



**QUANTUM CHEMICAL STUDY  
OF THE PROPERTIES  
OF GRIGNARD REAGENTS**

**JAANA TAMMIKU-TAUL**



**QUANTUM CHEMICAL STUDY  
OF THE PROPERTIES  
OF GRIGNARD REAGENTS**

**JAANA TAMMIKU-TAUL**



TARTU UNIVERSITY  
PRESS

Department of Chemistry, University of Tartu, Estonia

Dissertation is accepted for the commencement of the degree of Doctor of Philosophy in Chemistry on September 11, 2003, by the Doctoral Committee of the Department of Chemistry, University of Tartu.

Opponents:            Professor José-Luis M. Abboud, Madrid, CSIC  
                         Professor Ilmar Koppel, University of Tartu,  
                         Institute of Chemical Physics

Commencement:    December 03, 2003, 2 Jakobi St., room 430

© Jaana Tammiku-Taul, 2003  
Tartu Ülikooli Kirjastus  
[www.tyk.ut.ee](http://www.tyk.ut.ee)  
Tellimus nr. 655

*To my mother*

# CONTENTS

LIST OF ORIGINAL PUBLICATIONS .....	8
ABBREVIATIONS .....	9
1. INTRODUCTION .....	10
2. LITERATURE OVERVIEW .....	12
2.1. 1,10-Phenanthroline and its complexes with metal ions and compounds. Absorption spectra.....	12
2.2. The Schlenk equilibrium.....	13
2.3. Grignard reaction with alkynes.....	14
3. EXPERIMENTAL AND CALCULATION METHODS .....	16
3.1. Experimental methods .....	16
3.2. Calculation methods .....	16
4. RESULTS AND DISCUSSION.....	18
4.1. 1,10-Phenanthroline and its complexes with magnesium compounds. The absorption spectra .....	18
4.1.1. 1,10-Phenanthroline and its complex with ethylmagnesium bromide.....	18
4.1.2. Absorption spectra of 1,10-phenanthroline .....	19
4.1.3. Absorption spectra of the complex EtMgBr(phen) .....	19
4.1.4. Analysis of the disappearance of the red colour of the complex RMgX(phen).....	24
4.2. The Schlenk equilibrium.....	28
4.2.1. The Schlenk equilibrium in the gas phase and in Et <sub>2</sub> O solution .....	28
4.2.2. The Schlenk equilibrium in THF solution.....	29
4.3. Grignard reaction with alkynes.....	31
4.3.1. Mechanism of Grignard reaction with alkyne .....	31
4.3.2. The transition state of Grignard reaction with alkyne.....	32
5. CONCLUSIONS .....	34
SUMMARY IN ESTONIAN.....	36
REFERENCES .....	38
ACKNOWLEDGEMENTS.....	41
PUBLICATIONS.....	43

## LIST OF ORIGINAL PUBLICATIONS

This thesis is based on the following original papers, which are referred to in the text by their Roman numerals:

- I J. Tammiku, P. Burk, A. Tuulmets, UV-VIS Spectrum of 1,10-Phenanthroline — Ethylmagnesium Bromide Complex. An Experimental and Computational Study. *Main Group Metal Chem.* **2000**, 23 (5), 301–305.
- II J. Tammiku, P. Burk, A. Tuulmets, 1,10-Phenanthroline and Its Complexes with Magnesium Compounds. Disproportionation Equilibria. *J. Phys. Chem. A* **2001**, 105 (37), 8554–8561.
- III J. Tammiku-Taul, P. Burk, A. Tuulmets, Theoretical Study of Magnesium Compounds. The Schlenk Equilibrium in the Gas Phase and in the Presence of Et<sub>2</sub>O and THF molecules. *J. Phys. Chem. A* **2003**, *submitted*.
- IV A. Tuulmets, V. Pällin, J. Tammiku-Taul, P. Burk, K. Raie, Solvent Effects in the Grignard Reaction with Alkynes. *J. Phys. Org. Chem.* **2002**, 15 (10), 701–705.
- V A. Tuulmets, J. Tammiku-Taul, P. Burk, Computational Study of the Grignard Reaction with Alkynes. *J. Mol. Struct. (Theochem)* **2003**, *submitted*.

## ABBREVIATIONS

BLYP	Becke Lee-Yang-Parr functional
B3LYP	Becke's three parameter hybrid functional using the Lee-Yang-Parr correlation functional
BSSE	basis set superposition error
CIS	single-excitation configuration interaction
CNDO	complete neglect of differential overlap
CP	counterpoise
CT	charge transfer
DFT	density functional theory
Et	ethyl
Et <sub>2</sub> O	diethyl ether
eV	electron-volt
HF	Hartree-Fock method
HMO	Hückel molecular orbital method
IR	infrared
Me	methyl
Me <sub>3</sub> N	trimethylamine
MeO	methoxy
Me <sub>2</sub> O	dimethyl ether
MO	molecular orbital
mp	melting point
MP	Møller-Plesset perturbation theory
MPW1PW91	Barone and Adamo's one parameter hybrid functional with modified Perdew-Wang exchange and correlation
NBO	natural bond orbital
NImag	number of imaginary frequencies
NMR	nuclear magnetic resonance
Ph	phenyl
phen	1,10-phenanthroline
PPP	Pariser-Parr-Pople method
RHF	restricted Hartree-Fock method
TD-DFT	time-dependent density functional theory
THF	tetrahydrofuran
TS	transition state
UV	ultraviolet
UV-Vis	ultraviolet visible
ZINDO	Zerner's implementation of intermediate neglect of differential overlap approximation to the calculation of electronic spectra
ZPVE	zero-point vibrational energy

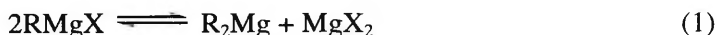


# 1. INTRODUCTION

Grignard reagents, which can be expressed by the simple empirical formula  $\text{RMgX}$  ( $\text{R}$  = organic group,  $\text{X}$  = halogen), have been known for more than hundred years<sup>1</sup> and have found widespread applications in organic synthesis.<sup>2,3</sup> Grignard reagents are still complicated systems for organic chemists. E.C. Ashby has said "Part of the problem seems to be that it takes an organic chemist to recognise the importance of this problem, a physical chemist to make the type of measurements which could be informative in what has become a complex physical-chemist problem, and an organometallic chemist with the background and experience to handle studies involving such sensitive organometallic compounds. Each person, having faced the Grignard problem, soon recognises his weakness in at least one of the above areas."<sup>4</sup> Nowadays computer modelling can provide answers to complicated and often experimentally inaccessible problems about energetics, geometries, and spectra of molecules, reaction mechanisms, etc.

One of the simplest methods for determination of a Grignard reagent concentration is the titration of its solution with *sec*-butanol or *n*-butanol<sup>5</sup> in the presence of 1,10-phenanthroline (**phen**) as an indicator. **Phen** is thought to form simple 1:1 charge transfer complexes<sup>5</sup> with organomagnesium compounds such as  $\text{RMgX}$  and  $\text{R}_2\text{Mg}$ .<sup>5,6,7</sup> There is, however, some controversy about the colour of a Grignard reagent complex with **phen** in literature. The bright violet colour of the complex has been mentioned,<sup>5,8</sup> as well as the red<sup>6</sup> or burgundy.<sup>8</sup> Prior this work no information was available regarding the processes, which take place during titration of a Grignard reagent with an alcohol in the presence of **phen** and the reasons for the disappearance of the colour of the solution near the titration end point.

Although the stoichiometry of a Grignard reagent is simple, the real composition of the reagent is far more complex, both in solution and in the solid state. The primary equilibrium, known generally as the Schlenk equilibrium (1),<sup>9</sup> is the dismutation process.



The position of the Schlenk equilibrium depends upon the solvent, the concentration of the solution, also the nature of the organic group and the halide, as well as the temperature.<sup>2,10</sup>

One of the goals of this study was to investigate the complexes between **phen** and magnesium compounds both experimentally and computationally. The solvation, complexation, and disproportionation equilibria (the Schlenk equilibrium), which might be important during titration of a Grignard reagent

with an alcohol in the presence of **phen**, have been studied using several computational methods.

Acetylenic Grignard compounds and the corresponding organometallic derivatives are important intermediates in many syntheses of acetylenic compounds.<sup>11</sup> Attention has been focused on elucidation of the mechanism of the Grignard reaction with alkynes. Although a cyclic structure of the transition state has been suggested,<sup>12</sup> no necessary experimental data are available to give more fundamental information about the transition state.

Another goal of this study was to obtain a more detailed insight into the mechanism of the reaction of Grignard reagent with alkyne by means of the methods of quantum chemistry.

## 2. LITERATURE OVERVIEW

### 2.1. 1,10-Phenanthroline and its complexes with metal ions and compounds. Absorption spectra

Many experimental data is available about UV spectrum of 1,10-phenanthroline (**phen**),<sup>13,14,15,16,17,18,19</sup> as well as theoretical studies using several semiempirical methods like Pariser-Parr-Pople (PPP) method,<sup>16</sup> CNDO method,<sup>20</sup> a modified PPP method on the basis of  $\pi$ -electron approach,<sup>21</sup> and CNDO/2 method.<sup>22</sup>

There are some weak bands at 338, 329, 324, and 309 nm and the two very intense absorption maxima at 263 and 231 nm with a shoulder at 226 nm in the experimental UV spectrum of **phen**.<sup>19</sup> 0-0' transition, which has very weak intensity, emerges at 338 nm.<sup>19</sup> No evidence has been found for  $n\text{-}\pi^*$  transitions in the absorption spectrum of **phen**. This conclusion has been based on the absence of the solvent effect with a variation of solvent polarity.<sup>16,23</sup>  $n\text{-}\pi^*$  transition shifts towards shorter wavelengths in polar solvents (ethanol, water, etc.) and towards longer wavelengths in nonpolar solvents (cyclohexane, carbon tetrachloride, etc.).<sup>23</sup>

Mono- and diprotonated forms of **phen** are used for interpretation of spectra of metal complexes, as most of the absorption bands are red-shifted both by protonation and metal complex formation.<sup>13,15,21,24</sup>

**Phen** forms charge transfer (CT) complexes with metal ions and compounds. Complexes of **phen** with open-shell transition-metal ions (metal-to-ligand charge-transfer complexes, e.g.,  $[\text{Fe}(\text{phen})_3]^{2+}$ ) are coloured<sup>16</sup> in contrast to those of  $nd^{10}$  closed-shell metal ions (ligand-to-ligand charge-transfer complexes, e.g.,  $\text{Mg}(\text{phen})^{2+}$ ,  $\text{Ca}(\text{phen})^{2+}$ ,  $\text{Zn}(\text{phen})^{2+}$ ,  $\text{Cd}(\text{phen})^{2+}$ ,<sup>24</sup>  $\text{ZnX}_2(\text{phen})$ ,  $\text{CdX}_2(\text{phen})$ ,  $\text{X} = \text{Cl}, \text{Br}, \text{I}$ ),<sup>25a-c</sup> where the participation of metal d-orbitals in the low-lying excited states of the complexes is thought to be insignificantly small. However, the complexes of **phen** with organozinc compounds, e.g.,  $\text{R}_2\text{Zn}(\text{phen})$  are yellow ( $\text{R} = \text{Me}, \text{Ph}$ )<sup>26a-c</sup> or orange-red ( $\text{R} = \text{Et}$ ),<sup>27</sup> and with organocadmium compounds, e.g.,  $\text{R}_2\text{Cd}(\text{phen})$  are yellow-orange ( $\text{R} = \text{Me}$ ).<sup>26c</sup> The complexes formed by **phen** with organomagnesium reagents such as  $\text{RMgX}$  and  $\text{R}_2\text{Mg}$  are also intensely coloured CT complexes.<sup>5-7</sup> Therefore, **phen** is widely used as an indicator for quantitative analysis of these species,<sup>5,8</sup> as well as for organolithium<sup>5</sup> and organozinc<sup>27</sup> compounds. These organometallic compounds can be directly titrated with an alcohol (acid) in the presence of **phen** (base) to a visible, well-defined, stoichiometric end point.<sup>5</sup> The quality of the end points is not dependent on the organic group attached to the magnesium atom.<sup>8</sup>

The absorption spectra of free **phen**,<sup>16,20,21</sup> its mono- and diprotonated forms,<sup>21</sup> and its complexes with the iron(II) ion<sup>16,20</sup> have been interpreted on the basis of the results of theoretical calculations using different semiempirical

methods. The *ab initio* calculations on the energetics of the complexation of alkaline metal cations ( $\text{Li}^+$ ,  $\text{Na}^+$ ,  $\text{K}^+$ ) with **phen** have been presented.<sup>28</sup> No theoretical studies regarding complexes of **phen** with the magnesium(II) ion or magnesium compounds were found in literature, except for well-resolved electron spin resonance spectra for complexes  $[\text{phen}(\text{MgR})]^+$ ,<sup>6,7</sup> which were analysed on the basis of Hückel MO (HMO) calculations.<sup>7</sup>

## 2.2. The Schlenk equilibrium

The original formula,  $\text{RMgX}$ , first proposed for the Grignard reagent, by Victor Grignard himself,<sup>1</sup> has a convenience and economy of style that belies its true nature. Following the initial reports, it became quickly apparent that the actual structure is far more complex, both in solution and in the solid state. It should be expressed by equilibrium of the type



where the middle part is known as the Schlenk equilibrium<sup>9</sup> and the associated species can exist as dimers, also as trimers and higher aggregates. The Schlenk equilibrium is dynamic and can be shifted very fast.

The position of the Schlenk equilibrium depends upon the solvent, the concentration of the solution, the nature of the organic group and the halide, as well as the temperature. The most important factors are solvent and concentration. All alkyl- and arylmagnesium chlorides, bromides, and iodides are monomeric in tetrahydrofuran (THF) over a wide concentration range (0.1–3.5 M).<sup>2,10,29</sup> Alkyl- and arylmagnesium bromides and iodides contain essentially monomeric species at low concentrations (less than 0.1 M) and dimeric species at higher concentrations (0.5–1.0 M) in diethyl ether ( $\text{Et}_2\text{O}$ ). The alkylmagnesium chlorides are essentially dimeric even at the low concentrations.<sup>2,10,29,30a</sup> The difference in Grignard reagent association behaviour in THF and  $\text{Et}_2\text{O}$  is attributed to the relative Lewis basicities of the two solvents. Solvent-metal bonding competes with the bridging characteristics of the halide, and THF competes more favourably than  $\text{Et}_2\text{O}$ . The associated complexes are believed to bridge predominantly through halide substituents.<sup>10,29</sup> Variable temperature NMR studies indicate that the rate of alkyl exchange is a function of the structure of the alkyl group, e.g., methyl group exchange is much faster than *tert*-butyl group exchange. Temperature effects on the composition of Grignard reagents in solution can be either kinetic or thermodynamic. Increasing temperature usually results in a faster exchange of ligands among magnesium complexes, which translates to faster equilibration

rates.<sup>2,10,31a,b</sup> Thus, all factors which affect the position of equilibrium are in close connection with one another.

The Schlenk equilibrium constant is usually expressed as

$$K_s = \frac{[RMgX]^2}{[R_2Mg] \cdot [MgX_2]} \quad (3)$$

If  $[R_2Mg] \approx [MgX_2]$ , which is frequently the case, a determination of the ratio  $[RMgX]/[R_2Mg]$  can be used. The equilibrium constants are also calculated from the equation

$$\Delta G = -RT \ln K \quad (4)$$

where R is universal gas constant (8.314 J/mol·K) and T is temperature.

The Schlenk equilibrium has been the subject of various experimental investigations. Calorimetric studies of the heats of reaction between  $MgX_2$  and  $R_2Mg$  in dilute solutions of  $Et_2O$ <sup>32a-c</sup> and THF<sup>33</sup> (thermochemical titration) have provided thermodynamic parameters and equilibrium constants for several systems. A number of constants, thermodynamic parameters, and qualitative kinetic data for the exchange process has been obtained by variable temperature NMR-spectroscopy.<sup>31a-d</sup> Also IR-spectroscopy,<sup>34</sup> polarography,<sup>35</sup> analysis of kinetic investigations of Grignard reactions,<sup>36a,b</sup> and molecular weight measurements<sup>30a,b</sup> have been used. Many crystallographic data are available for the structures of solvated monomeric magnesium compounds.<sup>37,38,39,40,41</sup>

Several theoretical studies about the Schlenk equilibrium, solvent effects, association processes in Grignard reagents, etc. have been carried out by semiempirical calculations, using the extended HMO<sup>42</sup> (solvents are  $Me_2O$  and  $Me_3N$ ) and CNDO/2<sup>43</sup> (only gas-phase calculations) methods, and by high level *ab initio* calculations, using both Hartree-Fock (HF) and Møller-Plesset (MP) perturbation calculations<sup>44</sup> (solvent is  $Me_2O$ ), the density functional theory (DFT), where solvent is  $Et_2O$ .<sup>45</sup>

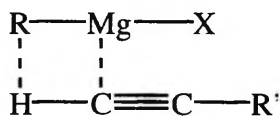
### 2.3. Grignard reaction with alkynes

Acetylenic Grignard compounds and the corresponding organometallic derivatives are important intermediates in many syntheses of acetylenic compounds.<sup>11</sup>

The first acetylenic Grignard reagents of the type  $RC\equiv CMgX$  ( $R = C_6H_5$ ,  $n-C_5H_{11}$ ) were obtained by J. Iotsitch.<sup>46</sup> Subsequently the reactions of acetylenic compounds with Grignard reagents have been investigated occasionally over many years.<sup>2,3</sup> A change in relative rates of the reaction of various Grignard reagents with hex-1-yne was studied by Dessy *et al.*,<sup>12,47,48</sup> discovering a simple

correlation between the numbers of  $\beta$ -hydrogens and the reactivity, i.e., isopropyl > ethyl > *n*-propyl > methyl,<sup>12,47</sup> and besides that halogen-free diethylmagnesium reacts with hex-1-yne three times as fast as ethylmagnesium bromide.<sup>48</sup> Kinetics of the reaction between acetylene HC≡CH and phenylmagnesium bromide PhMgBr in diethyl ether<sup>49,50</sup> and in tetrahydrofuran<sup>51</sup> in the presence of various additions of triethylamine and without a catalyst were carried out by Tuulmets' group to investigate the mechanism and solvent effects of this reaction.

A cyclic structure of the transition state (Scheme 1) suggested by Dessy *et al.*<sup>12</sup> and supported *inter alia* by the significance of the nucleophilic assistance by the acetylenic group<sup>50</sup> is merely a symbolic sketch, representing no real bond lengths and angles or any atomic charges.



**Scheme 1.** A cyclic structure of the transition state for a complex between magnesium compound and alkyne molecule.

No necessary experimental data are available to give more fundamental information about the transition state. The transition state can elucidate the mechanism of the Grignard reaction with alkyne and the solvent effects in reactions of acetylenic compounds with Grignard reagents.

## 3. EXPERIMENTAL AND CALCULATION METHODS

### 3.1. Experimental methods

Commercial 1,10-phenanthroline monohydrate (mp 108–110°C)<sup>52</sup> was purified by multiple recrystallization from benzene. The crystals were dried over P<sub>2</sub>O<sub>5</sub> in an exsiccator (mp 116.1°C, literature: mp 117.0–117.5°C).<sup>19</sup> The purity was checked by chromatomass spectrometry.

Ethylmagnesium bromide was prepared in diethyl ether by the standard method.<sup>53</sup> The complex EtMgBr(phen) was obtained by dissolving crystals of **phen** in the Grignard reagent at room temperature under the atmosphere of dry argon. The complex EtMgBr(phen) has deep red colour.

The absorption spectra of **phen** (in CH<sub>3</sub>CN; reference solution CH<sub>3</sub>CN) and of the complex EtMgBr(phen) (in Et<sub>2</sub>O; reference solution EtMgBr in Et<sub>2</sub>O) were measured at room temperature on a Perkin-Elmer UV-Vis spectrophotometer Lambda 2S. The spectrophotometer was controlled from a PC, and the spectra were stored in digital form. Fused silica cells with an optical path length of 1 cm were used. The spectrophotometer cells were capped with rubber septa to protect the Grignard reagent and the complex from moisture and air.

### 3.2. Calculation methods

The calculations were carried out using the GAUSSIAN 98<sup>54</sup> program package.

All geometry optimizations and vibrational analysis were done using either the conventional restricted Hartree-Fock (RHF) calculations with the 3-21G\* basis set or the density functional theory (DFT) with hybrid B3LYP functional and the 6-31+G\* basis set. All stationary points were found to be true minima (number of imaginary frequencies, NImag = 0). The calculated frequencies were also used for calculations of enthalpies and Gibbs energies.

Also, the natural bond orbital (NBO)<sup>55</sup> analysis was made both at the RHF/3-21G\* and the B3LYP/6-31G\* levels.

The absorption spectra of **phen** and its complexes with magnesium compounds were calculated at different levels of theory using semiempirical ZINDO method, *ab initio* CIS/6-31+G\* method, the time-dependent density functional theory (TD-DFT) TD/B3LYP/6-31+G\*, TD/BLYP/6-31+G\*, and TD/MPW1PW91/6-311+G\*\* methods.

Solvation was modelled using the supermolecule approach, which is the best method to describe the specific solvent effects. Solvent molecules were added to the studied species.

The basis set superposition error (BSSE) estimated according to the counterpoise (CP) correction<sup>56</sup> was taken into account. The BSSE arises from the mathematical fact that the basis sets are not complete and it should be considered in the case of complexation energies. The dimer (complex) energy minus the monomer energies is the directly calculated complexation energy,  $\Delta E_{\text{complexation}}$ .

$$\Delta E_{\text{complexation}} = E(AB)_{ab}^* - E(A)_a - E(B)_b \quad (5)$$

To estimate how much of this complexation energy is due to BSSE, additional energy calculations were needed. The CP correction is defined as

$$\Delta E_{CP} = E(A)_{ab}^* + E(B)_{ab}^* - E(A)_a^* - E(B)_b^* \quad (6)$$

where  $E(A)_{ab}^*$  and  $E(B)_{ab}^*$  are the monomer energies with the basis set of complex,  $E(A)_a^*$  and  $E(B)_b^*$  are the monomer energies with their normal basis sets. In all cases the monomers were calculated with the geometry they have in complex. The counterpoise corrected complexation energy,  $\Delta E_{BSSE}$ , is given as

$$\Delta E_{BSSE} = \Delta E_{\text{complexation}} - \Delta E_{CP} \quad (7)$$

The BSSE had a particularly strong influence on the complexation energies of the bromine-containing compounds compared to the corresponding chlorine compounds, indicating somewhat less satisfactory description of bromine basis set.

In transition state calculations the first order saddle point was found on the surface of potential energy (NImag = 1). The reaction path from the obtained transition state was followed both in reverse (towards the reagents) and forward (towards the products) direction to verify that the correct transition state, which connects the reactants and products, was obtained.<sup>57</sup> The activation energies were calculated without BSSE corrections, as there is no general rule how to separate the transition state into interacting fragments.



## 4. RESULTS AND DISCUSSION

### 4.1. 1,10-Phenanthroline and its complexes with magnesium compounds. The absorption spectra

#### 4.1.1. 1,10-Phenanthroline and its complex with ethylmagnesium bromide<sup>1</sup>

Geometries of **phen**, ethylmagnesium bromide, and the complex formed between **phen** and ethylmagnesium bromide (Figure 1) were optimized at RHF/3-21G\* level.

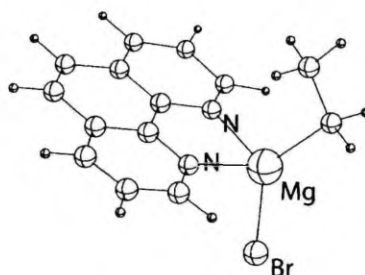


**Figure 1.** The optimized structure of the complex of 1,10-phenanthroline with ethylmagnesium bromide.

The complex  $\text{EtMgBr}(\text{phen})$  is stable according to our *ab initio* calculations, the complexation enthalpy,  $\Delta H$ , is  $-39.7$  kcal/mol. This fairly high value indicates strong bonding in the complex, whereas for comparison, the complexes of **phen** with alkaline metal cations have the complexation enthalpies  $-85.1$ ,  $-60.9$ , and  $-41.1$  kcal/mol with  $\text{Li}^+$ ,  $\text{Na}^+$ , and  $\text{K}^+$ , respectively (RHF/MIDI calculations).<sup>28</sup> A trend in the stability of these complexes is in the order  $\text{Li}^+ > \text{Na}^+ > \text{K}^+$ , clearly depending on the radii of cations.<sup>28</sup> PPP calculations indicate that the complex  $[\text{Fe}(\text{phen})_3]^{2+}$  is stabilized by 26.3 kcal/mol relative to  $\text{Fe}^{2+}$  and free ligands.<sup>16</sup> Consequently, the stability of the complex  $\text{EtMgBr}(\text{phen})$  is comparable to those for  $\text{K}(\text{phen})^+$  and  $[\text{Fe}(\text{phen})_3]^{2+}$ . The stability of the studied complex is directly related to the high atomic charge at the magnesium atom (see Table 2 in I). Bonding of ligands to the magnesium atom in  $\text{EtMgBr}$  was found to be mainly ionic and the bonding between  $\text{EtMgBr}$  and **phen** was found to be electrostatic (an ion-dipole or a dipole-dipole interaction).

### 4.1.2. Absorption spectra of 1,10-phenanthroline<sup>1</sup>

The experimentally measured absorption spectrum of **phen** (in CH<sub>3</sub>CN, Figure 2a-d) is similar to those given in literature.<sup>13-21,25a</sup> There are some weak bands at 330, 322, and ~308 nm, a band of medium intensity in the region 274–286 nm, the two most intense bands at 262 and 230 nm with a shoulder, and a band of medium intensity at 196 nm in the experimental UV spectra. The last one was not described in literature because the earlier studies were performed decades ago with a limited measurement region.

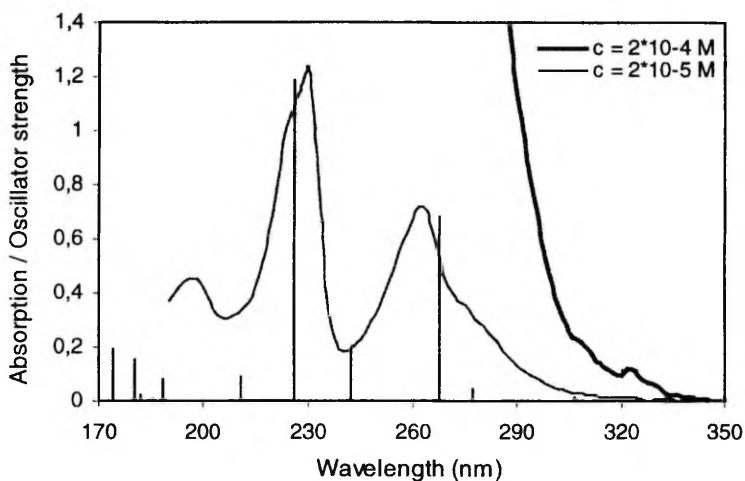
No 0-0' band (341 nm,<sup>17</sup> 339 nm<sup>14</sup> or 338 nm<sup>19</sup>) of very weak intensity was identified in our experiment. The strong band at 262 nm is assumed to be due to  $\pi$ - $\pi^*$  transition.

The absorption spectra were calculated at four different levels of theory. Good agreement was found between the experimental UV spectrum of **phen** and the excitation energies calculated with ZINDO method (Figure 2a). The theoretical spectrum obtained at *ab initio* CIS/6-31+G\* level of calculations has very similar pattern to the experimental spectrum in spite of a strong hypsochromic shift (Figure 2b). The results of TD/B3LYP/6-31+G\* calculations are not satisfactory (Figure 2c). Comparison of experimental and calculated spectra indicates that the best match was obtained using excitation energies calculated by the TD/BLYP/6-31+G\* method, the excitation energies being in error by 0.02, 0.17, and 0.01 eV, respectively (Figure 2d, see Table 3 in I). Our analysis of the bands on the basis of obtained MOs also confirm the conclusion that all observed bands in the spectrum of **phen** correspond to  $\pi$ - $\pi^*$  transitions. No  $n$ - $\pi^*$  transitions with noteworthy intensity were found.

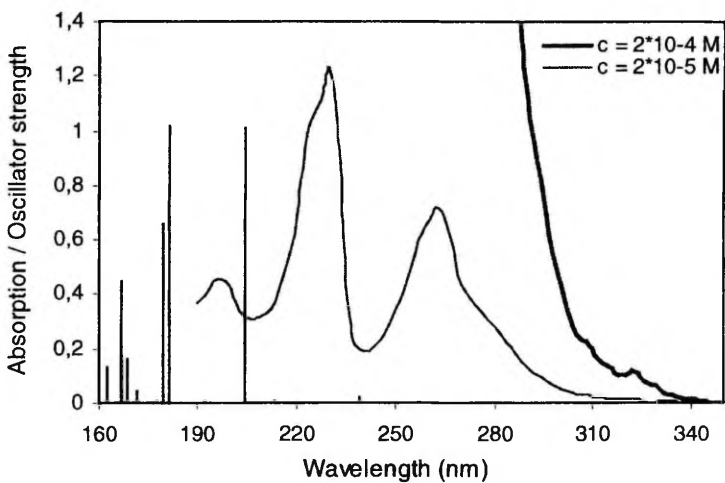
### 4.1.3. Absorption spectra of the complex EtMgBr(phen)<sup>1</sup>

The absorption spectrum of the complex EtMgBr(phen) is essentially different from that of **phen** as shown in Figure 3a-d. The absorption maxima emerge at much longer wavelengths compared to **phen**: at 522, 440, ~414, 392, and 316 nm.

The calculated UV-Vis spectra of the complex EtMgX(phen) by ZINDO (Figure 3a, X = Cl) and CIS/6-31+G\* methods (Figure 3b, X = Br) are not in agreement with the experiment. The CIS/6-31+G\* method is not appropriate for calculations of the spectra of CT complexes. Evidently this level of theory does not sufficiently include the electron correlation to describe the spectra of CT complexes. It should also be taken into account that our calculations refer to the isolated systems in the gas phase, while the experimental spectra are recorded in the solution, where the solvent effects can considerably affect the positions of bands, particularly for CT complexes, where considerable changes in dipole

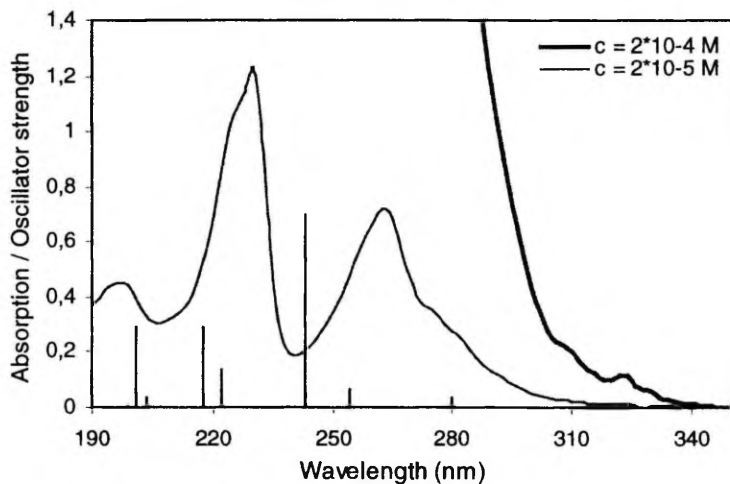


a) calculated by ZINDO method

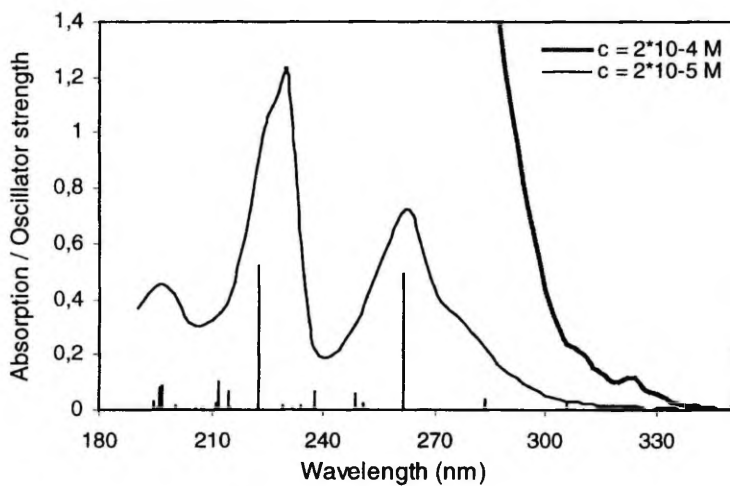


b) calculated by CIS/6-31+G\* method

**Figure 2a-b.** Absorption spectra of 1,10-phenanthroline compared with the theoretical results obtained by (a) semiempirical ZINDO method and (b) *ab initio* CIS/6-31+G\* method, being represented as vertical lines.

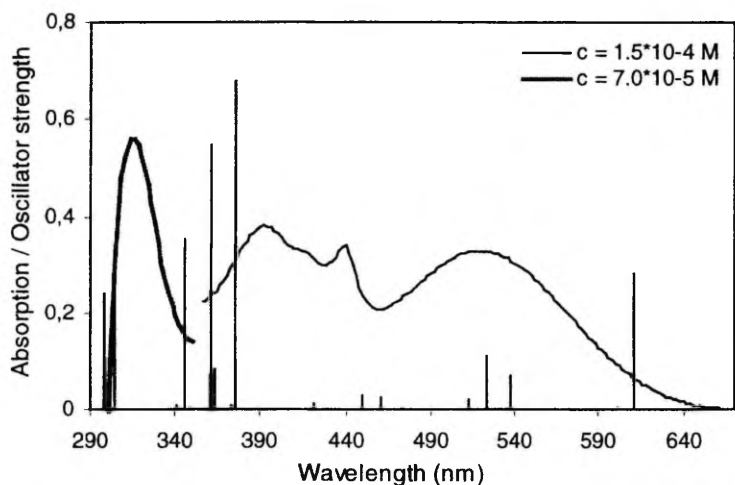


c) calculated by TD/B3LYP/6-31+G\* method

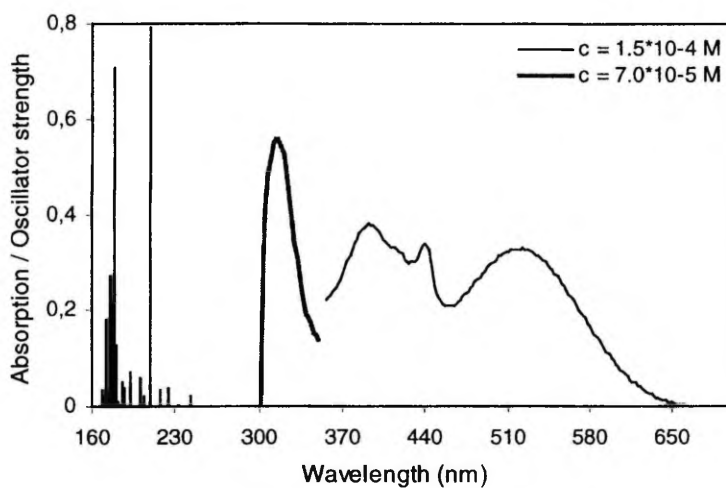


d) calculated by TD/BLYP/6-31+G\* method

**Figure 2c-d.** Absorption spectra of 1,10-phenanthroline compared with the theoretical results obtained by (c) TD-DFT/B3LYP/6-31+G\* method and (d) TD-DFT/BLYP/6-31+G\* method, being represented as vertical lines.



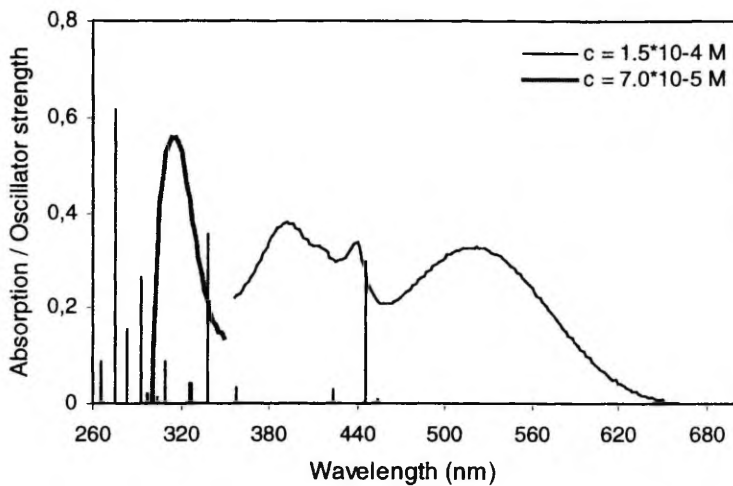
a) calculated by ZINDO method<sup>†</sup>



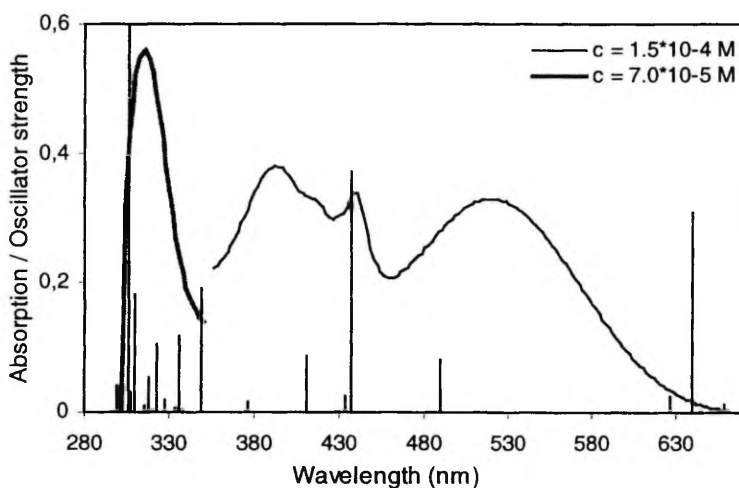
b) calculated by CIS/6-31+G\* method

**Figure 3a-b.** Absorption spectra of the complex EtMgBr(phen) compared with the theoretical results obtained by (a) semiempirical ZINDO method and (b) *ab initio* CIS/6-31+G\* method, being represented as vertical lines.

<sup>†</sup> Calculated for the complex EtMgCl(phen).



c) calculated by TD/B3LYP/6-31+G\* method<sup>‡</sup>



d) calculated by TD/BLYP/6-31+G\* method<sup>‡</sup>

**Figure 3c-d.** Absorption spectra of the complex EtMgBr(phen) compared with the theoretical results obtained by (c) TD-DFT/B3LYP/6-31+G\* method and (d) TD-DFT/BLYP/6-31+G\* method, being represented as vertical lines.

<sup>‡</sup> The values of oscillator strength are 20 times magnified.

moments upon excitation are expected. The results obtained by DFT methods (TD/B3LYP/6-31+G\* and TD/BLYP/6-31+G\*) are in much better agreement with the experiment, a hypsochromic shift appears in the case of TD/B3LYP/6-31+G\* level of theory (Figure 3c, X = Br) and a bathochromic shift appears in the case of TD/BLYP/6-31+G\* level of theory (Figure 3d, X = Br). The errors in transition energies are below 0.7 eV for TD/B3LYP/6-31+G\* and below 0.5 eV for TD/BLYP/6-31+G\* (see Table 3 in I). This allowed us to use the TD/BLYP/6-31+G\* results for the interpretation of spectral bands similarly to the case of **phen**.

The first most intense band at 522 nm in the experimental spectrum corresponds to the charge transfer from EtMgBr to **phen** and is responsible for the deep red colour of the complex. CT bands are always flat and have been assigned to a considerable change in the dipole moment. An inspection of the participating MOs indicates that excitation occurs mostly from the bromine lone pair orbital to the  $\pi$  system of **phen**. Thus, this transition can be classified as an  $n-\pi^*$  transition.

The next band at 440 nm also corresponds to the charge transfer from EtMgBr to **phen**. Here excitation occurs from the C-Mg bonding orbital to the  $\pi$  system of **phen**. As the C-Mg bonding orbital is located primarily on the carbon atom (the C-Mg bond is essentially ionic), the corresponding transition can also be classified as an  $n-\pi^*$  transition.

The third band at 392 nm is also a CT band, as the transition occurs from the Br-Mg bond to the  $\pi^*$  type MO of **phen**. The Br-Mg bond is ionic (as is the C-Mg bond), the corresponding MO is located mainly on bromine, and similarly to the previous excitation, we classify the band as an  $n-\pi^*$ .

The fourth band at 316 nm can be attributed to the  $\pi-\pi^*$  transitions in the  $\pi$  system of **phen**. This band corresponds to 305 nm in the spectrum of **phen** according to our TD/BLYP/6-31+G\* calculations.

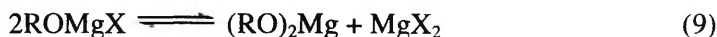
#### 4.1.4. Analysis of the disappearance of the red colour of the complex RMgX(phen)

The purpose of the present study was to clarify the reasons for the disappearance of the red colour of the solution during titration of a Grignard reagent with an alcohol in the presence of **phen**. It can be assumed that an alkoxy magnesium halide, which forms during the titration reaction



either does not form the complex with **phen** or the complex is colourless. As Grignard reagent exists in solution as an equilibrium mixture (Eqs. 1 and 2),

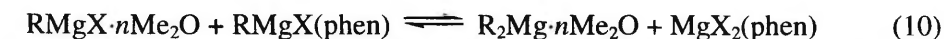
similar equilibrium reaction can take place in the case of alkoxy magnesium halide (i.e., the product of titration reaction).



As a result, the constitution of the titration mixture at the titration end point is not evident. For that reason, we carried out an extensive computational investigation at higher level of theory, using DFT B3LYP/6-31+G\* method for calculations of solvation energies for magnesium compounds, their complexation energies with **phen**, and disproportionation equilibria, and TD-DFT/MPW1PW91/6-311+G\*\* method for calculations of absorption spectra of the formed complexes.<sup>11</sup> The model system was studied, i.e., the magnesium compounds were  $\text{MgX}_2$ ,  $\text{MeMgX}$ ,  $\text{MeOMgX}$ ,  $\text{Me}_2\text{Mg}$ , and  $(\text{MeO})_2\text{Mg}$  ( $\text{X} = \text{Cl}, \text{Br}$ ) and the used solvent was  $\text{Me}_2\text{O}$ .

Comparison of experimental and calculated spectra of **phen** (Figure 4a) indicates that the calculated excitation energies are shifted to shorter wavelengths (a hypsochromic shift). In the case of calculated spectrum of the complex  $\text{MeMgCl}(\text{phen})$  appears a bathochromic shift relative to the experimentally measured absorption spectrum of the complex  $\text{EtMgBr}(\text{phen})$  (Figure 4b). The absorption of the complex  $\text{Me}_2\text{Mg}(\text{phen})$  also occurs in the visible region (Figure 4d), being in agreement with experimental data.<sup>6,7</sup> Our results indicate that all complexes of **phen** with alkyl- and alkoxy magnesium compounds have absorption maxima in the visible region (Figure 4b-e). Thus, the disappearance of the colour at the equivalence point of titration of a Grignard reagent with an alcohol in the presence of **phen** can not be attributed to the formation of the complex between  $\text{ROMgX}$  and **phen**, as the complex should be also coloured according to our calculations. The complex of **phen** with magnesium halide (Figure 4f) is the only one without absorption in the visible region. This leads to the necessity to investigate the disproportionation equilibria as an alkoxy complex, which forms during titration of a Grignard reagent with an alcohol, can disproportionate according to the Schlenk equilibrium.

In the case of titration of a Grignard reagent with an alcohol in the presence of **phen** as an indicator, there is, however, an excess of free  $\text{RMgX}$  or  $\text{ROMgX}$  in the solution and the Schlenk equilibria can be written as





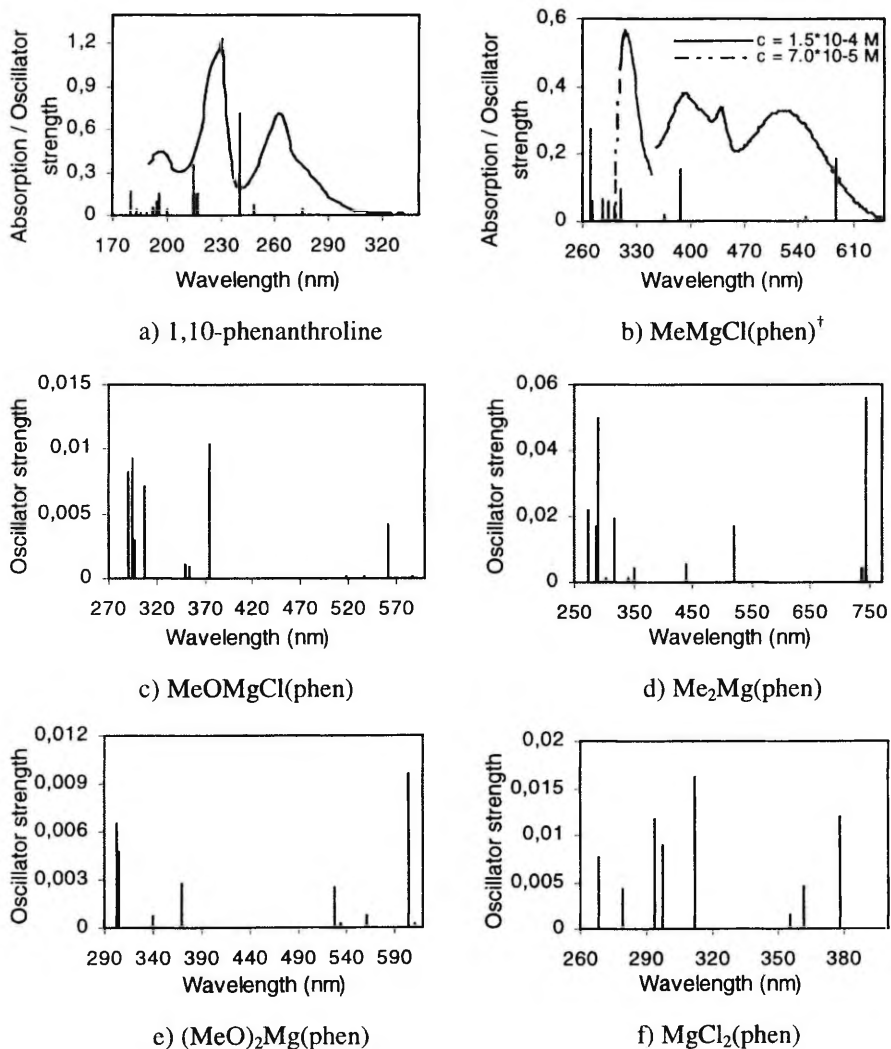


**Figure 4.** Calculated (at TD/MPW1PW91/6-311+G\*\* level of theory) absorption spectra of (a) 1,10-phenanthroline in comparison with experimental spectrum, (b) MeMgCl(phen) in comparison with experimental spectrum of EtMgBr(phen), (c) MeOMgCl(phen), (d) Me<sub>2</sub>Mg(phen), (e) (MeO)<sub>2</sub>Mg(phen), and (f) MgCl<sub>2</sub>(phen).

<sup>†</sup> The values of oscillator strength are 10 times magnified.

The formation of disproportionation products with reversed complexation, i.e.,  $R_2Mg(phen)$  and  $MgX_2 \cdot nMe_2O$ , is energetically less favourable. Namely, the complexation energy is the least negative for the complex of **phen** with  $Me_2Mg$  ( $\Delta H_0 = -23.7$  kcal/mol), which is sterically the most unfavourable and has the smallest positive charge on the magnesium atom according to the calculated NBO atomic charges (see Table 5 in II). The complexation of **phen** with  $(MeO)_2Mg$  is also excluded as **phen** forms with  $MgCl_2$  and  $MgBr_2$  the most stable complexes,  $\Delta H_0$  is  $-43.9$  and  $-39.8$  kcal/mol, respectively. This is apparently due to the fact that two electronegative halogen atoms withdraw larger amount of the electron density from the magnesium, thus, allowing stronger electrostatic interaction between the more positively charged magnesium and the negatively charged nitrogens of **phen**.

The calculated energies for disproportionation equilibria are given in Table 1.

**Table 1.** Energies ( $\Delta E$ , contains zero-point vibrational energy, ZPVE, correction), enthalpies ( $\Delta H$ ) and Gibbs energies ( $\Delta G$ ) for disproportionation equilibria of methylmagnesium halides and methoxymagnesium halides at B3LYP/6-31+G\* level. All values are in kcal/mol.

	$\Delta E$	$\Delta H$	$\Delta G$
$RMgX + RMgX(phen) \rightleftharpoons R_2Mg + MgX_2(phen)$			
MeMgCl	-6.02	-6.53	-4.27
MeMgBr	-7.55	-8.17	-5.72
MeOMgCl	-3.26	-3.20	-2.20
MeOMgBr	-6.65	-6.51	-5.98
$RMgX \cdot Me_2O + RMgX(phen) \rightleftharpoons R_2Mg \cdot Me_2O + MgX_2(phen)$			
MeMgCl	-0.82	-0.82	-0.31
MeMgBr	-2.28	-2.48	-1.54
MeOMgCl	-1.95	-1.95	-1.51
MeOMgBr	-5.14	-5.08	-5.27
$RMgX \cdot 2Me_2O + RMgX(phen) \rightleftharpoons R_2Mg \cdot 2Me_2O + MgX_2(phen)$			
MeMgCl	3.33	3.33	4.02
MeMgBr	4.22	4.01	4.86
MeOMgCl	-0.31	-0.31	0.44
MeOMgBr	-1.54	-1.44	-1.13

The modified Schlenk equilibria (Eqs. 10 and 11) are shifted towards the disproportionation products in the gas phase (the number of solvent molecule  $n = 0$ ) and in the case of monosolvated species ( $n = 1$ ) due to the stronger complex between **phen** and magnesium halide. In the case of disolvated species ( $n = 2$ ), which are the closest to the situation in real solution, the equilibrium is strongly shifted towards the nondisproportionated  $RMgX$ , while for  $ROMgX$

the equilibrium is shifted in the opposite direction. As a result, in solution of RMgX in the presence of **phen** alkylmagnesium halide complexes should prevail. Alkoxy magnesium halides should, in contrast, be strongly disproportionated, especially MeOMgBr.

So, according to our calculations, prior to the titration equivalence point **phen** is complexed with RMgX, while after equivalence point the complexes with MgX<sub>2</sub> should prevail. These results indicate that the disappearance of the red colour of the complex of **phen** with a Grignard reagent during titration with an alcohol is not due to the complex formation between alkoxy magnesium halide and **phen**. The alkoxy complex disproportionates to a dialkoxy magnesium compound and a magnesium halide, and **phen** gets entirely complexed with the magnesium halide in the equivalence point because the complex between magnesium halide and **phen** is much stronger than the other studied complexes. Thus, the complexation of MgX<sub>2</sub> with **phen** in the solution seems to be the reason of the disappearance of the red colour of the solution near the titration end point. The absorption spectrum of the complex MgCl<sub>2</sub>(phen) calculated by the TD/MPW1PW91/6-311+G\*\* method lies in the ultraviolet region (Figure 4f) supporting our hypothesis.

## 4.2. The Schlenk equilibrium

### 4.2.1. The Schlenk equilibrium in the gas phase and in Et<sub>2</sub>O solution

As the Schlenk equilibrium is a very intriguing subject in organic chemistry, it was studied thoroughly by means of the DFT B3LYP/6-31+G\* method. Grignard reagents are mostly prepared in diethyl ether (Et<sub>2</sub>O) and tetrahydrofuran (THF) solutions, thus, we carried out calculations for the systems, where R is Et and Ph groups besides Me group, and Et<sub>2</sub>O and THF were used as solvents<sup>III</sup> in addition to Me<sub>2</sub>O.<sup>II</sup>

The calculated energies for the Schlenk equilibria of monomeric Grignard reagents in the gas phase and in Et<sub>2</sub>O and THF solutions are given in Table 5 in III. The collected experimental data are listed in Table 6 in III for comparison.

The Schlenk equilibrium lies in favour of alkyl- and arylmagnesium halides in the gas phase,  $\Delta H$  ranges from 4.01 to 6.64 kcal/mol. The solvation by diethyl ether,<sup>III</sup> as well as by dimethyl ether<sup>II</sup> has a quite strong influence on the equilibrium, decreasing the endothermicity of disproportionation reactions. The addition of the first Et<sub>2</sub>O molecule has a stronger effect, disproportionation of monosolvated systems becomes by 1.69...3.21 kcal/mol less endothermic, and the addition of the second solvent molecule has a small 0.14...0.82 kcal/mol additional effect, except for PhMgCl where the second Et<sub>2</sub>O molecule increases the endothermicity by 0.76 kcal/mol. The effect of solvation is the strongest in

the case of PhMgBr, giving a value of  $\Delta\Delta H_2 = \Delta H_{\text{gas}} - \Delta H_2 = 4.03$  kcal/mol, in the case of another species it ranges from 1.42 kcal/mol for PhMgCl to 2.52 kcal/mol for EtMgBr. Comparison of experimental and calculated energies for the disolvated systems indicates that most values obtained by calculations are somewhat bigger, e.g.,  $\Delta\Delta H_{\text{calc}(2)\text{-exp}}$  is 0.85 kcal/mol for EtMgBr, 0.59 kcal/mol for PhMgBr, and  $\Delta\Delta G_{\text{calc}(2)\text{-exp}}$  is 1.30 kcal/mol for EtMgBr, but  $\Delta\Delta G_{\text{exp-calc}(2)}$  is 1.28 kcal/mol for PhMgBr. The calculated values of  $\Delta G$  for the monosolvated systems seem to be much more consistent with the experimental data for real solution,  $\Delta\Delta G_{\text{calc}(1)\text{-exp}}$  is 0.91 kcal/mol for EtMgBr and 0.20 kcal/mol for PhMgBr. However, the tendency that the predominant species in Et<sub>2</sub>O is RMgX, is still in agreement with experiment. We can not ignore the fact that magnesium compounds exist as aggregates in real diethyl ether solution. The dimerization processes were calculated by Bock *et al.* in Me<sub>2</sub>O<sup>44</sup> and by Lammertsma *et al.* in Et<sub>2</sub>O.<sup>45</sup> As the Schlenk equilibrium is only slightly influenced by the association of Grignard reagents<sup>45</sup> and the dimerization energies decrease in the order  $[\text{MgX}_2] > [\text{RMgX}] > [\text{R}_2\text{Mg}]$  (Cl > Br),<sup>44,45</sup> our calculations are limited to monomers.

#### 4.2.2. The Schlenk equilibrium in THF solution

THF, the stronger base, forms somewhat stronger Lewis acid-base complexes with studied magnesium compounds than Et<sub>2</sub>O. The energies of displacement of Et<sub>2</sub>O with THF for magnesium compounds indicate that the magnesium atom of each species prefers THF to Et<sub>2</sub>O (see Table 4 in III). Thus, the position of the Schlenk equilibrium in THF solution should be different from Et<sub>2</sub>O solution. Still, the equilibrium is shifted towards RMgX in the case of solvation with one and two THF molecules according to our DFT calculations, but from the experimental data it appears that the direction of reaction in THF shifts in favour of R<sub>2</sub>Mg + MgX<sub>2</sub>. It has been suggested that the difference in the Schlenk equilibrium between Et<sub>2</sub>O and THF results from the increased coordination number of magnesium halide in THF. As THF is sterically less demanding than Et<sub>2</sub>O, magnesium halide can probably coordinate at least four tetrahydrofurans, e.g., MgBr<sub>2</sub>·4THF, based on crystallographic data<sup>41a,b</sup> and conclusions by Smith and Becker about their calorimetric studies.<sup>33</sup>

However, our calculations indicate that the addition of the third THF molecule to MgCl<sub>2</sub> and MgBr<sub>2</sub> stabilizes the formed tris-tetrahydrofuranate complexes (see Figure 2a in III). The fourth THF molecule can have either a stabilizing or destabilizing effect on the energy of solvated complex, depending on the geometry of the complex. The tetrakis-tetrahydrofuranate complex of magnesium halide can exist in two forms. The formation of *cis*-dihalo-tetrakis(tetrahydrofurano)magnesium(II) (see Figure 2b in III) is energetically

less favourable than the formation of corresponding disolvated complexes, while *trans*-dihalotetrakis(tetrahydrofurano)magnesium(II) (see Figure 2c in III) is the most stable.

Our computational results using the energies of  $\text{MgX}_2\cdot 3\text{THF}$  for the calculations of the disproportionation reactions support the above-mentioned argument. The correlation between the calculated values of  $\Delta H$  without BSSE corrections and the corresponding experimental values is rather good,  $\Delta\Delta H_{\text{exp-calc}(3)}$  is 0.77 kcal/mol for EtMgCl, 0.79 kcal/mol for EtMgBr, and  $\Delta\Delta H_{\text{calc}(3)\text{-exp}}$  is 0.85 kcal/mol for PhMgCl and 0.08...1.73 kcal/mol for PhMgBr. The tendency that the alkyl- and arylmagnesium bromides are much more strongly disproportionated than the chlorides, is also in agreement with experiment. It also becomes evident from the calculations using the energies of *cis*  $\text{MgX}_2\cdot 4\text{THF}$  without BSSE corrections, but the extent of disproportionation is smaller in the case of bromine compounds and the equilibrium is shifted towards the formation of organomagnesium halides in the case of chloride compounds. The results using the energies of *trans*  $\text{MgX}_2\cdot 4\text{THF}$  are more reasonable with BSSE corrections. The extent of disproportionation is somewhat more pronounced in the case of chloride compounds, which is not consistent with experimental data.

It seems that the used method of BSSE corrections is mostly not justified in the cases when  $n = 3$  and 4, but it works well when  $n = 1$  and 2. Such behaviour can be attributed to the fact that the counterpoise correction seems to overestimate the magnitude of BSSE, especially for higher aggregates.

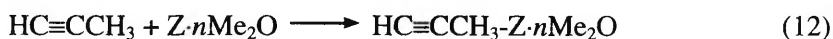
It should be noted that the values of  $\Delta G$  for the Schlenk equilibrium in the case of tri- and tetrasolvated complexes considerably differ from the  $\Delta E$  and  $\Delta H$ , having very high positive values. It seems to be a fault of the used thermochemical analysis method, which treats all vibrational modes other than the free rotations and translations of molecule or complex as harmonic vibrations. For molecules having hindered internal rotations, this can produce errors in the energy and heat capacity at room temperatures and can have a significant effect on the entropy. Thus, the obtained values of  $\Delta G$  are not reliable for the tris- and tetrakis-tetrahydrofuranate complexes of magnesium halides. Therefore, no equilibrium constants for the disproportionation reactions were calculated.

## 4.3. Grignard reaction with alkynes

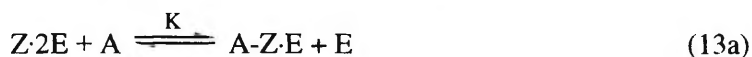
### 4.3.1. Mechanism of Grignard reaction with alkyne

The main question was whether an alkyne molecule can directly attack the organomagnesium compound via a  $S_{Ei}$  type reaction or whether a preliminary replacement of a solvent molecule is necessary. For that reason, a computational investigation was performed on the basis of the DFT B3LYP/6-31+G\* method,<sup>IV,V</sup> to get a more reliable understanding of the kinetic data obtained from the reaction of phenylmagnesium bromide with hex-1-yne in ethereal solutions.<sup>IV,58</sup> In order to save the computing time, all calculations were carried out for a model system, i.e., we used organomagnesium compounds with methyl group and propyne as alkyne. Their reactions were investigated in the gas phase and in the solvated state, using dimethyl ether as the donor.

The complexation energies calculated from Eq. 12, where Z is  $MgX_2$ ,  $MeMgX$ , and  $Me_2Mg$  ( $X = Cl, Br$ ) and  $n$  is the number of solvent molecules, 0 for unsolvated, 1 for mono-, and 2 for disolvated species, respectively,



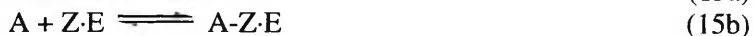
indicate that the complexes of disolvated magnesium compounds with propyne are weak (see Table 1 and Figure 1c-d in V). As a consequence, the reaction proceeds through replacement of a solvent molecule by the alkyne (Eq. 13a) and subsequent rate limiting conversion of the complex to products (Eq. 13b)



$$v = k[A \cdot Z \cdot E] = kK \frac{[Z \cdot 2E][A]}{[E]} \quad (14)$$

where Z denotes a magnesium compound, A an alkyne, and E an ether molecule.

The complex between the alkyne and monosolvated magnesium compound can form in two ways and, thus, the equilibrium constant K can be estimated either (i) from the equilibria (i.e.,  $S_{N1}$  mechanism of the ligand exchange)



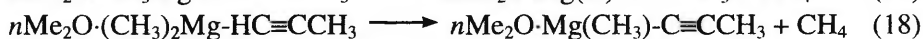
or (ii) from the equilibria (i.e., a  $S_{N2}$  like mechanism)





The thermodynamic effect is identical for the both cases and the results are presented in Table 2 in V. The equilibrium constants for an alkyne-Grignard complex formation are small, indicating that the concentration of the complex in the solution is extremely low. This seems to be the reason for the rather feeble reactivity of alkynes, although the rate of product formation from an alkyne-Grignard complex appears to be large. The addition of non-donating solvents, e.g., toluene, chlorobenzene and dichloromethane, to diethyl ether solution of Grignard reagent accelerated the reaction regardless of the polarity/polarizability of added cosolvents.<sup>IV</sup> Obviously reduced content of the ether in the reaction mixture shifted the equilibrium to the right, thus, enhancing the rate of the reaction. In the case of THF the accelerating effect of the additions is less pronounced in accordance with stronger solvating power of the donor.<sup>58</sup>

The formation energies of the end products were only calculated starting from the unsolvated ( $n = 0$ ) and monosolvated ( $n = 1$ ) complexes of organo-magnesium compounds with propyne according to Eqs. 17 and 18



The reaction towards the end products, acetylenic Grignard reagent and methane, is exothermic (see Table 3 in V). As expected, the reaction in solution is more exothermic than in the gas phase,  $\Delta H = -12.5 \dots -17.6$  kcal/mol for the unsolvated species and  $\Delta H = -18.5 \dots -23.3$  kcal/mol for the monosolvated species, respectively. This is in agreement with the experimental enthalpy of metallation of Brønsted acid  $\text{C}_6\text{H}_5\text{-C} \equiv \text{CH}$  with pentylmagnesium bromide in diethyl ether ( $\Delta H = -30.1$  kcal/mol) determined by Holm.<sup>59</sup>

#### 4.3.2. The transition state of Grignard reaction with alkyne

As the formation of the end products, acetylenic Grignard reagent and methane, from the propyne-Grignard complex is an exothermic process, the activation barrier for the reverse reaction (relative to the end products) is considerably higher than that for the forward reaction (relative to the propyne-Grignard complex). The activation energies for the gas-phase reagents are higher compared to the corresponding monosolvated reagents,  $\Delta H^\ddagger_{\text{forward}}$  is 27.6 and 27.9 kcal/mol for the unsolvated  $\text{MeMgCl}$  and  $\text{MeMgBr}$ , respectively, and 22.9 and 22.6 kcal/mol for the monosolvated  $\text{MeMgCl}$  and  $\text{MeMgBr}$ , respectively. The heights of the enthalpy barrier for the unsolvated and monosolvated products are comparable with each other,  $\Delta H^\ddagger_{\text{reverse}}$  ranges from 39.1 to 41.0

kcal/mol. Available rate constants for the reaction of Grignard reagent  $\text{PhCH}_2\text{MgCl}$  with proton donor  $\text{PhC}\equiv\text{CH}$  in diethyl ether<sup>60</sup> afforded a calculation of the activation energy equal to 16.7 kcal/mol, being in correlation with our computational activation energies for the monosolvated reagents.

The optimized structure of the transition state (see Figure 2b and 2e in V) is consistent with the cyclic four-centre transition state postulated by Dessy *et al.*,<sup>12</sup> however, the actual geometry of the transition state is almost triangular with practically linear proton transfer. The cycle formation is largely connected with the complexation of reagents. The entropy change during activation is negligible, but from the calculated values of complexation enthalpies,  $\Delta H$ , and Gibbs energies,  $\Delta G$ , (see Table 1 in V) becomes evident that the entropy change,  $\Delta S$ , lies in the range of  $-21.7\dots-31.2$  cal/K·mol, which is common for cycle formation (about  $-25\dots-30$  cal/K·mol). The analysis of bond lengths indicates that the transition state, which lies on the reaction path between reagents and products, slightly resembles the reagents. This is in accordance with the exothermicity of the reaction and with the enthalpy values for the activation, as well as with available values for kinetic isotope effects. Pocker and Exner<sup>60</sup> have found the kinetic deuterium isotope effect for the reactions of several organomagnesiums with phenylacetylene in diethyl ether to be  $4.6 \pm 0.2\dots 6.2 \pm 0.2$ . The same effect in tetrahydrofuran (THF) solution was equal to  $3.0 \pm 0.2\dots 3.6 \pm 0.2$ , accompanied with higher reactivity in THF medium.<sup>60</sup> The effect of stronger solvation, resulting in a shift of the transition state towards the reagents, can be observed also in our computational data, if to compare the lengthening of bond between Mg-atom and C-atom of Grignard reagent in the unsolvated and monosolvated transition states (see Table 5 in V).

A smaller polarity of the transition state in comparison with the reagents presents also evidence in favour of a cyclic structure of the transition state. Polarity of the studied systems can be estimated regarding their dipole moments. The most straightforward comparison can be done for the propyne-Grignard complex and the corresponding transition state. Although, the solvated complex  $\text{HC}\equiv\text{CCH}_3\text{-MeMgBr}\cdot\text{Me}_2\text{O}$  is the only initial system, which is slightly more polar than its transition state (see Table 6 in V), nevertheless, the changes in the polarity during activation is almost negligible for the other systems. The obtained dipole moments do not contradict to a slight suppressing effect of solvent polarity and polarizability found for the reaction of hex-1-yne with phenylmagnesium bromide solvated with diethyl ether<sup>IV</sup> and quantitatively described with Koppel-Palm equation.<sup>IV,61,62</sup>



## 5. CONCLUSIONS

The following conclusions can be drawn from the results of the present work:

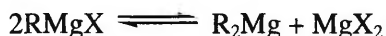
- There are two intense bands at 262 and 230 nm, and a band of medium intensity at 196 nm in the UV spectrum of 1,10-phenanthroline. *Ab initio* and DFT calculations confirm the conclusion found in literature that all observed intensive bands in the absorption spectrum of 1,10-phenanthroline correspond to  $\pi$ - $\pi^*$  transitions. No  $n$ - $\pi^*$  transitions of noteworthy oscillator strength were found.
- The experimental work evidenced that the complex between ethylmagnesium bromide and 1,10-phenanthroline has deep red colour. According to *ab initio* calculations the complex is stable. The measured UV-Vis spectrum of the complex EtMgBr(phen) had intense absorption maxima at 522, 440, and 392 nm corresponding to the  $n$ - $\pi^*$  excitations in the charge transfer complex, and at 316 nm corresponding to a  $\pi$ - $\pi^*$  transition in the  $\pi$  system of 1,10-phenanthroline.
- According to DFT calculations the disappearance of the red colour of the solution during titration of a Grignard reagent with an alcohol in the presence of 1,10-phenanthroline is not due to the complex formation between alkoxymagnesium halide and 1,10-phenanthroline. Prior to the titration equivalence point 1,10-phenanthroline is complexed with alkylmagnesium halide, while after the equivalence point the complexation with magnesium halide should be important, as the formed complex is much stronger than the organomagnesium complexes. Thus, the complexation of magnesium halide with 1,10-phenanthroline is the reason for the disappearance of the red colour of the solution.
- According to DFT calculations the magnesium halide is solvated with up to four solvent molecules in tetrahydrofuran solution, assuming that *trans*-dihalotetrakis(tetrahydrofurano)magnesium(II) complex forms. The formation of *cis*-dihalotetrakis(tetrahydrofurano)magnesium(II) is energetically even less favourable than the formation of corresponding disolvated complexes. The predominant species in the Schlenk equilibrium are RMgX in diethyl ether solution and  $R_2Mg + MgX_2$  in tetrahydrofuran solution, which is consistent with experimental data.
- According to DFT calculations the reaction between an alkyne and a disolvated Grignard reagent consists in the replacement of a coordinated solvent molecule by the alkyne, followed by fast conversion of the complex to products. The complex formation equilibrium is shifted towards the initial reagents, therefore, the overall reaction is slow. From experimental kinetic data becomes evident that the addition of non-donating solvents accelerates

the reaction presumably by shifting the equilibrium in favour of the complex formation. However, the reaction towards the end products, acetylenic Grignard reagent and alkane, is exothermic. The transition state has a cyclic structure with practically linear proton transfer and resembles more the reagents than the products.

## SUMMARY IN ESTONIAN

### Grignardi reaktiivide omaduste kvantkeemiline uurimine

1,10-fenantroliin (fen) moodustab magneesiumorgaaniliste ühenditega (RMgX ja R<sub>2</sub>Mg) intensiivse värvusega laenguülekandekomplekse ning seetõttu leiab ta laialdast kasutamist värvusindikaatorina nende ainete kvantitatiivsel määramisel. Käesoleva töö üheks eesmärgiks oli uurida 1,10-fenantroliini komplekse magneesiumiühenditega ning välja selgitada võimalik mehhanism, mis toimib Grignardi reaktiivi tiitrimisel alkoholi lahusega 1,10-fenantroliini juuresolekul. Arvutuslikult uuriti disproportsioneerumistasakaale (Schlenki tasakaal),



mis võivad püstitada Grignardi reaktiivi tiitrimisel alkoholi lahusega 1,10-fenantroliini juuresolekul.

1,10-fenantroliini neeldumisspektris esineb kaks intensiivset piiki maksimumidega lainepikkustel 262 ja 230 nm ning keskmise intensiivsusega piik maksimumiga lainepikkusel 196 nm. Nii *ab initio* kui ka tihedusfunktsionaali teooria arvutused kinnitavad fakti, et kõik intensiivsed piigid 1,10-fenantroliini spektris vastavad  $\pi$ - $\pi^*$  üleminekutele. Märgatava intensiivsusega  $n$ - $\pi^*$  üleminekut ei avastatud.

Meie eksperimentaalne mõõtmine tõestas, et 1,10-fenantroliini ja etüülmagneesiumbromiidi vaheline kompleks on tumepunase värvusega ning *ab initio* arvutuste kohaselt on tegemist stabiilse kompleksiga. Kompleksi EtMgBr(fen) mõõdetud neeldumisspektris asuvad maksimumid lainepikkustel 522, 440, 392 ja 316 nm. Kolme esimest piiki võib klassifitseerida kui  $n$ - $\pi^*$  üleminekut, viidates laenguülekandele etüülmagneesiumbromiidilt 1,10-fenantroliinile, ning viimast piiki kui  $\pi$ - $\pi^*$  üleminekut 1,10-fenantroliini  $\pi$ -süsteemis.

Tihedusfunktsionaali teooria arvutused näitavad, et lahuse punase värvuse valastumine Grignardi reaktiivi tiitrimisel alkoholi lahusega 1,10-fenantroliini juuresolekul ei tulene alkoksülmagneesiumhalogeniidi ja 1,10-fenantroliini vahelise kompleksi tekkest. Ilmneb, et enne stõhhiomeetriapunkti moodustab 1,10-fenantroliin kompleksi alküülmagneesiumhalogeniidiga ning pärast stõhhiomeetriapunkti magneesiumhalogeniidiga, mis on märgatavalt püsivam kui 1,10-fenantroliini kompleksid magneesiumorgaaniliste ühenditega. Lahuses esineva 1,10-fenantroliini komplekseerumine magneesiumhalogeniidiga ongi põhjuseks, miks stõhhiomeetriapunkti läheduses toimub tiitritava kompleksi RMgX(fen) punase värvuse valastumine.

Schlenki tasakaal on dünaamiline, sõltudes kõige enam solvendist ja lahuse kontsentratsioonist. Kuna tetrahüdrofuraan on steeriliselt vähenõudlikum kui dietüüleeter, on tal tugevam solvateerimisvõime, eelkõige magneesiumhalo-

geniidi suhtes. Tihedusfunktsionaali teooria arvutuste kohaselt on magneesium-halogeniid tetrahüdrofuraani lahuses solvateeritud kuni nelja solvendi molekuliga, eeldades et moodustub *trans*-dihalotetrakis(tetrahüdrofurano)magneesium(II) kompleks. *Cis*-dihalotetrakis(tetrahüdrofurano)magneesium(II) kompleksi moodustumine on energeetiliselt isegi veel ebasoodsam protsess kui vastavate disolvateeritud komplekside teke. Dietüüleetris on Schlenki tasakaal nihutatud  $\text{RMgX}$  tekke suunas, aga tetrahüdrofuraani lahuses disproportsioneerumisproduktide  $\text{R}_2\text{Mg} + \text{MgX}_2$  tekke suunas, olles kooskõlas eksperimendi tulemustega.

Atsetüleensed Grignardi ühendid  $\text{RC}\equiv\text{CMgX}$  ja nende vastavad metall-orgaanilised derivaadid on tähtsad vaheühendid atsetüleensete ühendite sünteesis. Töö teiseks eesmärgiks oli arvutuslikult välja selgitada Grignardi reaktsiooni ja alküüni vahelise reaktsiooni mehhanism. Uurimistulemusena leiti, et disolvateeritud Grignardi reaktsiooni ja alküüni vaheline reaktsioon koosneb kahest järjestikusest alareaktsioonist — esmalt asendub üks solvendi molekul alküüniga ning seejärel moodustuvad saadud kompleksist produktid. Kuna kompleksi moodustumise reaktsiooni tasakaal on nihutatud lähteainete suunas, on üldine reaktsioon väga aeglane. Eksperimentaalselt mõõdetud kineetilistest andmetest ilmneb, et mittedonoorsed solvendilisandid nihutavad tasakaalu kompleksi tekke suunas, mistõttu reaktsioon solvendisegudes kiirenes. Reaktsioon lõpp-produktide, atsetüleense Grignardi reaktsiooni ja alkaani tekke suunas on siiski eksotermiline protsess. Siirdeolek on tsüklilise struktuuriga, olles praktiliselt lineaarse prootoni ülekandega ning sarnanedes pigem lähteainete kui produktidega.

## REFERENCES

1. V. Grignard, *C. R. Hebd. Seances Acad. Sci.* **1900**, 130, 1322.
2. W.E. Lindsell, In *Comprehensive Organometallic Chemistry*, Vol. 1, G. Wilkinson (Ed.), Pergamon Press, 1982, Chapter 4.
3. W.E. Lindsell, In *Comprehensive Organometallic Chemistry II*, Vol. 1, G. Wilkinson, (Ed.), Pergamon Press, 1995, Chapter 3.
4. E.C. Ashby, *Quart. Revs.* **1967**, 21, 259.
5. S.C. Watson, J.F. Eastham, *J. Organomet. Chem.* **1967**, 9, 165.
6. W. Kaim, *J. Organomet. Chem.* **1981**, 222, C17.
7. W. Kaim, *J. Am. Chem. Soc.* **1982**, 104, 3833.
8. H.-S. Lin, L.A. Paquette, *Synth. Commun.* **1994**, 24, 2503.
9. W. Schlenk, W. Schlenk, *Chem. Ber.* **1929**, 62, 920.
10. K.S. Cannon, G.R. Krow, In *Handbook of Grignard Reagents*, G.S. Silverman, P.E. Rakita, (Eds.), Marcel Dekker: New York, 1996.
11. L. Brandsma, H.D. Verkruisje, *Synthesis of Acetylenes, Allenes and Cumulenes*. Elsevier: Amsterdam, 1981.
12. R.E. Dessy, J.H. Wotiz, C.A. Hollingsworth, *J. Am. Chem. Soc.* **1957**, 79, 358.
13. R.H. Linnell, A. Kaczmarczyk, *J. Phys. Chem.* **1961**, 65, 1196.
14. H. Gropper, F. Dörr, *Ber. Bunsen-Ges. Phys. Chem.* **1963**, 67, 46.
15. R.G. Bray, J. Ferguson, C.J. Hawkins, *Aust. J. Chem.* **1969**, 22, 2091.
16. T. Ito, N. Tanaka, I. Hanazaki, S. Nagakura, *Bull. Chem. Soc. Jpn.* **1969**, 42, 702.
17. T. Ohno, S. Kato, *Bull. Chem. Soc. Jpn.* **1974**, 47, 2953.
18. M. Yamada, M. Kimura, M. Nishizawa, S. Kuroda, I. Shimao, *Bull. Chem. Soc. Jpn.* **1991**, 64, 1821.
19. H.-H. Perkampus, *UV-VIS Atlas of Organic Compounds*, 2<sup>nd</sup> Ed., Part 2, Weinheim-New York-Basel-Cambridge, 1992, 1005.
20. N. Sanders, P. Day, *J. Chem. Soc. A* **1970**, 1190.
21. M. Berndt, W. Woznicki, *Acta Phys. Polon.* **1973**, A43, 101.
22. E.M. Kober, T.J. Meyer, *Inorg. Chem.* **1985**, 24, 106.
23. G.M. Badger, I.S. Walker, *J. Chem. Soc.* **1956**, 122.
24. K. Sone, P. Krumholz, H. Stammreich, *J. Am. Chem. Soc.* **1955**, 77, 777.
25. (a) S. Ikeda, S. Kimachi, T. Azumi, *J. Phys. Chem.* **1996**, 100, 10528. (b) S. Ikeda, S. Yamamoto, T. Azumi, G.A. Crosby, *J. Phys. Chem.* **1992**, 96, 6593. (c) S. Kimachi, S. Ikeda, T. Azumi, *J. Phys. Chem.* **1995**, 99, 7242.
26. (a) K.-H. Thiele, *Z. Anorg. Allgem. Chem.* **1963**, 325, 156. (b) K.-H. Thiele, J. Köhler, *Z. Anorg. Allgem. Chem.* **1965**, 337, 260. (c) K.-H. Thiele, *Z. Anorg. Allgem. Chem.* **1964**, 330, 8.
27. W.L. Everson, E.M. Ramirez, *Anal. Chem.* **1965**, 37, 812.
28. C.G. Sanchez, E.P.M. Leiva, S.A. Dassie, A.M. Baruzzi, *J. Electroanal. Chem.* **1998**, 451, 111.
29. F.W. Walker, E.C. Ashby, *J. Am. Chem. Soc.* **1969**, 91, 3845.
30. (a) E.C. Ashby, M.B. Smith, *J. Am. Chem. Soc.* **1964**, 86, 4363. (b) E.C. Ashby, W.E. Becker, *J. Am. Chem. Soc.* **1963**, 85, 118.
31. (a) D.F. Evans, V. Fazakerley, *J. Chem. Soc. A* **1971**, 184. (b) G.E. Parris, E.C. Ashby, *J. Am. Chem. Soc.* **1971**, 93, 1206. (c) D.F. Evans, V. Fazakerley, *Chem.*

- Commun.* **1968**, 974. (d) P.R. Markies, R.M. Altink, A. Villena, O.S. Akkerman, F. Bickelhaupt, *J. Organomet. Chem.* **1991**, 402, 289.
32. (a) M.B. Smith, W.E. Becker, *Tetrahedron Lett.* **1965**, 43, 3843. (b) M.B. Smith, W.E. Becker, *Tetrahedron* **1966**, 22, 3027. (c) T. Holm, *Acta Chem. Scand.* **1969**, 23, 579.
33. M.B. Smith, W.E. Becker, *Tetrahedron* **1967**, 23, 4215.
34. R.M. Salinger, H.S. Mosher, *J. Am. Chem. Soc.* **1964**, 86, 1782.
35. T. Psarras, R.E. Dessy, *J. Am. Chem. Soc.* **1966**, 88, 5132.
36. (a) E.C. Ashby, J. Laemmle, H.M. Neumann, *J. Am. Chem. Soc.* **1971**, 93, 4601. (b) E.C. Ashby, J. Laemmle, H.M. Neumann, *J. Am. Chem. Soc.* **1972**, 94, 5421.
37. (a) L.J. Guggenberger, R.E. Rundle, *J. Am. Chem. Soc.* **1964**, 86, 5344. (b) L.J. Guggenberger, R.E. Rundle, *J. Am. Chem. Soc.* **1986**, 90, 5375.
38. G. Stucky, R.E. Rundle, *J. Am. Chem. Soc.* **1964**, 86, 4825.
39. H. Schibilla, M.-T. Le Bihan, *Acta Cryst.* **1967**, 23, 332.
40. F. Schröder, Dissertation, Institut für Anorganische Chemie der Technischen Hochschule, Braunschweig, Germany, 1965.
41. (a) F. Schröder, H. Spandau, *Naturwiss.* **1966**, 53, 360. (b) M. Perucaud, J. Ducom, M. Vallino, *Compt. Rend.* **1967**, 264, 571.
42. K. Ohkubo, F. Watanabe, *Bull. Chem. Soc. Jpn.* **1971**, 44, 2867.
43. H. Kato, S. Tsuruya, *Bull. Chem. Soc. Jpn.* **1973**, 46, 1001.
44. J. Axten, J. Troy, P. Jiang, M. Trachtman, C.W. Bock, *Struct. Chem.* **1994**, 5, 99.
45. A.W. Ehlers, G.P.M. van Klink, M.J. van Eis, F. Bickelhaupt, P.H.J. Nederkoorn, K. Lammertsma, *J. Mol. Model.* **2000**, 6, 186.
46. J. Jotsitch, *Bull. Soc. Chim. Fr.* **1902**, 28, 922.
47. J.H. Wotiz, C.A. Hollingsworth, R.E. Dessy, *J. Am. Chem. Soc.* **1955**, 77, 103.
48. J.H. Wotiz, C.A. Hollingsworth, R.E. Dessy, *J. Am. Chem. Soc.* **1956**, 78, 1221.
49. V. Pällin, A. Tuulmets, *J. Organomet. Chem.* **1999**, 584, 185.
50. V. Pällin, E. Otsa, A. Tuulmets, *J. Organomet. Chem.* **1999**, 590, 149.
51. V. Pällin, A. Tuulmets, *Main Group Met. Chem.* **2000**, 23, 179.
52. A.I. Vogel, In *A Text-book of Practical Organic Chemistry Including Organic Qualitative Organic Analyses*, 3<sup>rd</sup> Ed., London, 1956, 992.
53. A.I. Vogel, In *Vogel's Textbook of Practical Organic Chemistry*, 5<sup>th</sup> Ed., London, 1994, 531.
54. *Gaussian 98, Revision A7*, M.J. Frisch, G.W. Trucks, H.B. Schlegel, G.E. Scuseria, M.A. Robb, J.R. Cheeseman, V.G. Zakrzewski, J.A. Montgomery, Jr., R.E. Stratmann, J.C. Burant, S. Dapprich, J.M. Millam, A.D. Daniels, K.N. Kudin, M.C. Strain, O. Farkas, J. Tomasi, V. Barone, M. Cossi, R. Cammi, B. Mennucci, C. Pomelli, C. Adamo, S. Clifford, J. Ochterski, G.A. Petersson, P.Y. Ayala, Q. Cui, K. Morokuma, D.K. Malick, A.D. Rabuck, K. Raghavachari, J.B. Foresman, J. Cioslowski, J.V. Ortiz, A.G. Baboul, B.B. Stefanov, G. Liu, A. Liashenko, P. Piskorz, I. Komaromi, R. Gomperts, R.L. Martin, D.J. Fox, T. Keith, M.A. Al-Laham, C.Y. Peng, A. Nanayakkara, C. Gonzalez, M. Challacombe, P.M.W. Gill, B. Johnson, W. Chen, M.W. Wong, J.L. Andres, C. Gonzalez, M. Head-Gordon, E.S. Replogle, J.A. Pople, Gaussian, Inc., Pittsburgh PA, 1998.
55. *NBO Version 3.1*, E.D. Glendening, A.E. Reed, J.E. Carpenter, F. Weinhold.

56. (a) S.F. Boys, F. Bernardi, *Mol. Phys.* **1976**, *19*, 325. (b) F.B. van Duijneveldt, J.G.C.M. van Duijneveldt-van de Rijdt, J.H. van Lenthe, *Chem. Rev.* **1994**, *94*, 1873.
57. J.B. Foresman, Æ. Frisch, *Exploring Chemistry with Electronic Structure methods*, 2<sup>nd</sup> Ed., Gaussian, Inc., Pittsburgh PA, 1996.
58. V. Pällin, A. Tuulmets, K. Raie, *Main Group Met. Chem.* **2002**, *25*, 297.
59. T. Holm, *Acta Chem. Scand. B* **1983**, *37*, 797.
60. Y. Pocker, J.H. Exner, *J. Am. Chem. Soc.* **1968**, *90*, 6764.
61. I.A. Koppel, V.A. Palm, In *Advances in Linear Free Energy Relationships*, N.B. Chapman, J. Shorter, (Eds.), Plenum Press: New York, 1972, Chapt. 5.
62. C. Reichardt, In *Solvents and Solvent Effects in Organic Chemistry*, VCH: Weinheim, 1988.

## ACKNOWLEDGEMENTS

I wish to express my greatest gratitude to my supervisors Professor Ants Tuulmets and Professor Peeter Burk for their professional guidance and magnificent collaboration. Being their student was a pleasant and valuable experience.

I am very thankful to Dr. Ivo Leito for his help in obtaining the UV-Vis spectra.

I also would like to thank all my colleagues and friends in the Department of Chemistry of the University of Tartu for the helpful and warm atmosphere.

The support from the Estonian Science Foundation (Grants No. 3058, 4630 and 5196) is gratefully acknowledged.

I deeply appreciate the support of my mother Virve Tammiku, as well as the support of my husband Kristo Taul and his family.



## **PUBLICATIONS**



Reproduced with permission from *Main Group Metal Chemistry*, **2000**,  
23 (5), 301–305.  
J. Tammiku, P. Burk, A. Tuulmets, UV-VIS Spectrum of 1,10-Phenanthroline —  
Ethylmagnesium Bromide Complex. An Experimental and Computational Study.

Copyright 2000 Freund Publishing House, Ltd.

# UV-VIS SPECTRUM OF THE 1,10-PHENANTHROLINE- ETHYLMAGNESIUM BROMIDE COMPLEX. AN EXPERIMENTAL AND COMPUTATIONAL STUDY

Jaana Tammiku<sup>1</sup>, Peeter Burk<sup>2</sup> and Ants Tuulmets\*<sup>1</sup>

University of Tartu, 2 Jakobi St., Tartu 51014, Estonia  
<sup>1</sup>Institute of Organic Chemistry <sup>2</sup>Institute of Chemical Physics

## ABSTRACT

The complex of 1,10-phenanthroline (**phen**) with C<sub>2</sub>H<sub>5</sub>MgBr was studied both experimentally and computationally. The UV-VIS absorption spectra of 1,10-phenanthroline and C<sub>2</sub>H<sub>5</sub>MgBr(**phen**) were measured. Full geometry optimizations, vibrational and NBO atomic charge analyses were performed for 1,10-phenanthroline, C<sub>2</sub>H<sub>5</sub>MgBr and C<sub>2</sub>H<sub>5</sub>MgBr(**phen**) using calculations with the RHF/3-21G\* methods. The stability of the investigated complex was estimated. The absorption spectra of 1,10-phenanthroline and C<sub>2</sub>H<sub>5</sub>MgBr(**phen**) were calculated at four different levels of theory - ZINDO, CIS/6-31+G\*, TD/B3LYP/6-31+G\* and TD/BLYP/6-31+G\*. The results of the calculations were used to assign the bands in experimental spectra.

## INTRODUCTION

1,10-phenanthroline (**phen**) is a well known indicator for the titration of organomagnesium [1,2] and organolithium compounds [1]. **Phen** forms charge transfer (CT) complexes with both metal ions and metal compounds. The effect of metalation on the spectrum of **phen** [3-5] is similar to that of protonation and diprotonation [6-8]. Most of the absorption bands are red-shifted both by protonation and metal complex formation.

Some complexes of **phen** with open-shell transition-metal ions ([Fe(**phen**)<sub>3</sub>]<sup>2+</sup>) are colored [9] in contrast to those of nd<sup>10</sup> closed-shell metal ions (ZnX<sub>2</sub>(**phen**), CdX<sub>2</sub>(**phen**), X = Cl, Br, I) [10-12] where the participation of metal d-orbitals in the low-lying excited states of the complexes is thought to be insignificantly small. The complex of **phen** with a Grignard reagent is also an intensely colored CT complex, and for that reason **phen** has been used as an indicator for quantitative analysis of Grignard reagents [1,2]. However, no information is available regarding the mechanism of the action of **phen** as an indicator. Therefore, possible sources of errors can neither be predicted nor taken into account.

The absorption spectra of free **phen** [4,8,9], its mono- and diprotonated forms [8], and its complexes with the iron(II) ion [4,9] have been interpreted on the basis of the results of theoretical calculations using different semiempirical methods. The *ab initio* calculations on the energetics of the complexation of alkaline metal cations with **phen** have been presented [13]. A number of theoretical studies on the structures, the total and relative energies and other properties of Grignard reagents have been carried out using the extended Hückel MO [14] and CNDO/2 [15] methods or different *ab initio* MO calculations [16-22]. No theoretical studies regarding complexes of **phen** with the magnesium(II) ion or magnesium compounds were found in literature.

The purpose of the present study was a more detailed investigation of the complex between **phen** and C<sub>2</sub>H<sub>5</sub>MgBr as no data were found for this complex in literature. Also, the capability of different advanced computational methods to predict the UV-VIS spectra of this charge transfer complex was investigated.

## EXPERIMENTAL

Commercial 1,10-phenanthroline monohydrate (mp 108-110°C [23]) was purified by multiple recrystallization from benzene. The crystals were dried over P<sub>2</sub>O<sub>5</sub> in an exsiccator (mp 116.1°C, lit.: mp 117.0-117.5°C [24]). The purity was checked by chromatomass spectrometry.

Ethylmagnesium bromide was prepared in diethyl ether by the standard method [25]. The complex C<sub>2</sub>H<sub>5</sub>MgBr(**phen**) was obtained by dissolving crystals of **phen** in the Grignard reagent at room temperature under the atmosphere of dry argon. The complex C<sub>2</sub>H<sub>5</sub>MgBr(**phen**) was deep red.

The absorption spectra of **phen** (in CH<sub>3</sub>CN; reference solution CH<sub>3</sub>CN) and of the complex C<sub>2</sub>H<sub>5</sub>MgBr(**phen**) (in Et<sub>2</sub>O; reference solution C<sub>2</sub>H<sub>5</sub>MgBr in Et<sub>2</sub>O) were measured at room temperature on a Perkin Elmer UV-VIS spectrometer Lambda 2S.

## CALCULATION METHODS

All calculations were carried out using the GAUSSIAN 94/98 [26] program packages.

Full geometry optimization and vibrational analysis of **phen** and C<sub>2</sub>H<sub>5</sub>MgBr were performed using the conventional restricted Hartree-Fock (RHF) calculations with the 3-21G\* basis set. All stationary points

were found to be true minima (number of imaginary frequencies,  $N_{\text{imag}} = 0$ ). The same procedure was repeated for the  $\text{C}_2\text{H}_5\text{MgBr}(\text{phen})$  complex. The stability of the complex was calculated considering the basis set superposition error (BSSE) estimated according to the counterpoise correction method of Boys and Bernardi [27]. Also, the natural bond orbital (NBO) [28] analysis was made for all the investigated species at the RHF/3-21G\* level. RHF/3-21G\* level was chosen for calculations primarily because the results for investigated systems were obtained in reasonable computational time.

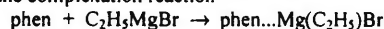
The absorption spectra of **phen** and of the complex  $\text{C}_2\text{H}_5\text{MgBr}(\text{phen})$  were calculated at four different levels of theory - ZINDO, CIS/6-31+G\*, TD/BLYP/6-31+G\* and TD/B3LYP/6-31+G\*.

## RESULTS AND DISCUSSION

### 1. Calculated geometry and properties

**Phen** has  $\text{C}_{2v}$  symmetry,  $\text{C}_2\text{H}_5\text{MgBr}$  and  $\text{C}_2\text{H}_5\text{MgBr}(\text{phen})$  possess  $\text{C}_s$  symmetry.

Energy change  $\Delta E$  for the complexation reaction



is equal to  $-40.0 \text{ kcal mol}^{-1}$  and the Gibbs free energy change  $\Delta G$  is  $-28.6 \text{ kcal mol}^{-1}$  according to our *ab initio* calculations. These fairly high values indicate strong bonding in the complex, whereas for comparison, the complexes of **phen** with alkaline metal cations have the complexation energies ( $\Delta G$ )  $-76.5$ ,  $-52.6$  and  $-33.5 \text{ kcal mol}^{-1}$  with  $\text{Li}^+$ ,  $\text{Na}^+$  and  $\text{K}^+$ , respectively (RHF/MIDI calculations) [13]. A trend in the stability of these complexes is in the order  $\text{Li}^+ > \text{Na}^+ > \text{K}^+$ , clearly depending on the radii of cations [13]. PPP calculations also indicate that  $[\text{Fe}(\text{phen})_3]^{2+}$  is stabilized by  $26.3 \text{ kcal mol}^{-1}$  relative to  $\text{Fe}^{2+}$  and free ligands [9]. However, this stabilization energy seems to be considerably underestimated. Consequently, the stability of the complex  $\text{C}_2\text{H}_5\text{MgBr}(\text{phen})$  is comparable to those for  $\text{Kphen}^+$  and  $[\text{Fe}(\text{phen})_3]^{2+}$ .

The most important geometrical parameters for the species studied are given in Table 1.

Table 1. Some geometrical parameters calculated at RHF/3-21G\* level

	$\text{C}_2\text{H}_5\text{MgBr}$	$\text{C}_2\text{H}_5\text{MgBr}(\text{phen})$
$r(\text{Mg-C})$ , Å	2.094	2.136
$r(\text{Mg-Br})$ , Å	2.316	2.404
$\angle(\text{C-Mg-Br})$	$179.21^\circ$	$135.83^\circ$

The most pronounced change upon complex formation is that in the C-Mg-Br angle. In free  $\text{C}_2\text{H}_5\text{MgBr}$  the angle is  $180^\circ$  while being bent to approximately  $130^\circ$  in the complex, indicating a strong repulsion between the substituents at the magnesium atom and the  $\pi$ -electron cloud of **phen**. Another evident change is the lengthening of Mg-Br and Mg-C bonds.

Atomic charges calculated using NBO analysis are given in Table 2.

Table 2. The NBO atomic charges calculated at RHF/3-21G\* level.

	Mg	C	Br	$\Sigma\text{H}$	N	phen
1,10-phenanthroline					-0.441	0.0
$\text{C}_2\text{H}_5\text{MgBr}$	1.488	-1.122	-0.783	1.078		
$\text{C}_2\text{H}_5\text{MgBr}(\text{phen})$	1.542	-1.116	-0.831	0.968	-0.592	0.094

The atomic charges on magnesium are high in both the investigated species, indicating that magnesium is bound to ligands primarily by ionic interaction. The natural bond orbital (NBO) analysis suggests further that the  $\text{C}_2\text{H}_5\text{MgBr}$  compound is best described as an ion-triplet consisting of positively charged  $\text{Mg}^{2+}$  and negatively charged  $\text{Br}^-$  and  $\text{C}_2\text{H}_5^-$ . Upon complex formation the charge on magnesium increases slightly (by 0.05 units), while the total charge on **phen** in the complex is 0.09. Consequently, charge transfer occurs to the ligands bonded to magnesium - primarily to the bromine atom (0.04 units) and to the hydrogens of the ethyl group (0.1 units). Negative atomic charges at the nitrogens of complexed **phen** are increased in comparison with free **phen** despite the overall positive charge of 1,10-phenanthroline. This indicates a strong polarization in **phen**. All these changes suggest an electrostatic binding between **phen** and  $\text{C}_2\text{H}_5\text{MgBr}$  (an ion-dipole or dipole-dipole interaction).

### 2. Absorption spectrum of 1,10-phenanthroline

The absorption spectrum of **phen** (in  $\text{CH}_3\text{CN}$ , Fig. 1) is similar to those given in literature [4-10,24,29,30]. There are some weak bands at 330, 322 and  $\sim 308 \text{ nm}$ , a band of medium intensity in the region 274-286 nm, the two most intense bands being at 262 and 230 nm with a shoulder and a band of

medium intensity at 196 nm in the experimental UV spectra. The last one was not described in literature because the earlier studies were performed decades ago with a limited measurement region.

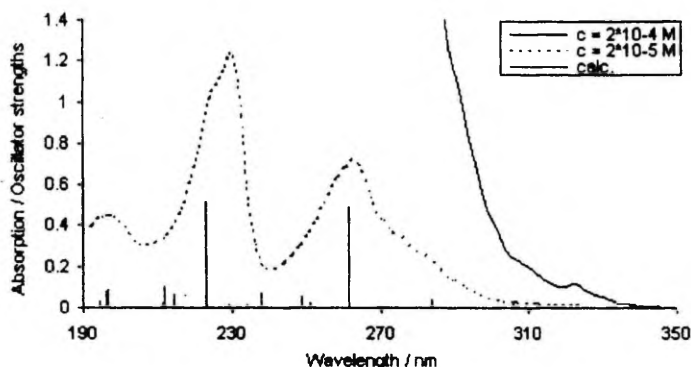


Figure 1. Experimental and calculated (TD/BLYP/6-31+G\*) absorption spectra of 1,10-phenanthroline.

The absorption bands of **phen** have been classified in different ways in literature [5,7,29,30]. No 0-0 band ( $29300\text{ cm}^{-1}$  [5],  $29500\text{ cm}^{-1}$  [29]) which is of very weak intensity, was identified in our experiment. The strong band at 262 nm is assumed to be due to  $\pi\text{-}\pi^*$  transition. No evidence has been found for  $n\text{-}\pi^*$  transitions in the absorption spectrum of **phen**. This conclusion has been based on the absence of the solvent effect with a variation of solvent polarity [9,31].

The computational methods used in this work are more sophisticated than those used earlier for the calculations of the absorption spectrum of **phen** [4,8,9]. Besides, we exploited the opportunity to test the suitability of the methods.

Comparison of experimental and calculated spectra (Table 3) indicates that the best match was obtained using excitation energies calculated by the DFT TD/BLYP/6-31+G\* method, the excitation energies being in error by 0.02, 0.17 and 0.01 eV, respectively (Fig. 1).

Our calculations also confirm the conclusion that all observed bands in the spectrum of **phen** correspond to  $\pi\text{-}\pi^*$  transitions. No  $n\text{-}\pi^*$  transitions with noteworthy intensity were found.

Table 3. Experimental and calculated excitation energies (nm and eV) and symmetry of bands.

	exptl		ZINDO			CIS/6-31+G*			TD/B3LYP/6-31+G*			TD/BLYP/6-31+G*		
	nm	eV	nm	eV	sym	nm	eV	sym	nm	eV	sym	nm	eV	sym
1	262	4.73	267	4.64	B <sub>2</sub>	204	6.07	B <sub>2</sub>	243	5.10	B <sub>2</sub>	261	4.75	B <sub>2</sub>
	230	5.39	226	5.47	B <sub>2</sub>	181	6.85	B <sub>2</sub>	222	5.58	A <sub>1</sub>	222	5.56	B <sub>2</sub>
			226	5.49	A <sub>1</sub>	179	6.91	A <sub>1</sub>	217	5.69	B <sub>2</sub>			
	196	6.33	188	6.58	A <sub>1</sub>	181	6.85	B <sub>2</sub>	203	6.09	A <sub>1</sub>	196	6.31	B <sub>2</sub>
180			6.87	B <sub>2</sub>	179	6.91	A <sub>1</sub>	201	6.16	B <sub>2</sub>	196	6.32	A <sub>1</sub>	
2	522	2.38	610	2.03	A'	208	5.94	-	446	2.77	A'	639	1.94	A'
	440	2.82	523	2.37	A''	179	6.91	-	358	3.46	A''	488	2.54	A''
	392	3.16	450	2.75	A'	177	6.98	-	339	3.66	A'	437	2.83	A'
	316	3.92	374	3.31	A''	175	7.05	-	283	4.38	A''	310	4.00	A''
							171	7.25	-					

1 – 1,10-phenanthroline

2 – C<sub>2</sub>H<sub>5</sub>MgBr(phen)

### 3. Absorption spectrum of the complex C<sub>2</sub>H<sub>5</sub>MgBr(phen)

The absorption spectra of Grignard reagents (CH<sub>3</sub>MgBr [32,33] and C<sub>2</sub>H<sub>5</sub>MgCl [32]) lie in the UV region similarly to the spectrum of Mg(phen)<sup>2+</sup> [3]. The absorption spectrum of the complex

$C_2H_5MgBr(phen)$  is essentially different from that of **phen** as shown in Fig. 2. The absorption maxima emerge at much longer wavelengths compared to **phen**: at 522, 440, ~414, 392 and 316 nm.

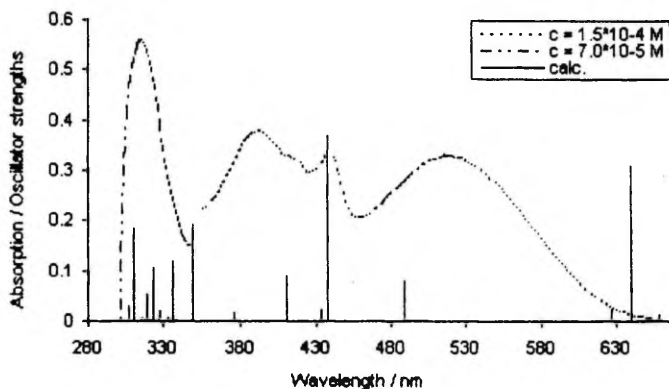


Figure 2. Experimental and calculated (TD/BLYP/6-31+G) absorption spectra of  $C_2H_5MgBr(phen)$ .

Comparison of experimental and calculated spectra (Table 3) indicates that the results obtained at TD/BLYP/6-31+G\* and TD/B3LYP/6-31+G\* levels of theory are in much better agreement with the experiment than those obtained by CIS/6-31+G\* and ZINDO. The errors in transition energies are below 0.5 eV for TD/BLYP/6-31+G\* and 0.7 eV for TD/B3LYP/6-31+G\*. This allowed us to use the TD/BLYP/6-31+G\* results for the interpretation of spectral bands similarly to the case of **phen**.

It should also be taken into account that our calculations refer to the isolated molecules and complexes in the gas phase while the experimental spectra are recorded in the solution where the solvent effects can considerably affect the positions of bands, particularly for CT complexes, where considerable changes in dipole moments upon excitation are expected.

The first most intense band at 522 nm in the experimental spectrum corresponds to the charge transfer from  $C_2H_5MgBr$  to **phen** and is responsible for the deep red colour of the complex. CT bands are always flat and have been assigned to a considerable change in the dipole moment. An inspection of the participating MO-s indicates that excitation occurs mostly from the bromine lone pair orbital to the  $\pi$  system of **phen**. This transition can thus be classified as an  $n-\pi^*$  transition.

The next band at 440 nm also corresponds to the charge transfer from  $C_2H_5MgBr$  to **phen**. Here excitation occurs from the C-Mg bonding orbital to the  $\pi$  system of **phen**. As the C-Mg bonding orbital is located primarily on the carbon atom (the C-Mg bond is essentially ionic), the corresponding transition can also be classified as an  $n-\pi^*$  transition.

The third band at 392 nm is also a CT band as the transition occurs from the Br-Mg bond to the  $\pi^*$  type MO of **phen**. The Br-Mg bond is ionic (as is the C-Mg bond), the corresponding MO is located mainly on bromine, and similarly to the previous excitation, we classify the band as an  $n-\pi^*$ . The fourth band at 316 nm can be attributed to the  $\pi-\pi^*$  transitions in the  $\pi$  system of **phen**. This band corresponds to 305 nm in the spectrum of **phen** according to our TD/BLYP/6-31+G\* calculations.

## CONCLUSIONS

The complex  $C_2H_5MgBr(phen)$  is stable according to our *ab initio* calculations ( $\Delta G = -28.6$  kcal  $mol^{-1}$ ), the stability of the complex being directly related to the atomic charge at the magnesium atom. Bonding of ligands to the magnesium atom in  $C_2H_5MgBr$  was found to be mainly ionic and the bonding between  $C_2H_5MgBr$  and **phen** was found to be electrostatic according to our *ab initio* calculations.

We noticed a new band at 196 nm in the absorption spectrum of **phen**.

Our *ab initio* and DFT calculations confirm the conclusion that all observed intensive bands in the absorption spectrum of **phen** correspond to  $\pi-\pi^*$  transitions. No  $n-\pi^*$  transitions of noteworthy oscillator strength were found. The theoretical spectra of **phen** calculated by semiempirical ZINDO, DFT TD/BLYP/6-31+G\* and *ab initio* CIS/6-31+G\* methods have a pattern similar to the experimental spectrum.

The experimentally measured CT complex  $C_2H_5MgBr(phen)$  has absorption maxima at 522, 440, 392 and 316 nm. The first three bands can be classified as  $n-\pi^*$  transitions and the last one as an  $\pi-\pi^*$  transition.

The CIS/6-31+G\* method is not appropriate for calculation of the spectra of CT complexes. The results of DFT methods (TD/B3LYP/6-31+G\* and TD/BLYP/6-31+G\*) are much better for the interpretation of the spectral bands.

#### ACKNOWLEDGEMENT

This work was supported by Estonian Science Foundation (Grant No. 3058).

#### REFERENCES

1. S. C. Watson, J. F. Eastham, *J. Organomet. Chem.*, 1967, 9, 165.
2. H.-S. Lin, L. A. Paquette, *Synth. Commun.*, 1994, 24, 2503.
3. K. Sone, P. Krumholz, H. Stammreich, *J. Am. Chem. Soc.*, 1955, 77, 777.
4. N. Sanders, P. Day, *J. Chem. Soc. A*, 1970, 1190.
5. T. Ohno, S. Kato, *Bull. Chem. Soc. Jpn.*, 1974, 47, 2953.
6. R. H. Linnell, A. Kaczmarczyk, *J. Phys. Chem.*, 1961, 65, 1196.
7. R. G. Bray, J. Ferguson, C. J. Hawkins, *Aust. J. Chem.*, 1969, 22, 2091.
8. M. Berndt, W. Woznicki, *Acta Phys. Polon.*, 1973, A43, 101.
9. T. Ito, N. Tanaka, I. Hanazaki, S. Nagakura, *Bull. Chem. Soc. Jpn.*, 1969, 42, 702.
10. S. Ikeda, S. Kimachi, T. Azumi, *J. Phys. Chem.*, 1996, 100, 10528.
11. S. Ikeda, S. Yamamoto, T. Azumi, G. A. Crosby, *J. Phys. Chem.*, 1992, 96, 6593.
12. S. Kimachi, S. Ikeda, T. Azumi, *J. Phys. Chem.*, 1995, 99, 7242.
13. C. G. Sanchez, E. P. M. Leiva, S. A. Dassie, A. M. Baruzzi, *J. Electroanal. Chem.*, 1998, 451, 111.
14. K. Ohkubo, F. Watanabe, *Bull. Chem. Soc. Jpn.*, 1971, 44, 2867.
15. H. Kato, S. Tsuruya, *Bull. Chem. Soc. Jpn.*, 1973, 46, 1001.
16. M. A. Ratner, J. W. Moskowitz, S. Topiol, *J. Am. Chem. Soc.*, 1978, 100, 2329.
17. S. Sakai, K. D. Jordan, *J. Am. Chem. Soc.*, 1982, 104, 4019.
18. P. G. Jasien, C. E. Dykstra, *J. Am. Chem. Soc.*, 1983, 105, 2089.
19. P. G. Jasien, C. E. Dykstra, *J. Am. Chem. Soc.*, 1985, 107, 1891.
20. S. R. Davis, *J. Am. Chem. Soc.*, 1991, 113, 4145.
21. A. V. Nemukhin, I. A. Topol, F. Weinhold, *Inorg. Chem.*, 1995, 34, 2980.
22. V. N. Solov'ev, G. B. Sergeev, A. V. Nemukhin, S. K. Burt, I. A. Topol, *J. Phys. Chem.*, 1997, 101, 8625.
23. A. I. Vogel, *A Text-book of Practical Organic Chemistry Including Organic Qualitative Organic Analyses*, 3<sup>rd</sup> Ed., London, 1956, 992.
24. H. H. Perkampus, *UV-VIS Atlas of Organic Compounds*, 2<sup>nd</sup> Ed., Part 2, Weinheim-New York-Basel-Cambridge, 1992, 1005.
25. A. I. Vogel, *Vogel's Textbook of Practical Organic Chemistry*, 5<sup>th</sup> Ed., London, 1994, 531.
26. Gaussian 98, Revision A.7, M. J. Frisch, G. W. Trucks, H. B. Schlegel, G. E. Scuseria, M. A. Robb, J. R. Cheeseman, V. G. Zakrzewski, J. A. Montgomery, Jr., R. E. Stratmann, J. C. Burant, S. Dapprich, J. M. Millam, A. D. Daniels, K. N. Kudin, M. C. Strain, O. Farkas, J. Tomasi, V. Barone, M. Cossi, R. Cammi, B. Mennucci, C. Pomelli, C. Adamo, S. Clifford, J. Ochterski, G. A. Petersson, P. Y. Ayala, Q. Cui, K. Morokuma, D. K. Malick, A. D. Rabuck, K. Raghavachari, J. B. Foresman, J. Cioslowski, J. V. Ortiz, A. G. Baboul, B. B. Stefanov, G. Liu, A. Liashenko, P. Piskorz, I. Komaromi, R. Gomperts, R. L. Martin, D. J. Fox, T. Keith, M. A. Al-Laham, C. Y. Peng, A. Nanayakkara, C. Gonzalez, M. Challacombe, P. M. W. Gill, B. Johnson, W. Chen, M. W. Wong, J. L. Andres, C. Gonzalez, M. Head-Gordon, E. S. Replogle, and J. A. Pople, Gaussian, Inc., Pittsburgh PA, 1998.
27. S. F. Boys, F. Bernardi, *Mol. Phys.*, 1976, 19, 325.
28. NBO Version 3.1, E. D. Glendening, A. E. Reed, J. E. Carpenter, F. Weinhold.
29. H. Gropper, F. Dörr, *Ber. Bunsen-Ges. Phys. Chem.*, 1963, 67, 46.
30. M. Yamada, M. Kimura, M. Nishizawa, S. Kuroda, I. Shima, *Bull. Chem. Soc. Jpn.*, 1991, 64, 1821.
31. G. M. Badger, I. S. Walker, *J. Chem. Soc.*, 1956, 122.
32. W. T. Ford, *J. Organomet. Chem.*, 1971, 32, 27.
33. Y. Imizu, K. J. Klabunde, *Inorg. Chem.*, 1984, 23, 3602.

Received: March 14, 2000 - Accepted: March 27, 2000 -  
Accepted in revised camera-ready format: March 31, 2000





Reproduced with permission from *Journal of Physical Chemistry A*, **2001**,  
105 (37), 8554–8561.

J. Tammiku, P. Burk, A. Tuulmets, 1,10-Phenanthroline and Its Complexes with  
Magnesium Compounds. Disproportionation Equilibria.

Copyright 2001 American Chemical Society

# 1,10-Phenanthroline and Its Complexes with Magnesium Compounds. Disproportionation Equilibria

Jaana Tammiku,<sup>†</sup> Peeter Burk,<sup>\*\*‡</sup> and Ants Tuulmets<sup>†</sup>

*Institute of Organic Chemistry, and Institute of Chemical Physics, University of Tartu, 2 Jakobi St., Tartu 51014, Estonia*

*Received: April 18, 2001; In Final Form: June 28, 2001*

The solvation, complexation, and disproportionation equilibria, which might be important during titration of a Grignard reagent RMgX with an alcohol in the presence of 1,10-phenanthroline (phen), have been studied both in the gas phase and solution using the density functional theory (DFT) B3LYP/6-31+G\* method. Solvation was modeled using the supermolecule approach. NBO atomic charge analyses were performed at the B3LYP/6-31G\* level. The absorption spectra of the complexes were calculated by the DFT TD/MPW1PW91/6-311+G\*\* method. According to our calculations the complexation of magnesium halide MgX<sub>2</sub> with 1,10-phenanthroline is the reason for the disappearance of the red color of the complex RMgX(phen) near the titration end point.

## 1. Introduction

Grignard reagents RMgX (X = halogen) have been known for more than hundred years<sup>1</sup> and have found widespread applications in organic synthesis.<sup>2,3</sup> One of the simplest methods for determination of a Grignard reagent concentration is the titration of its solution with *s*-butanol<sup>4</sup> in the presence of 1,10-phenanthroline (phen) as an indicator. This method yields the Grignard reagent concentration with ordinary volumetric precision.

Phen is thought to form simple reversibly coordinated 1:1 charge transfer (CT) complexes<sup>4</sup> with organomagnesium compounds such as RMgX and R<sub>2</sub>Mg.<sup>5,6</sup> There is, however, some controversy about the color of a Grignard reagent complex with phen in the literature. So, Lindsell<sup>2</sup> mentions the violet-green color of the complex, while other works<sup>5,7</sup> indicate that the complex should be red or burgundy. Our experimental work<sup>8</sup> also evidenced that the complex between a Grignard reagent and phen has deep red color. The measured absorption spectrum<sup>8</sup> of the complex C<sub>2</sub>H<sub>5</sub>MgBr(phen) had intense absorption maxima at 522, 440, and 392 nm corresponding to the n-π\* excitations in the CT complex, and at 316 nm corresponding to a π-π\* transition in the π-system of phen. However, it is known that R<sub>2</sub>Mg also forms colored complexes with phen.<sup>4-6</sup> To the best of our knowledge, no information is available regarding the processes which take place during titration of a Grignard reagent with an alcohol in the presence of phen and the reasons for the disappearance of the color of the solution near the titration end point. It can be assumed that an alkoxy-magnesium halide which forms during the titration reaction



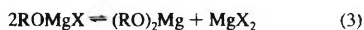
either does not form the complex with phen or the complex is colorless.

It should be also remembered that in solution Grignard reagents do not have a simple constitution but exist as an equilibrium mixture which may involve various solvated components. The primary equilibrium, known generally as the Schlenk equilibrium,<sup>9</sup> is the dismutation process, expressed simply by eq 2:



It is well-known that the Schlenk equilibrium depends on the solvent<sup>2,3</sup> but the dependence on the concentration of the solution is still unclear. As a rule the Schlenk equilibrium is shifted toward the formation of RMgX in diethyl ether.<sup>2,3</sup> In the case of THF the equilibrium is more shifted toward the formation of R<sub>2</sub>Mg and MgX<sub>2</sub> because of better solvation of the magnesium halide.<sup>2,3</sup>

Similar equilibrium reactions can take place in case of alkoxy-magnesium halide (i.e., the product of titration reaction):



As a result, the constitution of the titration mixture at the titration end point is not evident.

A number of theoretical studies on the structures, energies, atomic charges, mechanism of formation reaction, and other properties of Grignard reagents have been carried out using different ab initio calculations based on the Hartree-Fock (HF) method, the Møller-Plesset (MP) perturbation theory, the coupled cluster (CC) method, etc., and also the density functional theory (DFT).<sup>10-19</sup> To our knowledge the disproportionation equilibria of Grignard reagents have been investigated only by semiempirical calculations using the extended Hückel MO<sup>20</sup> and CNDO/2<sup>21</sup> methods.

In the current work we investigated the solvation, complexation, and disproportionation equilibria, which might take place during titration of a Grignard reagent with an alcohol in the presence of phen, by means of DFT calculations. The influence of solvent on these above-mentioned equilibria was also modeled. We also calculated (by TD-DFT method) the absorption spectra of all possible complexes of phen to clarify the

\* Corresponding author.

<sup>†</sup> Institute of Organic Chemistry.

<sup>‡</sup> Institute of Chemical Physics.

reasons for the disappearance of the red color of the solution near the titration end point.

## 2. Calculation Methods

All calculations were carried out using the GAUSSIAN 98<sup>22</sup> program package.

We investigated the disproportionation equilibria (the Schlenk equilibria) according to eqs 2 and 3 ( $R = CH_3$  and  $X = Cl, Br$ ) and complexation equilibria of all formed species with **phen**.

Optimizations and vibrational analysis were done using the density functional theory (DFT) with hybrid B3LYP functional and the 6-31+G\* basis set. All stationary points were found to be true minima (number of imaginary frequencies,  $N_{\text{imag}} = 0$ ). The calculated frequencies were also used for calculations of enthalpies and Gibbs free energies. The stability of the complexes of **phen** was calculated considering the basis set superposition error (BSSE) estimated according to the counterpoise correction method of Boys and Bernardi.<sup>23</sup>

Solvation was modeled using the supermolecule approach. Up to two molecules of dimethyl ether were added to the studied species. The basis set superposition error was taken into account here too. The BSSE had a particularly strong influence on both the complexation and solvation energies of the bromine containing compounds compared to the corresponding chlorine compounds.

Also, the natural bond orbital (NBO)<sup>24</sup> analysis was performed for all the investigated species at the B3LYP/6-31G\* level.

The absorption spectra of **phen** and its complexes with the studied magnesium compounds were calculated by the time-dependent density functional theory (TD-DFT) using hybrid MPW1PW91 density functional with the 6-311+G\*\* basis set. The DFT TD/MPW1PW91/6-311+G\*\* method has been found to give excitation energies in satisfactory agreement with experiment.<sup>25</sup>

## 3. Results and Discussion

**3.1. Calculated Absorption Spectra for Complexes of 1,10-Phenanthroline with  $CH_3MgCl$ ,  $CH_3OMgCl$  and Corresponding Disproportionation Products.** Calculated absorption spectra are given in Figure 1. Corresponding excitation energies and oscillator strengths are given in Table 1. The measured absorption spectrum of **phen**<sup>8</sup> (in  $CH_3CN$ ) had some weak bands at 330, 322, and 308 nm, a band of medium intensity in the region 274–286 nm, the two most intense bands at 262 and 230 nm with a shoulder, and a band of medium intensity at 196 nm. Comparison of experimental<sup>8</sup> and calculated spectra of **phen** (Table 1) indicates that the calculated excitation energies are shifted to shorter wavelengths (hypsochromic shift). Despite the fact that the calculated spectrum of  $CH_3MgCl(\text{phen})$  complex (Table 1) does not have a good correlation with the experimentally measured absorption spectrum<sup>8</sup> of  $C_2H_5MgBr(\text{phen})$  complex (see Introduction), the calculations still clearly predict the absorption in the visible region. The absorption of light by the complex  $(CH_3)_2Mg(\text{phen})$  (Table 1) also occurs in the visible region according to our calculations, in a good agreement with experimental data.<sup>5,6</sup> No information was found in the literature regarding the absorption spectrum of the  $(RO)_2Mg(\text{phen})$  complex.

So, our results indicate that all complexes of **phen** with alkyl- and alkoxy-magnesium compounds have intense absorption maxima in the visible region (Figure 1b–e). Thus, the disappearance of the color at the equivalence point of titration of a

**TABLE 1: Calculated Excitation Energies (nm) and Oscillator Strengths for 1,10-Phenanthroline and Its Complexes with Magnesium Compounds at DFT TD/MPW1PW91/6-311+G\*\* Level of Theory**

	nm	osc. strengths	
1,10-phenanthroline	275	0.0396	
	248	0.0768	
	240	0.7192	
	217	0.1567	
	214	0.3510	
	196	0.1557	
	195	0.0930	
	192	0.0519	
	179	0.1735	
	$CH_3MgCl(\text{phen})$	588	0.0187
386		0.0153	
309		0.0095	
301		0.0039	
294		0.0062	
286		0.0066	
273		0.0057	
271		0.0275	
$CH_3OMgCl(\text{phen})$		562	0.0041
		374	0.0103
	308	0.0071	
	296	0.0029	
	294	0.0093	
	291	0.0082	
	290	0.0042	
	$(CH_3)_2Mg(\text{phen})$	743	0.0558
		736	0.0042
		519	0.0172
439		0.0052	
349		0.0044	
318		0.0193	
289		0.0500	
287		0.0172	
$(CH_3O)_2Mg(\text{phen})$		273	0.0218
		606	0.0096
	529	0.0025	
	369	0.0028	
	305	0.0047	
	302	0.0065	
	$MgCl_2(\text{phen})$	378	0.0120
		361	0.0045
		312	0.0162
		297	0.0089
294		0.0116	
278		0.0043	
268	0.0076		

Grignard reagent with an alcohol in the presence of **phen** cannot be attributed to the formation of the complex between  $ROMgX$  and **phen** as the complex should be also colored according to our calculations.

The complex of **phen** with magnesium halide (Figure 1f) is the only one without absorption in the visible region. This leads to the necessity to investigate the Schlenk equilibrium (eq 2) as an alkoxy complex which forms during titration of a Grignard reagent with an alcohol can disproportionate according to the Schlenk equilibrium (eq 3).

**3.2. Solvation Equilibria.** The calculated solvation energies of studied species with one or two dimethyl ether molecules are given in Table 2. The geometries of mono- and disolvated species are shown in Figures 2 and 3. The tricoordinated magnesium is planar in the monosolvated complexes while the tetracoordinated magnesium forms with its ligands a deformed tetrahedron in the disolvated complexes, in accordance with the crystallographic data.<sup>26</sup> The solvation reaction is exothermic for all the studied species. The chlorine compounds are somewhat more strongly solvated than the corresponding bromine compounds. The solvation energies (with both one and two solvent

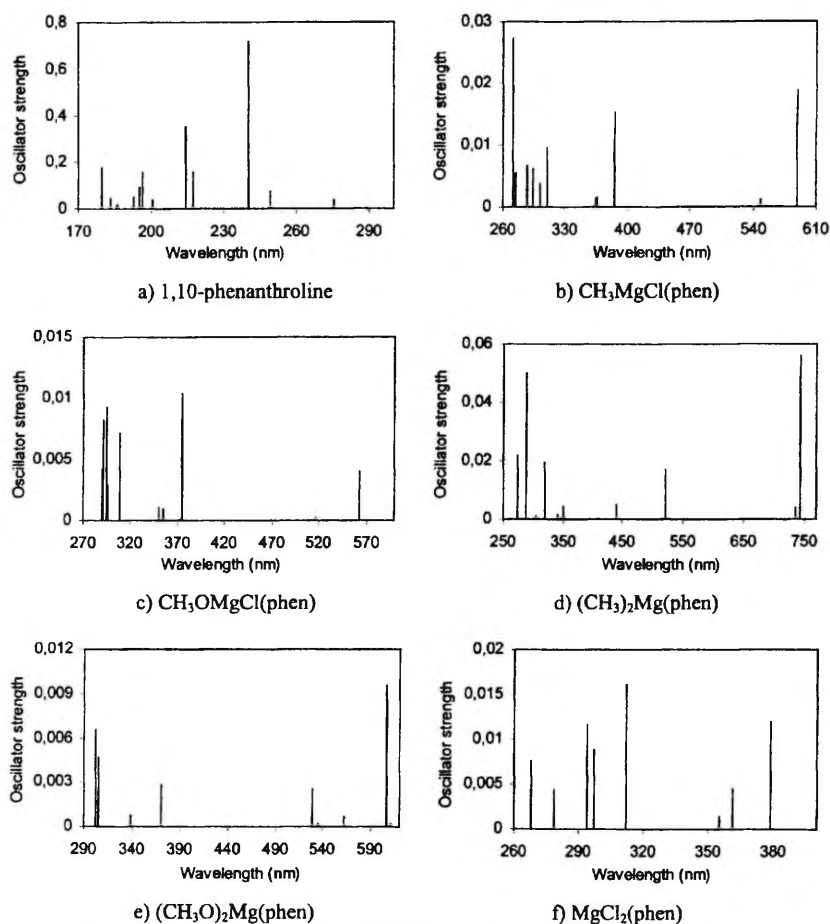


Figure 1. Calculated (at TD/MPW1PW91/6-311+G\*\* level of theory) absorption spectra of (a) 1,10-phenanthroline, (b)  $\text{CH}_3\text{MgCl}(\text{phen})$ , (c)  $\text{CH}_3\text{OMgCl}(\text{phen})$ , (d)  $(\text{CH}_3)_2\text{Mg}(\text{phen})$ , (e)  $(\text{CH}_3\text{O})_2\text{Mg}(\text{phen})$ , and (f)  $\text{MgCl}_2(\text{phen})$ .

TABLE 2: The Solvation Energies ( $\Delta E$ , contains zero-point vibrational energy (ZPVE) correction), Enthalpies ( $\Delta H$ ), and Gibbs Free Energies ( $\Delta G$ ) of Magnesium Compounds with One or Two Dimethyl Ether Molecules at B3LYP/6-31+G\* Level (All values are given in kcal/mol and are corrected for basis set superposition error (BSSE).)

Z	Z + n(CH <sub>3</sub> ) <sub>2</sub> O → Z·n(CH <sub>3</sub> ) <sub>2</sub> O					
	$\Delta E$		$\Delta H$		$\Delta G$	
	n = 1	n = 2	n = 1	n = 2	n = 1	n = 2
MgCl <sub>2</sub>	-23.0	-39.3	-23.0	-39.1	-13.8	-20.1
MgBr <sub>2</sub>	-19.2	-34.1	-19.3	-33.8	-9.7	-13.8
CH <sub>3</sub> MgCl	-16.7	-28.4	-16.5	-27.9	-6.9	-8.2
CH <sub>3</sub> MgBr	-14.8	-25.8	-14.6	-25.3	-5.2	-5.5
CH <sub>3</sub> OMgCl	-21.4	-36.4	-21.4	-35.9	-11.3	-15.6
CH <sub>3</sub> OMgBr	-20.1	-34.4	-20.0	-33.9	-9.8	-13.6
(CH <sub>3</sub> ) <sub>2</sub> Mg	-11.7	-19.5	-11.1	-18.5	-3.2	-0.4
(CH <sub>3</sub> O) <sub>2</sub> Mg	-20.2	-33.4	-20.2	-33.0	-10.6	-12.9

molecules) are higher for magnesium halides ( $\Delta H_1 = -23.0\dots-19.3$  and  $\Delta H_2 = -39.1\dots-33.8$  kcal/mol, respectively) and

TABLE 3: The Complexation Energies ( $\Delta E$ , contains zero-point vibrational energy (ZPVE) correction), Enthalpies ( $\Delta H$ ), and Gibbs Free Energies ( $\Delta G$ ) at B3LYP/6-31+G\* Level (All values are given in kcal/mol and are corrected for basis set superposition error (BSSE).)

Z	Z + phen → Z(phen)		
	$\Delta E$	$\Delta H$	$\Delta G$
MgCl <sub>2</sub>	-43.9	-43.9	-33.6
MgBr <sub>2</sub>	-39.9	-39.8	-29.3
CH <sub>3</sub> MgCl	-33.0	-32.6	-22.9
CH <sub>3</sub> MgBr	-31.8	-31.2	-21.9
CH <sub>3</sub> OMgCl	-38.6	-38.4	-28.6
CH <sub>3</sub> OMgBr	-36.9	-36.6	-26.1
(CH <sub>3</sub> ) <sub>2</sub> Mg	-24.5	-23.7	-15.2
(CH <sub>3</sub> O) <sub>2</sub> Mg	-34.0	-33.7	-23.7

methoxy compounds ( $\Delta H_1 = -21.4\dots-20.0$  and  $\Delta H_2 = -35.9\dots-33.0$  kcal/mol, respectively). This can evidently be related to a lesser steric hindrance to the interaction between the magnesium atom and the oxygen atom(s) of the solvent.

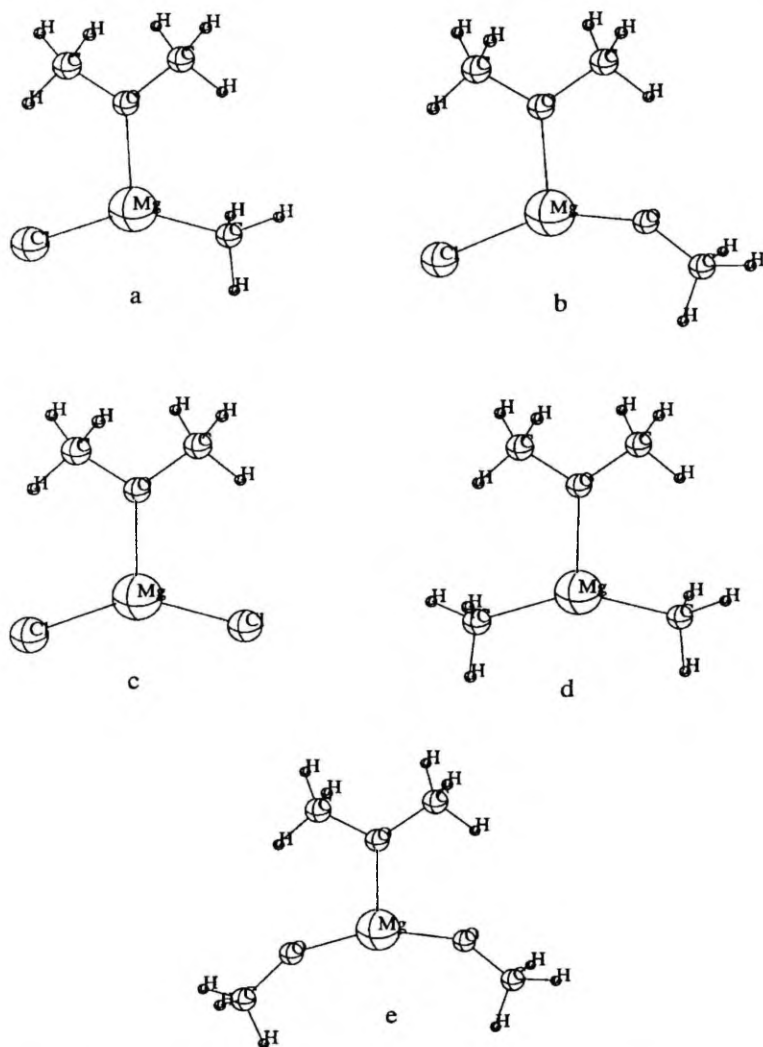


Figure 2. The optimized (at B3LYP/6-31+G\* level of theory) structures of monosolvated (a)  $\text{CH}_3\text{MgCl}$ , (b)  $\text{CH}_3\text{OMgCl}$ , (c)  $\text{MgCl}_2$ , (d)  $(\text{CH}_3)_2\text{Mg}$ , and (e)  $(\text{CH}_3\text{O})_2\text{Mg}$ .

The distances between the magnesium atom and the oxygen atom(s) of the solvent are 2.050–2.059 Å in the monosolvated and 2.094–2.099 Å in the disolvated magnesium halides, and 2.043–2.049 Å in the monosolvated and 2.095–2.097 Å in the disolvated methoxy compounds. Another possible reason (besides steric consideration) for higher solvation energies of magnesium halides and methoxy compounds is the higher positive charge on the metal atom in these species. The atomic (NBO) charge on magnesium is the highest in  $(\text{CH}_3\text{O})_2\text{Mg}$  for all cases (+1.727 in the unsolvated, +1.702 in the monosolvated, and +1.716 in the disolvated compound). The atomic

charges on magnesium are somewhat greater in the chlorine compounds compared to the corresponding bromine compounds (see Table 5). In accordance with a hypothesis that the solvation energy is determined by the charge on magnesium atom and the steric hindrance to the interaction of the solvent and metal atom (the bulkiness of ligands), the solvation energy is the lowest ( $\Delta H_1 = -11.1$  and  $\Delta H_2 = -18.5$  kcal/mol, respectively) in case of  $(\text{CH}_3)_2\text{Mg}$  which is sterically the most crowded with two relatively bulky methyl groups directly bound to the magnesium atom, and has the smallest atomic charge on magnesium (+1.370 in the unsolvated, +1.454 in the mono-

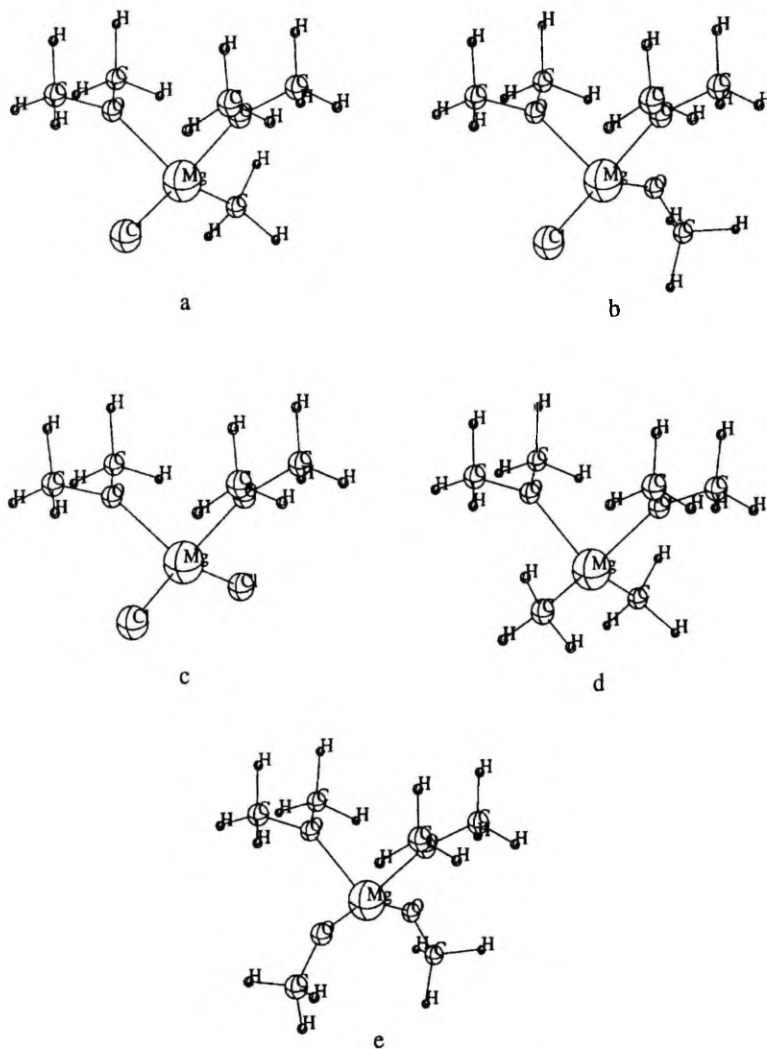
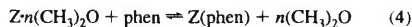


Figure 3. The optimized (at B3LYP/6-31+G\* level of theory) structures of disolvated (a)  $\text{CH}_3\text{MgCl}$ , (b)  $\text{CH}_3\text{OMgCl}$ , (c)  $\text{MgCl}_2$ , (d)  $(\text{CH}_3)_2\text{Mg}$ , and (e)  $(\text{CH}_3\text{O})_2\text{Mg}$ .

solvated, +1.517 in the disolvated compound, see Table 5). The distances between the magnesium atom and the oxygen atom(s) of the solvent is 2.147 Å in the monosolvated and 2.196 Å in the disolvated compound. The solvation energies with both one and two solvent molecules and the above-mentioned bond lengths stay between the two extremes in case of methylmagnesium halides ( $\Delta H_1 = -16.5 \dots -14.6$  kcal/mol,  $r_1 = 2.097 - 2.105$  Å, and  $\Delta H_2 = -27.9 \dots -25.3$  kcal/mol,  $r_2 = 2.137 - 2.145$  Å, respectively).

**3.3. The Complexation Energies.** The complexation energies of studied molecules (unsolvated, mono-, and disolvated) with

**phen** were calculated from eq 4 where  $Z = \text{MgX}_2$ ,  $\text{CH}_3\text{MgX}$ ,  $\text{CH}_3\text{OMgX}$ ,  $(\text{CH}_3)_2\text{Mg}$ , and  $(\text{CH}_3\text{O})_2\text{Mg}$ , and the number of solvent molecule(s)  $n = 0, 1$ , and 2.



The results are given in Tables 3 and 4. For the unsolvated (gas-phase) species the complexes of **phen** with magnesium halides are the most stable ( $\Delta H = -43.9 \dots -39.8$  kcal/mol). This is apparently due to the fact that two electronegative halogen atoms withdraw larger amount of the electron density

**TABLE 4: The Complexation Energies ( $\Delta E$ , contains zero-point vibrational energy (ZPVE) correction), Enthalpies ( $\Delta H$ ), and Gibbs Free Energies ( $\Delta G$ ) of Mono- and Disolvated Species at B3LYP/6-31+G\* Level (All values are given in kcal/mol and are corrected for basis set superposition error (BSSE).)**

Z	Z·n(CH <sub>3</sub> ) <sub>2</sub> O + phen → Z(phen) + n(CH <sub>3</sub> ) <sub>2</sub> O					
	$\Delta E$		$\Delta H$		$\Delta G$	
	n = 1	n = 2	n = 1	n = 2	n = 1	n = 2
MgCl <sub>2</sub>	-20.8	-4.5	-20.8	-4.8	-19.8	-13.5
MgBr <sub>2</sub>	-20.7	-5.8	-20.5	-6.0	-19.6	-15.4
CH <sub>3</sub> MgCl	-16.3	-4.6	-16.1	-4.7	-16.0	-14.7
CH <sub>3</sub> MgBr	-17.0	-6.0	-16.6	-5.9	-16.7	-16.4
CH <sub>3</sub> OMgCl	-17.2	-2.2	-17.1	-2.5	-17.4	-13.1
CH <sub>3</sub> OMgBr	-16.7	-2.5	-16.6	-2.7	-16.3	-12.5
(CH <sub>3</sub> ) <sub>2</sub> Mg	-12.9	-5.1	-12.7	-5.2	-12.0	-14.8
(CH <sub>3</sub> O) <sub>2</sub> Mg	-13.8	-0.6	-13.6	-0.7	-13.1	-10.8

from magnesium thus allowing stronger electrostatic interaction between the more positively charged magnesium and the negatively charged nitrogens of phen. The complexation energy is the lowest in case of the complex of phen with (CH<sub>3</sub>)<sub>2</sub>Mg ( $\Delta H = -23.7$  kcal/mol) which is sterically the most unfavorable and has the smallest positive charge on magnesium (+1.490).

The solvation of the magnesium compounds causes a remarkable decrease in the complexation energies as one of the reagents (magnesium compound) is stabilized by the specific solvation while the product (complex) is not solvated. The complexation energies of phen with disolvated MgCl<sub>2</sub>, CH<sub>3</sub>MgCl, and (CH<sub>3</sub>)<sub>2</sub>Mg are very close ( $\Delta H = -5.2$ ... $-4.7$  kcal/mol). The complexes of phen with MgBr<sub>2</sub> and CH<sub>3</sub>MgBr have also close stabilities relative to the disolvated magnesium compounds ( $\Delta H = -6.0$  and  $-5.9$  kcal/mol, respectively). However, the stabilities of those bromine-containing complexes are somewhat higher than

that of (CH<sub>3</sub>)<sub>2</sub>Mg. The complexes of methoxy compounds are much less stable relative the disolvated molecules ( $\Delta H = -2.5$ ... $-0.7$  kcal/mol). It should be noted that for the disolvated complexes, the values of  $\Delta G$  considerably differ from the values of  $\Delta E$  and  $\Delta H$ , thus indicating a significant contribution of entropy.

**3.4. Disproportionation (Schlenk) Equilibria.** The calculated energies for disproportionation equilibria are given in Table 6. The Schlenk equilibrium is shifted toward the formation of CH<sub>3</sub>MgX and CH<sub>3</sub>OMgX in the gas phase according to our B3LYP/6-31+G\* calculations. The relative concentration of magnesium halides should be relatively small, especially in the case of CH<sub>3</sub>MgX as the calculated equilibrium constants from eq 5:

$$\Delta G = -RT \ln K \quad (5)$$

are  $9.6 \times 10^{-5}$  (X = Cl) and  $2.1 \times 10^{-5}$  (X = Br). In the case of CH<sub>3</sub>OMgX these values are  $9.5 \times 10^{-3}$  (X = Cl) and  $1.5 \times 10^{-2}$  (X = Br), respectively.

The solvation has a strong influence on the Schlenk equilibrium decreasing the endothermicity of disproportionation reactions 2 and 3 but still the predominant species in solution should be CH<sub>3</sub>MgX and CH<sub>3</sub>OMgX. The effect of solvation is the strongest in the case of CH<sub>3</sub>MgCl where the addition of the first solvent molecule diminishes the endothermicity of reaction 2 by 1.06 kcal/mol ( $\Delta\Delta H$ ) and the second solvent molecule has an additional 0.76 kcal/mol effect. For the other studied species the effects are smaller and in case of the alkoxy-magnesium halides the second solvent molecule even increases the endothermicity. Nevertheless, the absolute endothermicities are in all cases bigger for the alkylmagnesium halides relative to the alkoxy compounds.

**TABLE 5: The NBO Atomic Charges Calculated at the B3LYP/6-31G\* Level**

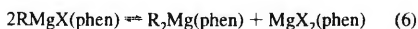
	Mg	C	Hal	$\Sigma H$	O	N	Phen
MgCl <sub>2</sub>	+1.587		-0.794				
MgBr <sub>2</sub>	+1.484		-0.742				
CH <sub>3</sub> MgCl	+1.454	-1.369	-0.804	+0.719			
CH <sub>3</sub> MgBr	+1.413	-1.371	-0.760	+0.719			
CH <sub>3</sub> OMgCl	+1.664	-0.266	-0.815	+0.560	-1.142		
CH <sub>3</sub> OMgBr	+1.617	-0.266	-0.770	+0.559	-1.139		
(CH <sub>3</sub> ) <sub>2</sub> Mg	+1.370	-1.374		+1.378			
(CH <sub>3</sub> O) <sub>2</sub> Mg	+1.727	-0.263		+1.095	-1.148		
MgCl <sub>2</sub> ·2(CH <sub>3</sub> ) <sub>2</sub> O	+1.609		-0.818				
MgBr <sub>2</sub> ·2(CH <sub>3</sub> ) <sub>2</sub> O	+1.527		-0.772				
CH <sub>3</sub> MgCl·(CH <sub>3</sub> ) <sub>2</sub> O	+1.515	-1.394	-0.824	+0.677			
CH <sub>3</sub> MgBr·(CH <sub>3</sub> ) <sub>2</sub> O	+1.482	-1.399	-0.785	+0.680			
CH <sub>3</sub> OMgCl·(CH <sub>3</sub> ) <sub>2</sub> O	+1.660	-0.268	-0.833	+0.532	-1.109		
CH <sub>3</sub> OMgBr·(CH <sub>3</sub> ) <sub>2</sub> O	+1.625	-0.269	-0.794	+0.533	-1.109		
(CH <sub>3</sub> ) <sub>2</sub> Mg·(CH <sub>3</sub> ) <sub>2</sub> O	+1.454	-1.394		+1.303			
(CH <sub>3</sub> O) <sub>2</sub> Mg·(CH <sub>3</sub> ) <sub>2</sub> O	+1.702	-0.268		+1.043	-1.111		
MgCl <sub>2</sub> ·2(CH <sub>3</sub> ) <sub>2</sub> O	+1.624		-0.831				
MgBr <sub>2</sub> ·2(CH <sub>3</sub> ) <sub>2</sub> O	+1.560		-0.795				
CH <sub>3</sub> MgCl·2(CH <sub>3</sub> ) <sub>2</sub> O	+1.561	-1.408	-0.837	+0.640			
CH <sub>3</sub> MgBr·2(CH <sub>3</sub> ) <sub>2</sub> O	+1.533	-1.405	-0.806	+0.639			
CH <sub>3</sub> OMgCl·2(CH <sub>3</sub> ) <sub>2</sub> O	+1.677	-0.269	-0.845	+0.512	-1.098		
CH <sub>3</sub> OMgBr·2(CH <sub>3</sub> ) <sub>2</sub> O	+1.648	-0.268	-0.810	+0.513	-1.096		
(CH <sub>3</sub> ) <sub>2</sub> Mg·2(CH <sub>3</sub> ) <sub>2</sub> O	+1.517	-1.401		+1.233			
(CH <sub>3</sub> O) <sub>2</sub> Mg·2(CH <sub>3</sub> ) <sub>2</sub> O	+1.716	-0.266		+1.001	-1.098		
1,10-phen						-0.415	0.000
MgCl <sub>2</sub> (phen)	+1.599		-0.836			-0.566	+0.073
MgBr <sub>2</sub> (phen)	+1.578		-0.818			-0.562	+0.058
CH <sub>3</sub> MgCl(phen)	+1.535	-1.389	-0.843	+0.639		-0.542	+0.058
CH <sub>3</sub> MgBr(phen)	+1.507	-1.394	-0.814	+0.646		-0.550	+0.056
CH <sub>3</sub> OMgCl(phen)	+1.647	-0.257	-0.849	+0.495	-1.098	-0.554	+0.061
CH <sub>3</sub> OMgBr(phen)	+1.618	-0.260	-0.818	+0.499	-1.096	-0.556	+0.057
(CH <sub>3</sub> ) <sub>2</sub> Mg(phen)	+1.490	-1.364		+1.228		-0.536	+0.010
(CH <sub>3</sub> O) <sub>2</sub> Mg(phen)	+1.684	-0.258		+0.974	-1.095	-0.548	+0.049



**TABLE 6: Energies ( $\Delta E$ , contains zero-point vibrational energy (ZPVE) correction), Enthalpies ( $\Delta H$ ), and Gibbs Free Energies ( $\Delta G$ ) for Disproportionation Equilibria of Methylmagnesium Halides and Methoxymagnesium Halides at B3LYP/6-31+G\* Level (All values are given in kcal/mol.)**

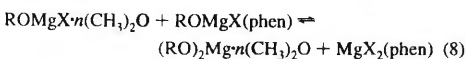
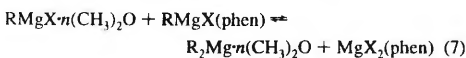
	$\Delta E$	$\Delta H$	$\Delta G$
$2RMgX \rightleftharpoons R_2Mg + MgX_2$			
CH <sub>3</sub> MgCl	5.27	5.08	6.84
CH <sub>3</sub> MgBr	5.24	5.15	6.38
CH <sub>3</sub> OMgCl	1.95	2.20	2.76
CH <sub>3</sub> OMgBr	1.58	1.90	2.47
$2[RMgX \cdot (CH_3)_2O] \rightleftharpoons R_2Mg \cdot (CH_3)_2O + MgX_2 \cdot (CH_3)_2O$			
CH <sub>3</sub> MgCl	3.89	4.02	3.70
CH <sub>3</sub> MgBr	4.52	4.54	4.48
CH <sub>3</sub> OMgCl	1.63	1.69	0.88
CH <sub>3</sub> OMgBr	2.19	2.24	1.41
$2[RMgX \cdot 2(CH_3)_2O] \rightleftharpoons R_2Mg \cdot 2(CH_3)_2O + MgX_2 \cdot 2(CH_3)_2O$			
CH <sub>3</sub> MgCl	3.14	3.26	2.70
CH <sub>3</sub> MgBr	4.51	4.54	4.40
CH <sub>3</sub> OMgCl	1.88	1.88	0.75
CH <sub>3</sub> OMgBr	2.40	2.50	2.45
$2RMgX(phen) \rightleftharpoons R_2Mg(phen) + MgX_2(phen)$			
CH <sub>3</sub> MgCl	2.76	2.76	3.83
CH <sub>3</sub> MgBr	6.05	5.64	7.33
CH <sub>3</sub> OMgCl	1.51	1.63	2.89
CH <sub>3</sub> OMgBr	1.40	1.55	1.57
$RMgX + RMgX(phen) \rightleftharpoons R_2Mg + MgX_2(phen)$			
CH <sub>3</sub> MgCl	-6.02	-6.53	-4.27
CH <sub>3</sub> MgBr	-7.55	-8.17	-5.72
CH <sub>3</sub> OMgCl	-3.26	-3.20	-2.20
CH <sub>3</sub> OMgBr	-6.65	-6.51	-5.98
$RMgX \cdot (CH_3)_2O + RMgX(phen) \rightleftharpoons R_2Mg \cdot (CH_3)_2O + MgX_2(phen)$			
CH <sub>3</sub> MgCl	-0.82	-0.82	-0.31
CH <sub>3</sub> MgBr	-2.28	-2.48	-1.54
CH <sub>3</sub> OMgCl	-1.95	-1.95	-1.51
CH <sub>3</sub> OMgBr	-5.14	-5.08	-5.27
$RMgX \cdot 2(CH_3)_2O + RMgX(phen) \rightleftharpoons R_2Mg \cdot 2(CH_3)_2O + MgX_2(phen)$			
CH <sub>3</sub> MgCl	3.33	3.33	4.02
CH <sub>3</sub> MgBr	4.22	4.01	4.86
CH <sub>3</sub> OMgCl	-0.31	-0.31	0.44
CH <sub>3</sub> OMgBr	-1.54	-1.44	-1.13

The disproportionation equilibrium should be modified if the solution contains **phen**. In case of excess (or equimolarity) of **phen** over organomagnesium compound the reaction goes as



The effect of **phen** on the equilibrium is similar to that of solvation. The reaction is less endothermic except for CH<sub>3</sub>MgBr where the influence of **phen** leads to an increase of the endothermicity by 0.49 kcal/mol ( $\Delta\Delta H$ ). The changes are the greatest for CH<sub>3</sub>MgCl where the endothermicity decreases by 2.32 kcal/mol. However, for all the studied species, the equilibrium is still shifted toward the formation of CH<sub>3</sub>MgX(phen) or CH<sub>3</sub>OMgX(phen).

In the case of titration of a Grignard reagent with an alcohol in the presence of **phen** as an indicator, there is, however, an excess of free RMgX or ROMgX in the solution and the Schlenk equilibria can be written as



The formation of disproportionation products with reversed

complexation, i.e., R<sub>2</sub>Mg(phen) and MgX<sub>2</sub>·n(CH<sub>3</sub>)<sub>2</sub>O, is energetically less favorable. The modified Schlenk equilibria (eqs 7 and 8) are shifted toward the disproportionation products in the gas phase (n = 0) and in case of the monosolvated species (n = 1) due to the stronger complex between **phen** and magnesium halide. In the case of the disolvated species which are the closest to the situation in real solution, the equilibrium is strongly (even stronger than in the absence of **phen**) shifted toward the nondisproportionated RMgX while for ROMgX the equilibrium is shifted in the opposite direction. As a result, in solution of RMgX in the presence of **phen**, alkylmagnesium halide complexes should prevail. Alkoxy magnesium halides should, in contrast, be strongly disproportionated, especially CH<sub>3</sub>OMgBr.

So, according to our calculations, prior to the titration equivalence point, **phen** is complexed with RMgX while after equivalence point the complexes with MgX<sub>2</sub> should prevail. These results indicate that the disappearance of the red color of the complex of **phen** with a Grignard reagent during titration with an alcohol is not due to the complex formation between alkoxy magnesium halide and **phen**. The alkoxy complex disproportionates to a dialkoxy magnesium compound and a magnesium halide, and **phen** gets entirely complexed with the magnesium halide in the equivalence point because the complex between magnesium halide and **phen** is much stronger than that of the other studied complexes. Thus, the complexation of MgX<sub>2</sub> with **phen** in the solution seems to be the reason of the disappearance of the red color of the solution near the titration end point. The absorption spectrum of the complex MgCl<sub>2</sub>(phen) calculated by the TD/MPW1PW91/6-311+G\*\* method lies in the ultraviolet region (Figure 1f) supporting our hypothesis.

#### 4. Conclusions

Our calculated absorption spectra of the complexes CH<sub>3</sub>MgCl(phen) and CH<sub>3</sub>OMgCl(phen) by the DFT TD/MPW1PW91/6-311+G\*\* method indicate that the disappearance of the red color of the solution during titration of a Grignard reagent RMgX with an alcohol in the presence of **phen** is not due to the complex formation between alkoxy magnesium halide ROMgX and **phen**. We have investigated disproportionation equilibria, e.g., the Schlenk equilibria, which can be important during titration of the complex RMgX(phen) with an alcohol both in the gas phase and in solution. Solvation was modeled using the supermolecule approach.

The solvation reaction is exothermic for all the studied magnesium compounds—CH<sub>3</sub>MgX, CH<sub>3</sub>OMgX, MgX<sub>2</sub>, (CH<sub>3</sub>)<sub>2</sub>Mg, and (CH<sub>3</sub>O)<sub>2</sub>Mg (X = Cl, Br). The tricoordinated magnesium is planar in the monosolvated complexes while the tetracoordinated magnesium forms with its ligands a deformed tetrahedron in the disolvated complexes.

The complexes of **phen** with MgCl<sub>2</sub> and MgBr<sub>2</sub> are the most stable according to our DFT B3LYP/6-31+G\* calculations,  $\Delta H$  is -43.9 and -39.8 kcal/mol, respectively. The complexation energy is the lowest in case of the complex of **phen** with (CH<sub>3</sub>)<sub>2</sub>Mg ( $\Delta H = -23.7$  kcal/mol). The solvation of studied compounds causes a remarkable decrease in the complexation energies as one of the reagents (magnesium compound) is stabilized by the specific solvation but the product (complex) is not solvated. The solvation has also a strong influence on the disproportionation equilibria.

According to the DFT B3LYP/6-31+G\* calculations, prior to the titration equivalence point **phen** is complexed with a Grignard reagent while after the equivalence point the com-

plexation with magnesium halide should be important as the complex between  $MgX_2$  and **phen** is much stronger than the other studied magnesium complexes. Thus, the complexation of  $MgX_2$  with **phen** in the solution seems to be the reason for the disappearance of the red color of the solution. The calculated absorption spectrum of  $MgCl_2(\text{phen})$  at the DFTTD/MPW1PW91/6-311+G\*\* level of theory confirms the hypothesis.

**Acknowledgment.** This work was supported by the Estonian Science Foundation (Grant No. 4630).

#### References and Notes

- (1) Grignard, V. C. R. *Hebd. Seances Acad. Sci.* **1900**, *130*, 1322.
- (2) Lindsell, W. E. In *Comprehensive Organometallic Chemistry*; Wilkinson, G., Ed.; Pergamon Press: Elmsford, NY, 1982; Vol. 1, Chapter 4.
- (3) Lindsell, W. E. In *Comprehensive Organometallic Chemistry II*; Wilkinson, G., Ed.; Pergamon Press: Elmsford, NY, 1995; Vol. 1, Chapter 3.
- (4) Watson, S. C.; Eastham, J. F. *J. Organomet. Chem.* **1967**, *9*, 165.
- (5) Kaim, W. *J. Organomet. Chem.* **1981**, *222*, C17.
- (6) Kaim, W. *J. Am. Chem. Soc.* **1982**, *104*, 3833.
- (7) Lin, H.-S.; Paquette, L. A. *Synth. Commun.* **1994**, *24*, 2503.
- (8) Tammi, J.; Burk, P.; Tuulmets, A. *Main Group Metal Chemistry* **2000**, *23*, 301.
- (9) Schlenk, W.; Schlenk, W. *Chem. Ber.* **1929**, *62*, 920.
- (10) Baskin, C. P.; Bender, C. F.; Lucchese, R. R.; Bauschlicher, C. W., Jr.; Schaefer, H. F., III. *J. Mol. Struct.* **1976**, *32*, 125.
- (11) Ratner, M. A.; Moskowitz, J. W.; Topiol, S. *J. Am. Chem. Soc.* **1978**, *100*, 2329.
- (12) Nagase, S.; Uchibori, Y. *Tetrahedron Lett.* **1982**, *23*, 2585.
- (13) Sakai, S.; Jordan, K. D. *J. Am. Chem. Soc.* **1982**, *104*, 4019.
- (14) Jasien, P. G.; Dykstra, C. E. *J. Am. Chem. Soc.* **1983**, *105*, 2089.
- (15) Jasien, P. G.; Dykstra, C. E. *J. Am. Chem. Soc.* **1985**, *107*, 1891.
- (16) Davis, S. R. *J. Am. Chem. Soc.* **1991**, *113*, 4145.
- (17) Liu, L.; Davis, S. R. *J. Phys. Chem.* **1991**, *95*, 8619.
- (18) Nemukhin, A. V.; Topol, I. A.; Weinhold, F. *Inorg. Chem.* **1995**, *34*, 2980.
- (19) Solov'ev, V. N.; Sergeev, G. B.; Nemukhin, A. V.; Burt, S. K.; Topol, I. A. *J. Phys. Chem. A* **1997**, *101*, 8625.
- (20) Ohkubo, K.; Watanabe, F. *Bull. Chem. Soc. Jpn.* **1971**, *44*, 2867.
- (21) Kato, H.; Tsuruya, S. *Bull. Chem. Soc. Jpn.* **1973**, *46*, 1001.
- (22) Frisch, M. J.; Trucks, G. W.; Schlegel, H. B.; Scuseria, G. E.; Robb, M. A.; Cheeseman, J. R.; Zakrzewski, V. G.; Montgomery, J. A., Jr.; Straumann, R. E.; Burant, J. C.; Dapprich, S.; Millam, J. M.; Daniels, A. D.; Kudin, K. N.; Strain, M. C.; Farkas, O.; Tomasi, J.; Barone, V.; Cossi, M.; Cammi, R.; Mennucci, B.; Pomelli, C.; Adamo, C.; Clifford, S.; Ochterski, J.; Petersson, G. A.; Ayala, P. Y.; Cui, Q.; Morokuma, K.; Malick, D. K.; Rabuck, A. D.; Raghavachari, K.; Foresman, J. B.; Cioslowski, J.; Ortiz, J. V.; Stefanov, B. B.; Liu, G.; Liashenko, A.; Piskorz, P.; Komaromi, I.; Gomperts, R.; Martin, R. L.; Fox, D. J.; Keith, T.; Al-Laham, M. A.; Peng, C. Y.; Nanayakkara, A.; Gonzalez, C.; Challacombe, M.; Gill, P. M. W.; Johnson, B.; Chen, W.; Wong, M. W.; Andres, J. L.; Gonzalez, C.; Head-Gordon, M.; Replogle, E. S.; Pople, J. A. *Gaussian 98, Revision A7*; Gaussian, Inc.: Pittsburgh, PA, 1998.
- (23) Boys, S. F.; Bernardi, F. *Mol. Phys.* **1976**, *19*, 325.
- (24) *NBO Version 3.1*, Glendening, E. D.; Reed, A. E.; Carpenter, J. E.; Weinhold, F.
- (25) Adamo, C.; Di Matteo, A.; Barone, V. *Adv. Quantum Chem.* **2000**, *36*, 45.
- (26) Guggenberger, L. J.; Rundle, R. E. *J. Am. Chem. Soc.* **1968**, *90*, 5375.



*Journal of Physical Chemistry A*, **2003**, submitted.  
J. Tammiku-Taul, P. Burk, A. Tuulmets, Theoretical Study of Magnesium Compounds.  
The Schlenk Equilibrium in the Gas Phase and in the Presence of Et<sub>2</sub>O and  
THF molecules.

# Theoretical Study of Magnesium Compounds. The Schlenk Equilibrium in the Gas Phase and in the Presence of Et<sub>2</sub>O and THF Molecules

Jaana Tammiku-Taul,<sup>a,b</sup> Peeter Burk,<sup>\*b</sup> and Ants Tuulmets<sup>a</sup>

University of Tartu, 2 Jakobi St., Tartu 51014, Estonia

<sup>a</sup>Institute of Organic and Bioorganic Chemistry, <sup>b</sup>Institute of Chemical Physics

The Schlenk equilibrium involving RMgX, R<sub>2</sub>Mg, and MgX<sub>2</sub> (R = Me, Et, Ph and X = Cl, Br) have been studied both in the gas phase and in diethyl ether (Et<sub>2</sub>O) and tetrahydrofuran (THF) solutions by means of the density functional theory (DFT) B3LYP/6-31+G\* method. Solvation was modeled using the supermolecule approach. The stabilization due to interaction with solvent molecules decreases in the order MgX<sub>2</sub> > RMgX > R<sub>2</sub>Mg and among the groups (R and X) Ph > Me > Et and Cl > Br. Studied magnesium compounds are more strongly solvated by THF compared to Et<sub>2</sub>O. The magnesium halide is solvated with up to four solvent molecules in THF solution, assuming that *trans*-dihalotetrakis(tetrahydrofurano)magnesium(II) complex forms. The formation of *cis*-dihalotetrakis(tetrahydrofurano)magnesium(II) is energetically less favorable than the formation of corresponding disolvated complexes. The predominant species in the Schlenk equilibrium are RMgX in Et<sub>2</sub>O and R<sub>2</sub>Mg + MgX<sub>2</sub> in THF, which is consistent with experimental data.

## 1. Introduction

Although the stoichiometry of a Grignard reagent<sup>1</sup> can be expressed as RMgX (R = organic group, X = halogen), the real composition of the reagent is far more complex, both in solution and in the solid state. It should be expressed by equilibrium of the type



where the middle part is known as the Schlenk equilibrium<sup>2</sup> and the associated species can exist as dimers, also as trimers and higher aggregates. The Schlenk equilibrium is dynamic and can be shifted very fast.

The position of the Schlenk equilibrium depends upon the solvent, the concentration of the solution, the nature of the organic group, and the halide as

---

\*Corresponding author. E-mail: burk@ut.ee

well as the temperature. The most important factors are solvent and concentration. All alkyl- and arylmagnesium chlorides, bromides, and iodides are monomeric in tetrahydrofuran (THF) over a wide concentration range (0.1-3.5 M).<sup>3-5</sup> Alkyl- and arylmagnesium bromides and iodides contain essentially monomeric species at low concentrations (less than 0.1 M) and dimeric species at higher concentrations (0.5-1.0 M) in diethyl ether (Et<sub>2</sub>O). The alkylmagnesium chlorides are essentially dimeric even at the low concentrations.<sup>3-6a</sup> The difference in Grignard reagent association behavior in THF and Et<sub>2</sub>O is attributed to the relative Lewis basicities of the two solvents. Solvent-metal bonding competes with the bridging characteristics of the halide, and THF competes more favorably than Et<sub>2</sub>O. The associated complexes are believed to bridge predominantly through halide substituents.<sup>3,5</sup> Variable temperature NMR studies indicate that the rate of alkyl exchange is a function of the structure of the alkyl group, e.g., methyl group exchange is much faster than *t*-butyl group exchange. Temperature effects on the composition of Grignard reagents in solution can be either kinetic or thermodynamic. Increasing temperature usually results in a faster exchange of ligands among magnesium complexes, which translates to faster equilibration rates.<sup>3,4,7a,b</sup> Thus, all factors which affect the position of equilibrium are in close connection with one another.

The Schlenk equilibrium constant is usually expressed as

$$K_s = \frac{[RMgX]^2}{[R_2Mg] \cdot [MgX_2]} \quad (2)$$

If  $[R_2Mg] \approx [MgX_2]$ , which is frequently the case, a determination of the ratio  $[RMgX]/[R_2Mg]$  can be used. The equilibrium constants are also calculated from the equation

$$\Delta G = -RT \ln K \quad (3)$$

where R is universal gas constant (8.314 J/mol·K) and T is temperature.

The Schlenk equilibrium has been the subject of various experimental investigations. Calorimetric studies of the heats of reaction between MgX<sub>2</sub> and R<sub>2</sub>Mg in dilute solutions of Et<sub>2</sub>O<sup>8a-c</sup> and THF<sup>9</sup> (thermochemical titration) have provided thermodynamic parameters and equilibrium constants for several systems. A number of constants, thermodynamic parameters, and qualitative kinetic data for the exchange process has been obtained by variable temperature NMR-spectroscopy.<sup>7a-d</sup> Also IR-spectroscopy,<sup>10</sup> polarography,<sup>11</sup> analysis of kinetic investigations of Grignard reactions,<sup>12a,b</sup> and molecular weight measurements<sup>6a,b</sup> have been used.

Several theoretical studies about the Schlenk equilibrium, solvent effects, association processes in Grignard reagents, etc. have been carried out by semiempirical calculations, using the extended Hückel MO<sup>13</sup> (solvents are Me<sub>2</sub>O and Me<sub>3</sub>N) and CNDO/2<sup>14</sup> (only gas-phase calculations) methods, and by high level ab initio calculations, using both Hartree-Fock (HF) and Møller-Plesset (MP) perturbation calculations<sup>15</sup> (solvent is Me<sub>2</sub>O), the density functional theory (DFT), where solvent is Me<sub>2</sub>O<sup>16</sup> or Et<sub>2</sub>O.<sup>17</sup>

Many crystallographic data are available for the structures of solvated monomeric magnesium compounds.<sup>18-22</sup> The structure in solution, however, can be different from the solid-state structure because of various intermolecular and intramolecular forces in these phases. In the current work we report the results of the density functional theory (DFT) calculations about the Schlenk equilibrium of RMgX, R<sub>2</sub>Mg, and MgX<sub>2</sub> (R = Me, Et, Ph and X = Cl, Br) in the gas phase and in solution. We have used the most common reaction media for Grignard reagents, diethyl ether (Et<sub>2</sub>O) and tetrahydrofuran (THF), as solvents.

## 2. Computational Methods

The calculations were carried out using the GAUSSIAN 98<sup>23</sup> program package.

All geometry optimizations and vibrational analysis were done using the density functional theory (DFT) with hybrid B3LYP functional and the 6-31+G\* basis set (B3LYP/6-31+G\*). All stationary points were found to be true minima (number of imaginary frequencies, NImag = 0). The calculated frequencies were also used for calculations of enthalpies and Gibbs energies.

Solvation was modeled using the supermolecule approach, which is the best method to describe the specific solvent effects. Up to two molecules of diethyl ether and up to four molecules of tetrahydrofuran were added to the studied species.

The stability of the solvated species was calculated considering the basis set superposition error (BSSE) estimated according to the counterpoise (CP) correction.<sup>24</sup> The BSSE arises from the mathematical fact that the basis sets are not complete and it should be considered in the case of complexation energies. The dimer (complex) energy minus the monomer energies is the directly calculated complexation energy,  $\Delta E_{\text{complexation}}$ .

$$\Delta E_{\text{complexation}} = E(AB)_{ab}^* - E(A)_a - E(B)_b \quad (4)$$

To estimate how much of this complexation energy is due to BSSE, four additional energy calculations were needed. The CP correction is defined as

$$\Delta E_{CP} = E(A)_{ab}^* + E(B)_{ab}^* - E(A)_a^* - E(B)_b^* \quad (5)$$

where  $E(A)_{ab}^*$  and  $E(B)_{ab}^*$  are the monomer energies with the basis set of complex,  $E(A)_a^*$  and  $E(B)_b^*$  are the monomer energies with their normal basis sets. In all cases the monomers were calculated with the geometry they have in complex. The counterpoise corrected complexation energy,  $\Delta E_{BSSE}$ , is given as

$$\Delta E_{BSSE} = \Delta E_{complexation} - \Delta E_{CP} \quad (6)$$

The BSSE was also taken into account in the case of the reactions of the Schlenk equilibrium. The BSSE had a particularly strong influence on both the solvation energies and the Schlenk equilibrium of the bromine-containing compounds compared to the corresponding chlorine compounds, indicating somewhat less satisfactory description of bromine basis set.

### 3. Results and Discussion

#### 3.1. Structures of solvated magnesium compounds

The optimized structures of some mono- and disolvated species are shown in Figure 1. The monosolvated structures contain an essentially planar tricoordinated magnesium (Figure 1a-b). The tetracoordinated magnesium forms with its ligands a deformed tetrahedron in the disolvated species (Figure 1c-d), in accordance with X-ray diffraction studies of the crystal structures of monomeric  $\text{EtMgBr} \cdot 2\text{Et}_2\text{O}$ ,<sup>18a,b</sup>  $\text{PhMgBr} \cdot 2\text{Et}_2\text{O}$  and  $\text{Ph}_2\text{Mg} \cdot 2\text{Et}_2\text{O}$ ,<sup>19</sup>  $\text{MgBr}_2 \cdot 2\text{Et}_2\text{O}$ ,<sup>20</sup> and  $\text{PhMgBr} \cdot 2\text{THF}$ .<sup>21</sup> The geometry of diethyl ether both in the monosolvated and disolvated species is like “propeller” similar to that obtained by Lammertsma’s group.<sup>17</sup> For the solid state, and possibly for the solution state as well, the structure of solvated magnesium compounds depends primarily on the steric requirements of the R group and solvent molecules attached to the magnesium atom. As tetrahydrofuran is sterically less demanding than diethyl ether, magnesium halide can probably coordinate at least four tetrahydrofurans, e.g.,  $\text{MgBr}_2 \cdot 4\text{THF}$ , based on crystallographic data<sup>22a,b</sup> and conclusions by Smith and Becker about their calorimetric studies.<sup>9</sup> The optimized structures of tri- and tetrasolvated tetrahydrofuranate complexes of  $\text{MgCl}_2$  are shown in Figure 2. The tris-tetrahydrofuranate complex of magnesium halide forms a deformed trigonal bipyramid, wherein the chlorine atoms and one THF molecule are equatorial (e) and two THF molecules are axial (a). The tetrakis-tetrahydrofuranate complex of magnesium halide can exist in two forms, as *cis*-dihalotetrakis(tetrahydrofurano)magnesium(II) and *trans*-dihalotetrakis(tet-



rahydrofurano)magnesium(II). The *cis* form is a deformed octahedron and as the chlorine atoms are located alongside, we label them as equatorial (e). Thus, two THF ligands are equatorial (e) and the other two THF ligands are axial (a). The *trans* form is also an octahedron, where equatorial and axial positions are indistinguishable.

The obtained bond lengths of mono- and disolvated magnesium compounds (Table 1) can evidently be related to a lesser steric hindrance to the interaction between the magnesium atom and the oxygen atom(s) of the solvent. The distances between the magnesium atom and the oxygen atom(s) of the solvent increase in the order  $MgX_2 < RMgX < R_2Mg$  and among the groups  $Ph < Me \approx Et$ . The bond lengths  $r(Mg-O)$  are somewhat unsymmetrical in the case of disolvated  $RMgX$  compounds,  $\Delta r = 0.003...0.011 \text{ \AA}$  in the  $Et_2O$  complexes, and  $\Delta r = 0.001...0.008 \text{ \AA}$  in the THF complexes. The bond lengths  $r(Mg-X)$  increase in the direction  $MgX_2 < RMgX$  ( $Ph < Me \approx Et$ ) and  $r(Mg-C)$  in the direction  $RMgX < R_2Mg$  ( $Ph \approx Me < Et$ ). The  $r(Mg-O)$  is shorter in the case of THF complexes, e.g.,  $\Delta r = 0.005...0.015 \text{ \AA}$  in the monosolvated, and  $\Delta r = 0.016...0.029 \text{ \AA}$  in the disolvated THF complexes compared to the corresponding  $Et_2O$  complexes, while  $r(Mg-X)$  and  $r(Mg-C)$  are more or less constant. All bond lengths are longer in the case of disolvated  $Et_2O$  and THF complexes compared to the monosolvated complexes. The  $Mg-X$  bond lengthens in  $MgX_2 \cdot nTHF$  complexes with the addition of the next THF molecule. The asymmetry of the  $Mg-O$  bonds also appears in tris- and *cis*-tetrakis-tetrahydrofuranate complexes. The axial  $Mg-O$  bonds are somewhat longer than the equatorial  $Mg-O$  bond in the  $MgX_2 \cdot 3THF$  complexes, but the situation is inverse in the case of *cis*  $MgX_2 \cdot 4THF$  complexes, the axial  $Mg-O$  bonds are shorter than the equatorial  $Mg-O$  bonds. The  $Mg-O$  bonds in the *trans*  $MgX_2 \cdot 4THF$  complexes are shorter than the axial and longer than the equatorial  $Mg-O$  bonds in the  $MgX_2 \cdot 3THF$  complexes.

### 3.2. Solvation energies for magnesium compounds

The solvation energies of studied species with diethyl ether and tetrahydrofuran molecules were calculated from eqs 7 and 8, where Z is  $MgX_2$ ,  $RMgX$ , and  $R_2Mg$ , and  $n$  is the number of solvent molecules.



The results are given in Tables 2 and 3. The solvation enthalpies are exothermic for all the studied species. The solvent stabilization (with both one,  $\Delta H_1$ , and two solvent molecules,  $\Delta H_2$ ) is largest for the magnesium halides,  $MgX_2$ , ( $\Delta H_1 = -17.9...-21.6 \text{ kcal/mol}$ ,  $\Delta H_2 = -29.8...-34.9 \text{ kcal/mol}$  in  $Et_2O$

solution, and  $\Delta H_1 = -21.9\dots-25.5$  kcal/mol,  $\Delta H_2 = -39.0\dots-43.7$  kcal/mol in THF solution) and least for the diorganyl magnesium compounds,  $R_2Mg$ , ( $\Delta H_1 = -9.2\dots-12.5$  kcal/mol,  $\Delta H_2 = -13.0\dots-18.6$  kcal/mol in  $Et_2O$  solution, and  $\Delta H_1 = -13.1\dots-16.3$  kcal/mol,  $\Delta H_2 = -22.0\dots-27.8$  kcal/mol in THF solution) with intermediate values for the organomagnesium halides,  $RMgX$ , ( $\Delta H_1 = -12.6\dots-15.9$  kcal/mol,  $\Delta H_2 = -20.4\dots-26.1$  kcal/mol in  $Et_2O$  solution, and  $\Delta H_1 = -16.5\dots-20.0$  kcal/mol,  $\Delta H_2 = -29.0\dots-35.1$  kcal/mol in THF solution). The phenyl derivatives have larger solvation energies compared to the alkyl derivatives, which are sterically the most unfavorable. There is hardly any difference in solvation energies between compounds carrying Me or Et groups, but the chlorine-containing compounds are somewhat more strongly solvated than the corresponding bromine-containing compounds because of more electronegative and smaller chlorine atom. The addition of the third THF molecule to  $MgCl_2$  and  $MgBr_2$  stabilizes the formed complexes only by 4.9 and 3.8 kcal/mol, respectively. The fourth THF molecule can have either a stabilizing or destabilizing effect on the energy of solvated complex, depending on the geometry of the complex. *Cis*  $MgX_2 \cdot 4THF$  complexes are by 5.7...5.8 kcal/mol less stable than  $MgX_2 \cdot 3THF + THF$  and by 0.9...2.0 kcal/mol less stable than  $MgX_2 \cdot 2THF + 2THF$ , while *trans*  $MgX_2 \cdot 4THF$  complexes are by 2.7...3.1 kcal/mol more stable than  $MgX_2 \cdot 3THF + THF$  and by 6.5...7.9 kcal/mol more stable than  $MgX_2 \cdot 2THF + 2THF$ .

THF, the stronger base, forms somewhat stronger Lewis acid-base complexes with studied magnesium compounds than  $Et_2O$ . It becomes evident from the energies of displacement of  $Et_2O$  with THF for magnesium compounds (Table 4) expressed by eq 9.



All displacement reactions are exothermic, indicating that the magnesium atom of each species prefers THF to  $Et_2O$ . The obtained energies of displacement are similar,  $\Delta H_1 = -3.7\dots-4.2$  kcal/mol,  $\Delta H_2 = -8.2\dots-10.0$  kcal/mol, respectively. The displacement of two  $Et_2O$  molecules with three or four THF molecules in the disolvated  $Et_2O$  complexes of  $MgX_2$  is -12.9...-13.6 kcal/mol ( $\Delta H_3$ ) and -7.1...-7.9 kcal/mol in the case of *cis* complexes and -15.6...-16.7 kcal/mol in the case of *trans* complexes ( $\Delta H_4$ ), respectively. The difference in energies between bromine-containing and chlorine-containing compounds is negligible,  $\Delta\Delta H_1 = 0.1\dots0.2$  kcal/mol,  $\Delta\Delta H_2 = 0.2\dots1.0$  kcal/mol,  $\Delta\Delta H_3 = 0.7$  kcal/mol, and  $\Delta\Delta H_4 = 0.8\dots1.1$  kcal/mol relative to bromine compounds, respectively. The experimental heats ( $\Delta H$ ) of displacement of  $Et_2O$  with THF are -19.1 kcal/mol for  $MgBr_2$ , -7.0 kcal/mol for  $EtMgBr$ , and -4.6 kcal/mol for  $Et_2Mg$ .<sup>9</sup> These data indicate that the degree of preference of THF over  $Et_2O$  is far greater for  $MgBr_2$  than for  $EtMgBr$  or  $Et_2Mg$ . The best

correspondence between the calculated and above-mentioned experimental heats is found for *trans* MgBr<sub>2</sub>·4THF ( $\Delta H_{\text{calc}} = -15.6$  kcal/mol), for EtMgBr·2THF ( $\Delta H_{\text{calc}} = -8.5$  kcal/mol) and for Et<sub>2</sub>Mg·THF ( $\Delta H_{\text{calc}} = -3.9$  kcal/mol).

### 3.3. The Schlenk equilibrium

The calculated energies for the Schlenk equilibria of monomeric Grignard reagents in the gas phase and in Et<sub>2</sub>O and THF solutions are given in Table 5. The collected experimental data are listed in Table 6 for comparison.

The Schlenk equilibrium lies in favor of alkyl- and arylmagnesium halides in the gas phase according to our B3LYP/6-31+G\* calculations,  $\Delta H$  ranges from 4.01 to 6.64 kcal/mol. The solvation by diethyl ether has a quite strong influence on the equilibrium, decreasing the endothermicity of disproportionation reactions. The addition of the first Et<sub>2</sub>O molecule has a stronger effect, disproportionation of monosolvated systems becomes by 1.69...3.21 kcal/mol less endothermic, and the addition of the second solvent molecule has a small 0.14...0.82 kcal/mol additional effect, except for PhMgCl where the second Et<sub>2</sub>O molecule increases the endothermicity by 0.76 kcal/mol. The effect of solvation is the strongest in the case of PhMgBr, giving a value of  $\Delta\Delta H_2 = \Delta H_{\text{gas}} - \Delta H_2 = 4.03$  kcal/mol, in the case of another species it ranges from 1.42 kcal/mol for PhMgCl to 2.52 kcal/mol for EtMgBr. Comparison of experimental and calculated energies for the disolvated systems indicates that most values obtained by calculations are somewhat bigger, e.g.,  $\Delta\Delta H_{\text{calc}(2)\text{-exp}}$  is 0.85 kcal/mol for EtMgBr, 0.59 kcal/mol for PhMgBr, and  $\Delta\Delta G_{\text{calc}(2)\text{-exp}}$  is 1.30 kcal/mol for EtMgBr, but  $\Delta\Delta G_{\text{exp-calc}(2)}$  is 1.28 kcal/mol for PhMgBr. The calculated values of  $\Delta G$  for the monosolvated systems seem to be much more consistent with the experimental data for real solution,  $\Delta\Delta G_{\text{calc}(1)\text{-exp}}$  is 0.91 kcal/mol for EtMgBr and 0.20 kcal/mol for PhMgBr. However, the tendency that the predominant species in Et<sub>2</sub>O is RMgX, is still in agreement with experiment. We can not ignore the fact that magnesium compounds exist as aggregates in real diethyl ether solution. The dimerization processes were calculated by Bock et al. in Me<sub>2</sub>O<sup>15</sup> and by Lammertsma et al. in Et<sub>2</sub>O.<sup>17</sup> As the Schlenk equilibrium is only slightly influenced by the association of Grignard reagents<sup>17</sup> and the dimerization energies decrease in the order  $[\text{MgX}_2] > [\text{RMgX}] > [\text{R}_2\text{Mg}]$  (Cl > Br),<sup>15,17</sup> our calculations are limited to monomers.

The Schlenk equilibrium is shifted toward RMgX also in the case of solvation with one and two THF molecules according to our DFT calculations. From the experimental data it appears that the direction of reaction in THF shifts in favor of R<sub>2</sub>Mg + MgX<sub>2</sub>. It has been suggested that the difference in the Schlenk equilibrium between Et<sub>2</sub>O and THF results from the increased coordination number of magnesium halide in THF (see section 3.1. in the

current paper). Our computational results using the energies of  $\text{MgX}_2 \cdot 3\text{THF}$  for the calculations of the disproportionation reactions support this argument. The correlation between the calculated values of  $\Delta H$  without BSSE corrections and the corresponding experimental values is rather good,  $\Delta\Delta H_{\text{exp-calc}(3)}$  is 0.77 kcal/mol for  $\text{EtMgCl}$ , 0.79 kcal/mol for  $\text{EtMgBr}$ , and  $\Delta\Delta H_{\text{calc}(3)\text{-exp}}$  is 0.85 kcal/mol for  $\text{PhMgCl}$  and 0.08...1.73 kcal/mol for  $\text{PhMgBr}$ . The tendency that the alkyl- and arylmagnesium bromides are much more strongly disproportionated than the chlorides, is also in agreement with experiment. It also becomes evident from the calculations using the energies of *cis*  $\text{MgX}_2 \cdot 4\text{THF}$  without BSSE corrections, but the extent of disproportionation is smaller in the case of bromine compounds and the equilibrium is shifted toward the formation of organomagnesium halides in the case of chloride compounds. The results using the energies of *trans*  $\text{MgX}_2 \cdot 4\text{THF}$  are more reasonable with BSSE corrections. The extent of disproportionation is somewhat more pronounced in the case of chloride compounds, which is not consistent with experimental data.

It seems that the used method of BSSE corrections is mostly not justified in the cases when  $n = 3$  and 4, but it works well when  $n = 1$  and 2. Such behavior can be attributed to the fact that the counterpoise correction seems to overestimate the magnitude of BSSE, especially for higher aggregates.

It should be noted that for the di-, tri- and tetrasolvated complexes the values of  $\Delta G$  considerably differ from the  $\Delta E$  and  $\Delta H$ , having even some positive values. It seems to be a fault of the used thermochemical analysis method, which treats all vibrational modes other than the free rotations and translations of molecule or complex as harmonic vibrations. For molecules having hindered internal rotations, this can produce errors in the energy and heat capacity at room temperatures and can have a significant effect on the entropy. Thus, the obtained values of  $\Delta G$  are not reliable, especially in the case of solvation Gibbs energies and Gibbs energies for the Schlenk equilibrium using the corresponding total energies of tris- and tetrakis-tetrahydrofuranate complexes of magnesium halides. Therefore, no equilibrium constants for the disproportionation reactions were calculated.

#### 4. Conclusions

The most important factor affecting the position of the Schlenk equilibrium is solvent. From the experimental data it appears that the predominant species is alkyl- or arylmagnesium halide,  $\text{RMgX}$ , in diethyl ether solution and the disproportionation products,  $\text{R}_2\text{Mg} + \text{MgX}_2$ , are favored in tetrahydrofuran solution. The magnesium atom in  $\text{RMgX}$ ,  $\text{R}_2\text{Mg}$ , and  $\text{MgX}_2$  compounds can coordinate with two molecules of solvent in  $\text{Et}_2\text{O}$  in addition to the two covalent bonds. The difference in the Schlenk equilibrium between

Et<sub>2</sub>O and THF can be due to the increased coordination number of magnesium halide in THF, e.g., MgX<sub>2</sub>·*n*THF (*n* ≥ 3).

The tricoordinated magnesium is essentially planar in the monosolvated species, while the tetracoordinated magnesium forms with its ligands a deformed tetrahedron in the disolvated species. The tris-tetrahydrofuranate complex of magnesium halide is a deformed trigonal bipyramid and the both tetrakis-tetrahydrofuranate complexes of magnesium halide, *cis*-dihalotetrakis(tetrahydrofurano)magnesium(II) and *trans*-dihalotetrakis(tetrahydrofurano)magnesium(II) are deformed octahedrons.

The solvation enthalpies are exothermic for all the studied magnesium compounds – RMgX, R<sub>2</sub>Mg, and MgX<sub>2</sub> (R = Me, Et, Ph and X = Cl, Br). According to our DFT B3LYP/6-31+G\* calculations the stabilization due to interaction with solvent molecules decreases in the order MgX<sub>2</sub> > RMgX > R<sub>2</sub>Mg and among the groups Ph > Me > Et and Cl > Br. THF, the stronger base, forms somewhat stronger Lewis acid-base complexes with studied species than Et<sub>2</sub>O.

Disproportionation reactions are slightly endothermic, favoring the organomagnesium halides in Et<sub>2</sub>O solution. The Schlenk equilibrium is shifted toward the formation of the disproportionation products both in the case of tris-tetrahydrofuranate complex of MgX<sub>2</sub> and *trans*-tetrakis-tetrahydrofuranate complex of MgX<sub>2</sub> according to our calculations. Thus, magnesium halide is able to coordinate with up to four THF molecules, assuming that *trans*-dihalotetrakis(tetrahydrofurano)magnesium(II) forms. The formation of *cis*-dihalotetrakis(tetrahydrofurano)magnesium(II) is energetically even less favorable than the corresponding disolvated complexes.

## Acknowledgement

This work was supported by Estonian Science Foundation (Grants No. 4630 and 5196). We are thankful to reviewers for their helpful suggestions.

**Supporting Information Available:** Optimized structures of mono- and disolvated phenylmagnesium chloride and diphenylmagnesium.

## References and Notes

1. Grignard, V. *C. R. Hebd. Seances Acad. Sci.* **1900**, *130*, 1322.
2. Schlenk, W.; Schlenk W. Jr. *Chem. Ber.* **1929**, *62*, 920.
3. Cannon, K. S.; Krow, G. R. In *Handbook of Grignard Reagents* and references cited therein; Silverman, G. S.; Rakita, P. E., Eds. Marcel Dekker: New York, 1996.

4. Lindsell, W. E. In *Comprehensive Organometallic Chemistry* and references cited therein; Wilkinson, G., Ed.; Pergamon Press: Elmsford, NY, 1982; Vol. 1, Chapter 4.
5. Walker, F. W.; Ashby, E. C. *J. Am. Chem. Soc.* **1969**, *91*, 3845.
6. (a) Ashby, E. C.; Smith, M. B. *J. Am. Chem. Soc.* **1964**, *86*, 4363. (b) Ashby, E. C.; Becker, W. E. *J. Am. Chem. Soc.* **1963**, *85*, 118.
7. (a) Evans, D. F.; Fazakerley, V. J. *Chem. Soc. A* **1971**, 184. (b) Parris, G. E.; Ashby, E. C. *J. Am. Chem. Soc.* **1971**, *93*, 1206. (c) Evans, D. F.; Fazakerley, V. *Chem. Commun.* **1968**, 974. (d) Markies, P. R.; Altink, R. M.; Villena, A.; Akkerman, O. S.; Bickelhaupt, F. J. *Organomet. Chem.* **1991**, *402*, 289.
8. (a) Smith, M. B.; Becker, W. E. *Tetrahedron Lett.* **1965**, *43*, 3843. (b) Smith, M. B.; Becker, W. E. *Tetrahedron* **1966**, *22*, 3027. (c) Holm, T. *Acta Chem. Scand.* **1969**, *23*, 579.
9. Smith, M. B.; Becker, W. E. *Tetrahedron* **1967**, *23*, 4215.
10. Salinger, R. M.; Mosher, H. S. *J. Am. Chem. Soc.* **1964**, *86*, 1782.
11. Psarras, T.; Dessy, R. E. *J. Am. Chem. Soc.* **1966**, *88*, 5132.
12. (a) Ashby, E. C.; Laemmle, J.; Neumann, H. M. *J. Am. Chem. Soc.* **1971**, *93*, 4601. (b) Ashby, E. C.; Laemmle, J.; Neumann, H. M. *J. Am. Chem. Soc.* **1972**, *94*, 5421.
13. Ohkubo, K.; Watanabe, F. *Bull. Chem. Soc. Jpn.* **1971**, *44*, 2867.
14. Kato, H.; Tsuruya, S. *Bull. Chem. Soc. Jpn.* **1973**, *46*, 1001.
15. Axten, J.; Troy, J.; Jiang, P.; Trachtman, M.; Bock, C. W. *Struct. Chem.* **1994**, *5*, 99.
16. Tammiku, J.; Burk, P.; Tuulmets, A. *J. Phys. Chem. A* **2001**, *105*, 8554.
17. Ehlers, A. W.; van Klink, G. P. M.; van Eis, M. J.; Bickelhaupt, F.; Nederkoorn, P. H. J.; Lammertsma, K. *J. Mol. Model.* **2000**, *6*, 186.
18. (a) Guggenberger, L. J.; Rundle, R. E. *J. Am. Chem. Soc.* **1964**, *86*, 5344. (b) Guggenberger, L. J.; Rundle, R. E. *J. Am. Chem. Soc.* **1986**, *90*, 5375.
19. Stucky, G.; Rundle, R. E. *J. Am. Chem. Soc.* **1964**, *86*, 4825.
20. Schibilla, H.; Le Bihan, M.-T. *Acta Cryst.* **1967**, *23*, 332.
21. Schröder, F. Dissertation, Institut für Anorganische Chemie der Technischen Hochschule, Braunschweig, Germany, 1965.
22. (a) Schröder, F.; Spandau, H. *Naturwiss.* **1966**, *53*, 360. (b) Perucaud, M.; Ducom, J.; Vallino, M. *Compt. Rend.* **1967**, *264*, 571.
23. *Gaussian 98, Revision A7*, Frisch, M. J.; Trucks, G. W.; Schlegel, H. B.; Scuseria, G. E.; Robb, M. A.; Cheeseman, J. R.; Zakrzewski, V. G.; Montgomery, Jr., J. A.; Stratmann, R. E.; Burant, J. C.; Dapprich, S.; Millam, J. M.; Daniels, A. D.; Kudin, K. N.; Strain, M. C.; Farkas, O.; Tomasi, J.; Barone, V.; Cossi, M.; Cammi, R.; Mennucci, B.; Pomelli, C.; Adamo, C.; Clifford, S.; Ochterski, J.; Petersson, G. A.; Ayala, P. Y.; Cui, Q.; Morokuma, K.; Malick, D. K.; Rabuck, A. D.;

Raghavachari, K.; Foresman, J. B.; Cioslowski, J.; Ortiz, J. V.; Stefanov, B. B.; Liu, G.; Liashenko, A.; Piskorz, P.; Komaromi, I.; Gomperts, R.; Martin, R. L.; Fox, D. J.; Keith, T.; Al-Laham, M. A.; Peng, C. Y.; Nanayakkara, A.; Gonzalez, C.; Challacombe, M.; Gill, P. M. W.; Johnson, B.; Chen, W.; Wong, M. W.; Andres, J. L.; Gonzalez, C.; Head-Gordon, M.; Replogle, E. S.; Pople, J. A. Gaussian, Inc., Pittsburgh PA, 1998.

24. Van Duijneveldt, F. B.; van Duijneveldt-van de Rijdt, J. G. C. M.; van Lenthe, J. H. *Chem. Rev.* **1994**, *94*, 1873.

**TABLE 1. Selected bond lengths of solvated magnesium compounds at B3LYP/6-31+G\* level. All distances are in angstroms, Å.**

<i>Z</i> - <i>n</i> Et <sub>2</sub> O	<i>r</i> (Mg-O)		<i>r</i> (Mg-X)		<i>r</i> (Mg-C)	
	<i>n</i> = 1	<i>n</i> = 2	<i>n</i> = 1	<i>n</i> = 2	<i>n</i> = 1	<i>n</i> = 2
MgCl <sub>2</sub>	2.038	2.091	2.238	2.286	-	-
MgBr <sub>2</sub>	2.046	2.091	2.380	2.427	-	-
MeMgCl	2.085	2.137; 2.140	2.269	2.319	2.104	2.129
MeMgBr	2.089	2.131; 2.140	2.411	2.469	2.102	2.123
EtMgCl	2.088	2.138; 2.141	2.270	2.319	2.119	2.142
EtMgBr	2.087	2.129; 2.140	2.411	2.467	2.117	2.139
PhMgCl	2.075	2.122; 2.126	2.259	2.309	2.108	2.139
PhMgBr	2.082	2.116; 2.120	2.395	2.452	2.102	2.128
Me <sub>2</sub> Mg	2.137	2.190	-	-	2.127	2.154
Et <sub>2</sub> Mg	2.138	2.201	-	-	2.144	2.168
Ph <sub>2</sub> Mg	2.104	2.157; 2.161	-	-	2.125	2.156
<i>Z</i> - <i>n</i> THF	<i>n</i> = 1	<i>n</i> = 2	<i>n</i> = 1	<i>n</i> = 2	<i>n</i> = 1	<i>n</i> = 2
MgCl <sub>2</sub>	2.033	2.075	2.237	2.286	-	-
MgBr <sub>2</sub>	2.038	2.068	2.379	2.426	-	-
MeMgCl	2.078	2.118; 2.123	2.268	2.321	2.103	2.129
MeMgBr	2.078	2.114; 2.115	2.410	2.467	2.102	2.121
EtMgCl	2.078	2.122; 2.123	2.269	2.322	2.118	2.142
EtMgBr	2.078	2.111; 2.119	2.410	2.469	2.116	2.135
PhMgCl	2.063	2.107; 2.110	2.259	2.313	2.106	2.136
PhMgBr	2.067	2.100; 2.101	2.395	2.460	2.103	2.131
Me <sub>2</sub> Mg	2.128	2.170	-	-	2.127	2.154
Et <sub>2</sub> Mg	2.129	2.172	-	-	2.143	2.169
Ph <sub>2</sub> Mg	2.099	2.130; 2.145	-	-	2.124	2.153; 2.157
<i>Z</i> - <i>n</i> THF	<i>n</i> = 3		<i>n</i> = 3		<i>n</i> = 3	
MgCl <sub>2</sub>	2.205 (a) 2.097 (e)		2.340 (e)		-	
MgBr <sub>2</sub>	2.198 (a) 2.203 (a) 2.073 (e)		2.471 (e) 2.475 (e)		-	
<i>Z</i> - <i>n</i> THF	<i>cis</i> <i>n</i> = 4	<i>trans</i> <i>n</i> = 4	<i>cis</i> <i>n</i> = 4	<i>trans</i> <i>n</i> = 4	<i>cis</i> <i>n</i> = 4	<i>trans</i> <i>n</i> = 4
MgCl <sub>2</sub>	2.235 (a) 2.240 (a) 2.322 (e) 2.323 (e)	2.199	2.409 (e)	2.429 2.432	-	-
MgBr <sub>2</sub>	2.222 (a) 2.298 (e)	2.191	2.551 (e)	2.577 2.579	-	-



**TABLE 2.** Solvation energies ( $\Delta E$ , contains zero-point vibrational energy (ZPVE) correction), enthalpies ( $\Delta H$ ), and Gibbs energies ( $\Delta G$ ) of magnesium compounds with one or two diethyl ether molecules at B3LYP/6-31+G\* level. All values are in kcal/mol and include BSSE corrections.

Z	$Z + n\text{Et}_2\text{O} \longrightarrow Z \cdot n\text{Et}_2\text{O}$					
	$\Delta E$		$\Delta H$		$\Delta G$	
	$n = 1$	$n = 2$	$n = 1$	$n = 2$	$n = 1$	$n = 2$
MgCl <sub>2</sub>	-21.6	-35.3	-21.6	-34.9	-11.7	-14.3
MgBr <sub>2</sub>	-18.0	-30.1	-17.9	-29.8	-8.2	-8.1
MeMgCl	-14.9	-23.8	-14.6	-23.2	-5.4	-3.7
MeMgBr	-13.0	-21.1	-12.7	-20.6	-3.2	0.7
EtMgCl	-14.8	-23.5	-14.4	-22.9	-4.2	-1.5
EtMgBr	-13.0	-21.1	-12.6	-20.4	-2.2	1.7
PhMgCl	-16.3	-26.7	-15.9	-26.1	-6.3	-4.3
PhMgBr	-13.9	-22.8	-13.6	-22.2	-3.2	0.3
Me <sub>2</sub> Mg	-9.6	-14.3	-9.4	-13.8	0.4	7.3
Et <sub>2</sub> Mg	-9.5	-13.5	-9.2	-13.0	1.9	10.0
Ph <sub>2</sub> Mg	-12.9	-19.4	-12.5	-18.6	-2.3	3.2

**TABLE 3. Solvation energies ( $\Delta E$ , contains zero-point vibrational energy (ZPVE) correction), enthalpies ( $\Delta H$ ), and Gibbs energies ( $\Delta G$ ) of magnesium compounds with one up to four tetrahydrofuran molecules at B3LYP/6-31+G\* level. All values are in kcal/mol and include BSSE corrections.**

Z	$Z + n\text{THF} \longrightarrow Z \cdot n\text{THF}$					
	$\Delta E$		$\Delta H$		$\Delta G$	
	$n = 1$	$n = 2$	$n = 1$	$n = 2$	$n = 1$	$n = 2$
MgCl <sub>2</sub>	-25.5	-44.0	-25.5	-43.7	-15.9	-22.7
MgBr <sub>2</sub>	-22.1	-39.3	-21.9	-39.0	-13.0	-17.8
MeMgCl	-18.7	-32.2	-18.4	-31.6	-9.1	-11.5
MeMgBr	-17.0	-29.8	-16.5	-29.2	-7.7	-7.9
EtMgCl	-18.6	-31.9	-18.3	-31.2	-8.1	-9.9
EtMgBr	-17.0	-29.7	-16.6	-29.0	-7.2	-7.2
PhMgCl	-20.3	-35.7	-20.0	-35.1	-9.8	-13.3
PhMgBr	-18.1	-33.0	-17.8	-32.2	-6.8	-10.3
Me <sub>2</sub> Mg	-13.3	-22.5	-13.1	-22.0	-3.2	-0.5
Et <sub>2</sub> Mg	-13.4	-22.2	-13.1	-21.7	-1.8	1.8
Ph <sub>2</sub> Mg	-16.7	-28.6	-16.3	-27.8	-5.6	-5.9
	$n = 3$		$n = 3$		$n = 3$	
MgCl <sub>2</sub>	-49.2		-48.6		-15.7	
MgBr <sub>2</sub>	-43.4		-42.8		-8.9	
	<i>cis</i>	<i>trans</i>	<i>cis</i>	<i>trans</i>	<i>cis</i>	<i>trans</i>
	$n = 4$	$n = 4$	$n = 4$	$n = 4$	$n = 4$	$n = 4$
MgCl <sub>2</sub>	-43.6	-52.9	-42.8	-51.6	3.9	-7.0
MgBr <sub>2</sub>	-37.7	-46.2	-37.0	-45.5	11.0	3.1

**TABLE 4.** Energies ( $\Delta E$ , contains zero-point vibrational energy (ZPVE) correction), enthalpies ( $\Delta H$ ), and Gibbs energies ( $\Delta G$ ) of displacement of diethyl ether with tetrahydrofuran for magnesium compounds at B3LYP/6-31+G\* level. All values are in kcal/mol and include BSSE corrections.

Z	$\Delta E$		$\Delta H$		$\Delta G$	
	$Z \cdot nEt_2O + nTHF \longrightarrow Z \cdot nTHF + nEt_2O$					
	$n = 1$	$n = 2$	$n = 1$	$n = 2$	$n = 1$	$n = 2$
MgCl <sub>2</sub>	-3.9	-8.7	-3.9	-8.8	-4.2	-8.3
MgBr <sub>2</sub>	-4.1	-9.2	-4.1	-9.1	-4.8	-9.6
MeMgCl	-3.8	-8.5	-3.8	-8.4	-3.7	-7.8
MeMgBr	-4.0	-8.7	-3.9	-8.6	-4.5	-8.5
EtMgCl	-3.8	-8.3	-3.8	-8.3	-3.8	-8.4
EtMgBr	-4.0	-8.6	-4.0	-8.5	-5.0	-9.0
PhMgCl	-4.0	-9.0	-4.0	-9.0	-3.4	-9.0
PhMgBr	-4.1	-10.2	-4.2	-10.0	-3.5	-10.6
Me <sub>2</sub> Mg	-3.7	-8.2	-3.7	-8.2	-3.7	-7.8
Et <sub>2</sub> Mg	-3.9	-8.7	-3.9	-8.7	-3.7	-8.3
Ph <sub>2</sub> Mg	-3.8	-9.2	-3.8	-9.2	-3.3	-9.1
	$Z \cdot 2Et_2O + nTHF \longrightarrow Z \cdot nTHF + 2Et_2O$					
	$n = 3$		$n = 3$		$n = 3$	
MgCl <sub>2</sub>	-14.0		-13.6		-1.3	
MgBr <sub>2</sub>	-13.3		-12.9		-0.7	
	<i>cis</i>	<i>trans</i>	<i>cis</i>	<i>trans</i>	<i>cis</i>	<i>trans</i>
	$n = 4$	$n = 4$	$n = 4$	$n = 4$	$n = 4$	$n = 4$
MgCl <sub>2</sub>	-8.3	-17.6	-7.9	-16.7	18.2	7.4
MgBr <sub>2</sub>	-7.6	-16.1	-7.1	-15.6	19.1	11.2

**TABLE 5. Energies ( $\Delta E$ , contains zero-point vibrational energy (ZPVE) correction), enthalpies ( $\Delta H$ ), and Gibbs energies ( $\Delta G$ ) for the Schlenk equilibria of Grignard reagents in the gas phase and in Et<sub>2</sub>O and THF solutions at B3LYP/6-31+G\* level. All values are in kcal/mol and include BSSE corrections if not stated otherwise.**

	$\Delta E$	$\Delta H$	$\Delta G$
$2\text{RMgX} \rightleftharpoons \text{R}_2\text{Mg} + \text{MgX}_2$			
MeMgCl	5.35	5.66	5.19
MeMgBr	5.25	5.72	4.81
EtMgCl	5.89	6.24	6.50
EtMgBr	6.14	6.55	6.48
PhMgCl	3.68	4.01	4.38
PhMgBr	6.19	6.64	6.62
$2(\text{RMgX}\cdot\text{Et}_2\text{O}) \rightleftharpoons \text{R}_2\text{Mg}\cdot\text{Et}_2\text{O} + \text{MgX}_2\cdot\text{Et}_2\text{O}$			
MeMgCl	4.00	3.97	4.75
MeMgBr	3.69	3.84	3.41
EtMgCl	4.32	4.29	5.08
EtMgBr	4.66	4.73	4.57
PhMgCl	1.91	1.83	3.06
PhMgBr	3.25	3.43	2.57
$2(\text{RMgX}\cdot 2\text{Et}_2\text{O}) \rightleftharpoons \text{R}_2\text{Mg}\cdot 2\text{Et}_2\text{O} + \text{MgX}_2\cdot 2\text{Et}_2\text{O}$			
MeMgCl	3.34	3.30	5.52
MeMgBr	3.07	3.20	2.70
EtMgCl	4.11	4.04	5.18
EtMgBr	4.65	4.59	4.96
PhMgCl	2.47	2.59	1.85
PhMgBr	2.22	2.61	1.09
$2(\text{RMgX}\cdot\text{THF}) \rightleftharpoons \text{R}_2\text{Mg}\cdot\text{THF} + \text{MgX}_2\cdot\text{THF}$			
MeMgCl	3.99	3.99	4.27
MeMgBr	3.74	3.80	3.95
EtMgCl	4.20	4.16	4.87
EtMgBr	4.72	4.69	6.05
PhMgCl	2.17	2.17	2.40
PhMgBr	3.53	3.99	1.55
$2(\text{RMgX}\cdot 2\text{THF}) \rightleftharpoons \text{R}_2\text{Mg}\cdot 2\text{THF} + \text{MgX}_2\cdot 2\text{THF}$			
MeMgCl	3.29	3.18	4.96
MeMgBr	2.97	3.07	2.31
EtMgCl	3.35	3.18	5.41
EtMgBr	3.98	3.79	4.97
PhMgCl	2.53	2.60	2.36
PhMgBr	4.18	4.28	3.64

**TABLE 5. Continues.**

	$2(\text{RMgX}\cdot 2\text{THF}) + \text{THF} \rightleftharpoons$	$\text{R}_2\text{Mg}\cdot 2\text{THF} + \text{MgX}_2\cdot 3\text{THF}$	
MeMgCl	-1.92, -3.23*	-1.68, -3.00*	11.94, 10.63*
MeMgBr	-1.13, -6.17*	-0.75, -5.79*	11.22, 6.19*
EtMgCl	-1.85, -3.20*	-1.68, -3.03*	12.39, 11.04*
EtMgBr	-0.12, -5.40*	-0.03, -5.31*	13.87, 8.59*
PhMgCl	-2.68, -3.99*	-2.26, -3.57*	9.34, 8.03*
PhMgBr	0.08, -4.93*	0.46, -4.55*	12.55, 7.54*
	$2(\text{RMgX}\cdot 2\text{THF}) + 2\text{THF} \rightleftharpoons$	$\text{R}_2\text{Mg}\cdot 2\text{THF} + \text{cis MgX}_2\cdot 4\text{THF}$	
MeMgCl	3.69, 1.68*	4.06, 2.04*	31.49, 29.48*
MeMgBr	4.60, -4.71*	5.07, -4.24*	31.03, 21.72*
EtMgCl	3.76, 1.71*	4.05, 2.01*	31.94, 29.89*
EtMgBr	5.62, -3.95*	5.80, -3.76*	33.69, 24.12*
PhMgCl	2.93, 0.93*	3.48, 1.47*	28.89, 26.88*
PhMgBr	5.82, -3.47*	6.28, -3.01*	32.36, 23.07*
	$2(\text{RMgX}\cdot 2\text{THF}) + 2\text{THF} \rightleftharpoons$	$\text{R}_2\text{Mg}\cdot 2\text{THF} + \text{trans MgX}_2\cdot 4\text{THF}$	
MeMgCl	-5.54, -8.27*	-4.75, -7.47*	20.66, 17.93*
MeMgBr	-3.90, -21.99*	-3.45, -21.54*	23.19, 5.10*
EtMgCl	-5.48, -8.24*	-4.75, -7.51*	21.10, 18.35*
EtMgBr	-2.89, -21.23*	-2.72, -21.06*	25.85, 7.51*
PhMgCl	-6.30, -9.02*	-5.33, -8.04*	18.06, 15.34*
PhMgBr	-2.68, -20.75*	-2.23, -20.30*	24.52, 6.45*

\*Values without BSSE corrections.

**TABLE 6. Collected experimental data for the Schlenk equilibrium  $2\text{RMgX} \rightleftharpoons \text{R}_2\text{Mg} + \text{MgX}_2$  at 298 K.**

Grignard reagent	Solvent	$\Delta H$ (kcal/mol)	$\Delta F$ or $\Delta G$ (kcal/mol)	$1/K_s$	Method of analysis	Ref.
MeMgCl	THF			$1.0 \pm 0.72$	NMR	7b
				4.5	IR	10
MeMgBr	Et <sub>2</sub> O			320	calorimetric	8c
				450	kinetic + UV	12a,b
	THF			$4.0 \pm 2.6$	NMR	7b
				3.5	IR	10
EtMgCl	THF	-3.80	1.010	5.52	calorimetric	9
EtMgBr	Et <sub>2</sub> O	3.74	3.66	480	calorimetric	8a,b
	THF	-6.10	0.965	5.09	calorimetric	9
PhMgCl	THF	-2.72	0.300	1.66	calorimetric	9
PhMgBr	Et <sub>2</sub> O	2.02	2.37	55-62	calorimetric	8b
	THF	-2.82	0.787	3.77	calorimetric	9
		$-3.2 \pm 0.5$		$4.0 \pm 0.8$	NMR	7a,c
		-4.47		7.46	NMR	7d
EtMgBr	dimethoxyethane			$2.2 \pm 0.3$	polarographic	11
PhMgBr	dimethoxyethane			$6.1 \pm 0.3$	polarographic	11

\*T = 209-236 K

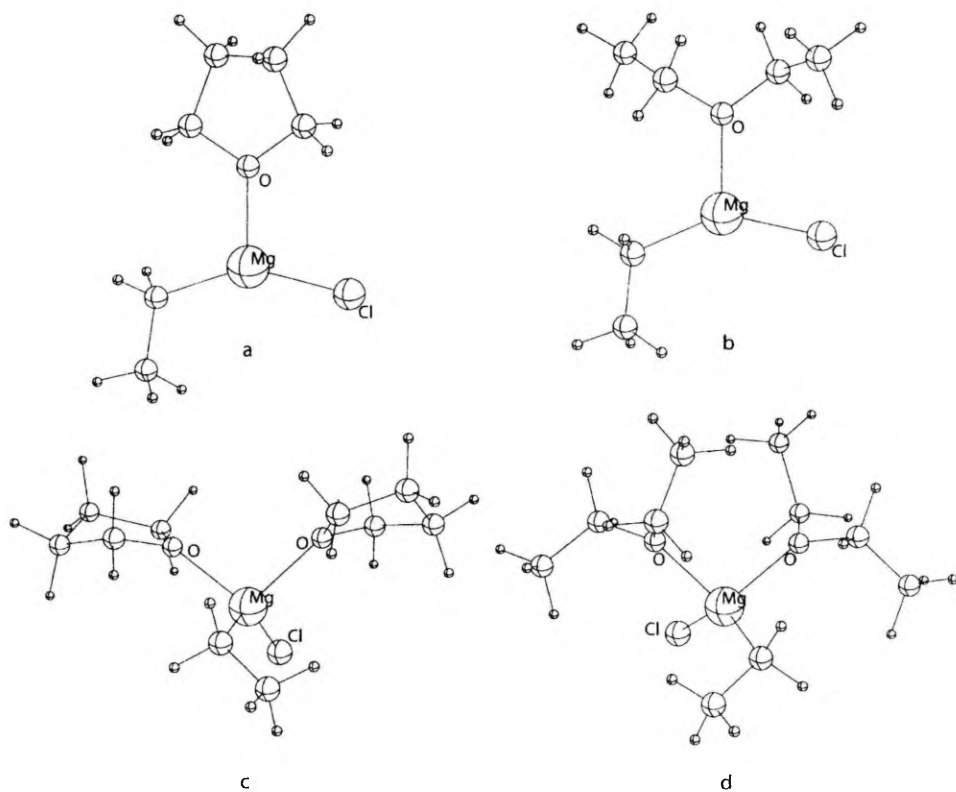


**Figure 1.** The optimized (at B3LYP/6-31+G\* level of theory) structures of monosolvated and disolvated species: (a) EtMgCl·THF, (b) EtMgCl·Et<sub>2</sub>O, (c) EtMgCl·2THF, and (d) EtMgCl·2Et<sub>2</sub>O.

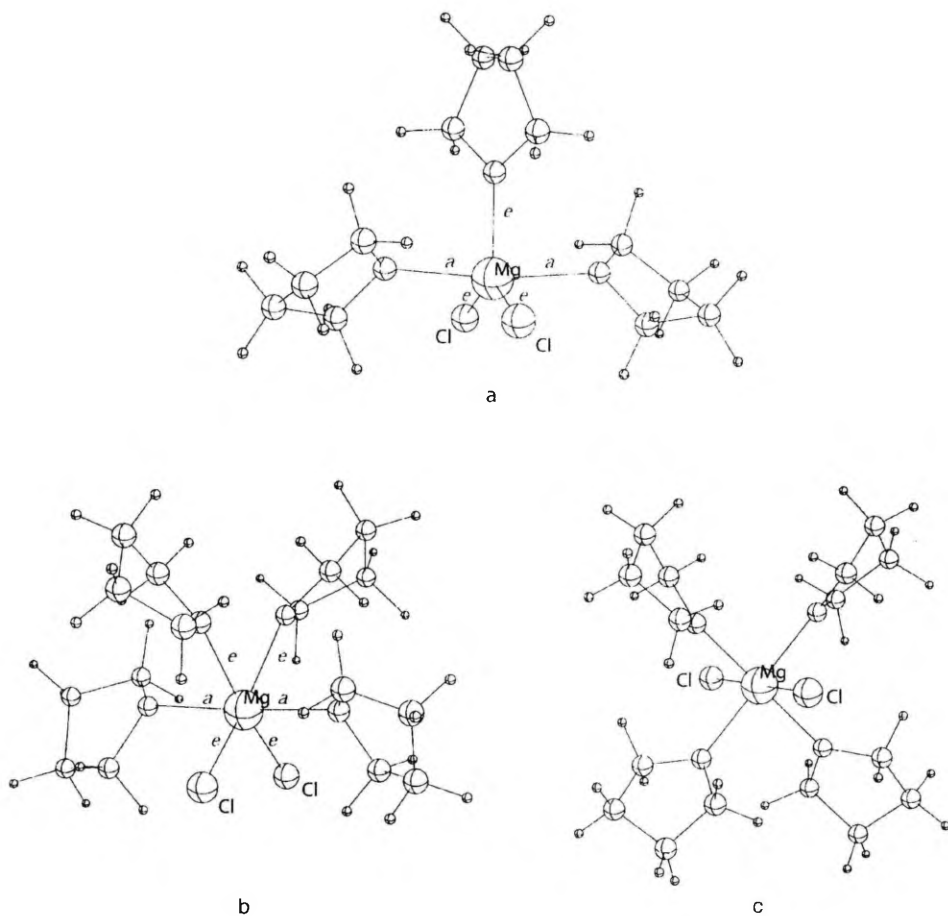


**Figure 2.** The optimized (at B3LYP/6-31+G\* level of theory) structures of tris-tetrahydrofuranate and tetrakis-tetrahydrofuranate complexes of magnesium halide: (a)  $\text{MgCl}_2 \cdot 3\text{THF}$ , (b) *cis*  $\text{MgCl}_2 \cdot 4\text{THF}$ , and (c) *trans*  $\text{MgCl}_2 \cdot 4\text{THF}$ .





Reproduced with permission from *Journal of Physical Organic Chemistry*, **2002**,  
15 (10), 701–705.

A. Tuulmets, V. Pällin, J. Tammiku-Taul, P. Burk, K. Raie,  
Solvent Effects in the Grignard Reaction with Alkynes.

Copyright 2002 John Wiley & Sons, Ltd.

# Solvent effects in the Grignard reaction with alkynes

A. Tuulmets,<sup>1\*</sup> V. Pällin,<sup>1</sup> J. Tammiku-Taul,<sup>1</sup> P. Burk<sup>2</sup> and K. Raie<sup>1</sup><sup>1</sup>Institute of Organic and Bioorganic Chemistry, University of Tartu, Tartu 51014, Estonia<sup>2</sup>Institute of Chemical Physics, University of Tartu, Tartu 51014, Estonia

Received 5 February 2002; revised 31 March 2002; accepted 23 April 2002

**ABSTRACT:** Kinetic studies were carried out on the reaction of phenylmagnesium bromide with hex-1-yne in diethyl ether, and in binary mixtures of diethyl ether with toluene, chlorobenzene and dichloromethane. The reaction was accelerated by addition of non-donating solvents. The replacement of a coordinated solvent molecule by the alkyne is necessary for the reaction to proceed, according to density functional theory (DFT) calculations with B3LYP/6-31 + G\* method. The non-donating solvents accelerate the reaction by shifting the replacement equilibrium in favour of the complex formation. An analysis in terms of the Koppel–Palm equation revealed a rate decrease with increase in solvent polarity and polarizability. Copyright © 2002 John Wiley & Sons, Ltd.

**KEYWORDS:** Grignard compounds; Grignard reaction; alkynes; kinetics; solvent effects; DFT calculations

## INTRODUCTION

Recently, we carried out a kinetic investigation of the Grignard reaction with acetylene.<sup>1,2</sup> In a solution to new details of the reaction mechanism, we observed large solvation effects which depend strongly on the steric requirements of both the Grignard reagent and the donors. However, the non-specific solvation effects were not investigated in that work.

In addition to a general interest, the effects of non-specific solvation can be informative concerning the reaction mechanism. In an earlier series of studies we were able to show quantitatively that in the Grignard addition reaction to ketones the transition states are of lower polarity than the reagents and, therefore probably have a cyclic structure.<sup>3–6</sup> A change in the polarity of the medium was achieved by addition of *n*-heptane or dichloromethane to the Grignard reagent prepared in a donor solvent. Linear plots of log *k* vs Kirkwood function were obtained for the reactions of pinacolone with ethylmagnesium and *n*-propylmagnesium bromides,<sup>4</sup> dipropylmagnesium<sup>3,5</sup> and diphenylmagnesium.<sup>6</sup> The susceptibility of the reactions to the polarity of the medium was remarkably dependent on the donating ability of donors (ethers, amines).<sup>6,7</sup>

In this work, we attempted to apply the same method to the Grignard reaction of alkynes with the goal of obtaining an insight into the solvation phenomena. The

reaction of hex-1-yne with phenylmagnesium bromide was selected as a model process.

## RESULTS AND DISCUSSION

The kinetics of the slow but sufficiently exothermic reaction were followed thermographically by means of the initial rates method in the same way as in our previous work<sup>8</sup> (for details, see Experimental). Phenylmagnesium bromide was prepared in diethyl ether and the required reagent solutions were obtained by addition of appropriate amounts of toluene, chlorobenzene or dichloromethane to the initial reagent. The previously used *n*-heptane<sup>3–6</sup> was not suitable since it caused precipitation of the reagents. Reaction media of different polarity/polarizability were generated in this way, while the specific solvation of the reagents presumably remained unchanged. The addition of toluene decreased the polarity and increased the polarizability of the solution, as can be seen in Table 1, whereas admixtures of chlorobenzene and dichloromethane caused increases in both the polarity and polarizability.

The results of the kinetic measurements are presented in Table 2. The rate constants are mean values for 3–4 parallel runs. The reproducibility of the data is within ±5%. The rate constant for the reaction in pure diethyl ether,  $5 \times 10^{-5} \text{ M}^{-1} \text{ s}^{-1}$  at 20 °C, is in reasonable agreement with  $k_{\text{H}} = 2 \times 10^{-4} \text{ M}^{-1} \text{ s}^{-1}$  at 31.5 °C determined by Dessy and Salinger.<sup>10</sup> It can be seen from Table 2 that all the added non-donating solvents increase the reaction rate regardless of their possible polarity/polarizability contribution.

\*Correspondence to: A. Tuulmets, Institute of Organic and Bioorganic Chemistry, University of Tartu, 2 Jakobi Str., Tartu 51014, Estonia. E-mail: tuulmets@chem.ut.ee

Contract/grant sponsor: Estonian Science Foundation; Contract/grant number: 4630.

**Table 1.** Polarity and polarizability parameters of the solvents investigated<sup>9</sup>

Solvent	Dielectric constant, $\epsilon$	Refractive index, $n$
Diethyl ether	4.267	1.353
Toluene	2.38	1.496
Chlorobenzene	5.69	1.524
Dichloromethane	8.93	1.424

The solvent polarizability effect was excluded for the Grignard reaction with ketones on the basis that the experimental points for both *n*-heptane and dichloromethane additions fit the same  $\log k$  vs Kirkwood function correlation.<sup>4</sup> For the reaction with alkynes, both medium effects can be involved. The rate constants were accordingly analyzed with the Koppel–Palm equation<sup>11,12</sup> [Eqn. (1)] where the terms for constant specific solvation were omitted:

$$\log k = \log k_0 + \gamma Y + pP \quad (1)$$

According to Ref. 11, the polarity,  $Y$ , and polarizability,  $P$ , were calculated as

$$Y = (\epsilon - 1)/(2\epsilon + 1) \quad (2)$$

$$P = (n^2 - 1)/(n^2 + 1) \quad (3)$$

The dielectric constants ( $\epsilon$ ) and refractive indexes ( $n$ ) for the solvent mixtures were calculated assuming additivity of the properties (by volume fractions). The Grignard reagents were considered as solvated with two ether molecules on average, so in the calculations 2 mol of ether per mole of reagent were not included in the solvent composition.

From the data in Table 2, we obtained the following equation for phenylmagnesium bromide solvated with

diethyl ether:

$$\log k_{II} = -5.65(\pm 0.36) - (1.02 \pm 0.61)Y + (9.4 \pm 1.4)P \quad (4)$$

$$R = 0.925, \quad SE = 0.068, \quad n = 12$$

Although the overall correlation is satisfactory, the polarity and polarizability terms are statistically significant at the 95% confidence level. The absolute value of the susceptibility factor in the polarity term is considerably smaller than those for the reactions with ketones.<sup>4-6</sup> However, the negative sign of the constant indicates a smaller polarity of the transition state in comparison with the reactants. This seems to be consistent with the four-centre mechanism postulated by Dessy *et al.*<sup>13</sup> for this reaction and subsequently supported by evidence of nucleophilic assistance in the reaction (see, e.g., Refs 1, 14 and 15). In contrast, the preponderant solvent polarizability term, suggesting a charge separation during the activation process, is less readily understood in this context. Therefore, a significant contribution of solvation equilibria shifts in the last term of Eqn. (4) as an artifact cannot be excluded.

To obtain a more reliable understanding of the data, DFT calculations were performed. The main question was whether an alkyne molecule can directly attack the organomagnesium compound via an  $S_{Ei}$  type of reaction or whether a preliminary replacement of a solvent molecule is necessary. The species involved in a Grignard reagent and their coordination complexes with an alkyne were studied in the gas phase using the DFT B3LYP/6-31 + G\* method. Solvation was modelled using the supermolecule approach (for details, see Calculation Methods). We present here only the most relevant data since an extensive computational investigation of the reaction is in progress, the results which will be published elsewhere.

In order to save computing time, Grignard reagents were modeled by MeMgBr, dimethyl ether was taken for

**Table 2.** Kinetic data for the reaction in various media at 20°C

Solvent	Molar fraction of the ether	Concentration (mol l <sup>-1</sup> )		Initial rate (dC/dt) × 10 <sup>5</sup> (mol l <sup>-1</sup> s <sup>-1</sup> )	$k_{II} \times 10^5$ (l mol <sup>-1</sup> s <sup>-1</sup> )	$k_{II}[E] \times 10^5$	$Y$	$P$
		PhMgBr	Hex-1-yne					
Et <sub>2</sub> O	1.0	0.503	0.528	1.25	4.72	36.53	0.343	0.178
Et <sub>2</sub> O + PhMe	0.92	0.503	0.528	1.24	4.68	33.39	0.338	0.182
Et <sub>2</sub> O + PhMe	0.62	0.503	0.528	1.42	5.38	25.42	0.315	0.198
Et <sub>2</sub> O + PhMe	0.23	0.503	0.528	4.13	15.6	26.36	0.274	0.216
Et <sub>2</sub> O + PhCl	0.96	0.487	0.512	1.19	4.80	35.71	0.345	0.181
Et <sub>2</sub> O + PhCl	0.92	0.473	0.496	1.24	5.28	37.70	0.346	0.183
Et <sub>2</sub> O + PhCl	0.84	0.446	0.469	1.34	6.31	41.20	0.350	0.188
Et <sub>2</sub> O + PhCl	0.22	0.503	0.528	2.85	10.7	18.08	0.372	0.223
Et <sub>2</sub> O + CH <sub>2</sub> Cl <sub>2</sub>	0.94	0.487	0.512	1.20	4.82	35.86	0.352	0.180
Et <sub>2</sub> O + CH <sub>2</sub> Cl <sub>2</sub>	0.88	0.473	0.496	1.19	5.11	36.48	0.359	0.181
Et <sub>2</sub> O + CH <sub>2</sub> Cl <sub>2</sub>	0.77	0.446	0.469	1.19	5.71	37.28	0.372	0.184
Et <sub>2</sub> O + CH <sub>2</sub> Cl <sub>2</sub>	0.15	0.503	0.528	1.85	6.46	10.92	0.414	0.200

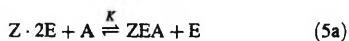
**Table 3.** Complexation energies ( $\Delta E$ ), enthalpies ( $\Delta H$ ) and Gibbs free energies ( $\Delta G$ ) for the reaction  $Z + \text{HC}\equiv\text{CCH}_3 \rightarrow Z\cdot\text{HC}\equiv\text{CCH}_3$  calculated at the B3LYP/6-31 + G\* level of theory [all values are given in kcal mol<sup>-1</sup> and are corrected for basis set superposition error (BSSE)]

Z	$\Delta E$	$\Delta H$	$\Delta G$
MgBr <sub>2</sub>	-8.35	-8.31	-0.25
MgBr <sub>2</sub> ·Me <sub>2</sub> O	-4.88	-4.38	4.50
MeMgBr	-5.37	-5.06	2.81
MeMgBr·Me <sub>2</sub> O	-2.84	-2.46	6.82
Me <sub>2</sub> Mg	-3.92	-3.66	4.45
Me <sub>2</sub> Mg·Me <sub>2</sub> O	-1.58	-1.08	7.07

the ether and propyne for alkynes. The gas-phase data are reasonably applicable to poorly polar ether solutions.

As shown in Table 3, the solvation of the magnesium compounds causes a substantial decrease in the complexation energies. It should be noted that the  $\Delta G$  values differ considerably from the  $\Delta E$  and  $\Delta H$  values, thus indicating a significant contribution of entropy. The complexes are weak and  $\Delta G$  of their formation is positive. Complexation of an alkyne with bisolvated magnesium species appeared to be energetically unfavourable (see also Fig. 1) and should be ruled out.

As a consequence, the reaction proceeds through the replacement of a solvent molecule by the alkyne and subsequent rate-limiting conversion of the complex to products:



$$v = k[ZEA] = kK \frac{[Z \cdot 2E][A]}{[E]} \quad (6)$$

where Z denotes a magnesium compound, A the alkyne and E an ether molecule.

The equilibrium constant  $K$  can be estimated from the

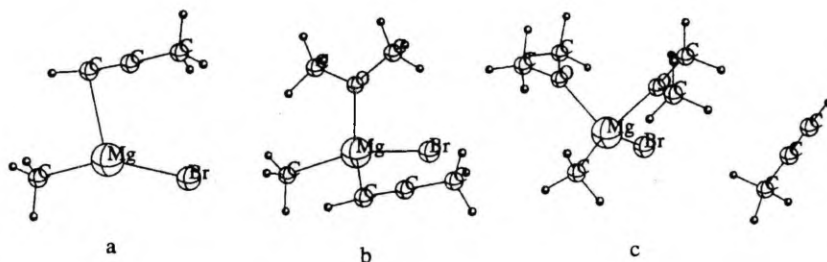


**Figure 1.** The optimized (at the B3LYP/6-31 + G\* level of theory) structures of the propyne complexes with (a) unsolvated methylmagnesium bromide, (b) monosolvated methylmagnesium bromide and (c) disolvated methylmagnesium bromide

**Table 4.** Estimated Gibbs free energies and equilibrium constants at 20 °C for the complex formation with propyne in dimethyl ether solution according to Eqns (7a) and (7b)

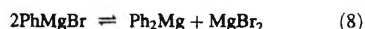
Complex	$\Delta G$ (kcal mol <sup>-1</sup> )	$K$
MgBr <sub>2</sub> ·Me <sub>2</sub> O·HC≡CCH <sub>3</sub>	8.68	$3.3 \times 10^{-7}$
MeMgBr·Me <sub>2</sub> O·HC≡CCH <sub>3</sub>	7.14	$4.7 \times 10^{-6}$
Me <sub>2</sub> Mg·Me <sub>2</sub> O·HC≡CCH <sub>3</sub>	4.22	$7.1 \times 10^{-4}$

equilibria



combining the data from Table 3 and the Gibbs free energies of solvation calculated in our previous work.<sup>16</sup> The results are presented in Table 4. When the Lewis acidity of the species decreases, the replacement of the ligands becomes easier. However, all the equilibria are shifted far to the left.

The nature of the phenylmagnesium bromide solution can also be represented by the Schlenk equilibrium:



shifted towards PhMgBr in diethyl ether ([PhMgBr]/[Ph<sub>2</sub>Mg] ≈ 8, from Refs 17 and 18). A semiquantitative treatment of the Lewis acidities of Grignard entities<sup>7</sup> indicated somewhat lower acidity of PhMgBr and Ph<sub>2</sub>Mg species in comparison with corresponding methyl compounds. Moreover, diethyl ether, as a weaker Lewis acid due to the steric demands, should enhance the acidity of the magnesium center compared with dimethyl ether. Consequently, the equilibrium constants for the complex formation in the phenylmagnesium bromide–hex-1-yne system must be greater to some extent than those in Table 4. Nevertheless, the concentrations of the complexes in

the reaction solution remain extremely low. This seems to be the reason for the rather feeble reactivity of alkynes, although the rate of product formation from an alkyne-Grignard complex appears to be unexpectedly large.

The equilibrium (5a) is shifted far to the left and the equilibrium can be taken into account by multiplying the observed rate constants by molar concentration of the free ether:

$$k_{\text{II}} = \frac{kK}{[\text{E}]} \quad (9)$$

Rate constants corrected in this way (Table 2) were correlated according to Eqn. (1) and the following equation was obtained:

$$\log [k_{\text{II}}[\text{E}]] = -1.02(\pm 0.54) - (2.6 \pm 0.9)Y - (8.4 \pm 2.0)P \quad (10)$$

$$R = 0.841, \quad SE = 0.101, \quad n = 12.$$

The concentration of free ether in the solution can be only roughly estimated, because the contribution of the Schlenk equilibrium [Eqn. (8)] and of the association equilibria of the species involved cannot be taken into account. This seems to be the reason for the relatively poor correlation of the data. However, the polarity and polarizability terms in Eqn. (10) are statistically significant and their signs are now coherent. Decelerating effects of solvent polarity and polarizability indicate a smaller polarity of the transition state in comparison with the reagents, thus presenting evidence in favour of a cyclic structure of the transition state.

The fast reactions of ketones can hence be rationalized on the basis of extensive complex formation with Grignard reagents. As the values for the equilibrium constants are large (for a review, see Ref. 19), with an excess of one of the reagents the other is almost completely bound and the changes in the solvent composition, similar to those in the present work, only slightly affect the positions of the equilibria. This explains why good linear  $\log k$  vs Kirkwood function plots have been obtained for the reactions of ketones.<sup>3-6</sup> Moreover, the refractive indexes of ethers and of non-donating additives used in those studies differed only slightly and therefore the contribution of solvent polarizability remained undetected.

## CONCLUSIONS

The reaction between an alkyne and Grignard reagent involves two consecutive steps, the first consisting in the replacement of a coordinated solvent molecule by the alkyne, followed by a unimolecular reaction of the complex. The complex formation equilibrium is shifted far towards the initial reagents and therefore, despite a

fast rearrangement of the complex to products, the overall reaction is slow.

Addition of non-donating solvents accelerates the reaction, presumably by shifting the replacement equilibrium in favour of the complex formation. In addition, a susceptibility of the reaction rate to changes in the solvent polarity and polarizability was revealed by a correlation analysis. This points to a smaller polarity of the transition state in comparison with the reagents, thus presenting evidence in favour of a cyclic structure of the transition state.

## EXPERIMENTAL

**Materials.** All the procedures with the reagents and solutions were carried out under dry argon. The Grignard reagents in diethyl ether were prepared in the conventional manner. The reagents in binary solutions were obtained by diluting the Grignard reagents with appropriate amounts of the ether and/or of the non-donating solvent.

**Kinetic measurements.** The reaction was carried out in a glass vessel mantled with foam plastic and placed in a thermostated housing. The equipment was sealed with a thermostated lid. The reaction cell was provided with a mechanical stirrer and a thermistor, which was connected through a bridge circuit to a recording potentiometer.

All parts of the equipment and the reagents were thermostated. The reaction vessel was purged thoroughly with pure argon, 15 ml of the Grignard reagent were cannulated into the cell and the stirring was started. After thermal equilibrium, 0.92 ml of hex-1-yne was introduced and the temperature change of the reaction solution (usually 0.1–0.2°C) was recorded as a plot of temperature versus time. Because the system was nearly adiabatic, the heat exchange with the internal part of the calorimeter caused only a little heat loss.

The zero-order initial rate constants in  $\text{mol l}^{-1} \text{s}^{-1}$  were obtained dividing the rate constants, determined as the slope of the tangent to the kinetic curve at the initial point, by the molar temperature rise of the reaction. The latter was determined from a separate run with the same reagent containing about 10 mol% triethylamine. The rapid and complete reaction of 30  $\mu\text{l}$  of hex-1-yne raised the temperature by about 0.6°C and provided the total heat of the reaction under the experimental conditions. The second-order rate constants were obtained dividing the initial rate constants by initial concentrations of hex-1-yne and the Grignard reagents.

## CALCULATION METHODS

All calculations were carried out using the Gaussian 98 program package.<sup>20</sup>

Optimizations and vibrational analysis were done using DFT with hybrid B3LYP functional and the 6-31 + G\* basis set. All stationary points were found to be true minima (number of imaginary frequencies,  $N_{\text{Imag}} = 0$ ). The calculated frequencies were also used for calculations of enthalpies and Gibbs free energies. The stability of the complexes was calculated considering the basis set superposition error estimated according to the counterpoise correction method of Boys and Bernardi.<sup>21</sup>

## REFERENCES

- Pällin V, Otsa E, Tuulmets A. *J. Organomet. Chem.* 1999; **590**: 149–152.
- Pällin V, Tuulmets A. *Main Group Met. Chem.* 2000; **23**: 179–182.
- Koppel J, Tuulmets A. *Reakts. Sposobn. Org. Soedin.* 1970; **7**: 911–918.
- Koppel J, Loit J, Luuk M, Tuulmets A. *Reakts. Sposobn. Org. Soedin.* 1971; **8**: 1155–1164.
- Koppel J, Tuulmets A. *Reakts. Sposobn. Org. Soedin.* 1972; **9**: 399–411.
- Viiraid S, Kurrikoff S, Tuulmets A. *Org. React. (Tartu)* 1974; **11**: 73–80.
- Tuulmets A. *Org. React. (Tartu)* 1974; **11**: 81–100.
- Pällin V, Tuulmets A. *J. Organomet. Chem.* 1999; **584**: 185–189.
- Handbook of Chemistry and Physics* (79th edn) Lide DR (ed). CRC Press: Boca Raton, FL, 1998–99.
- Dessy RE, Salinger RM. *J. Org. Chem.* 1961; **26**: 3519–3520.
- Koppel IA, Palm VA. In *Advances in Linear Free Energy Relationships*, Chapman NB, Shorter J (eds). Plenum Press: New York, 1972; chapt. 5.
- Reichardt C. *Solvents and Solvent Effects in Organic Chemistry*. VCH: Weinheim, 1988.
- Dessy RE, Wotiz JH, Hollingsworth CC. *J. Am. Chem. Soc.* 1957; **79**: 358–362.
- Dessy RE, Paulik E. *J. Am. Chem. Soc.* 1963; **83**: 1812–1819.
- Abraham MH, Hill JA. *J. Organomet. Chem.* 1967; **7**: 11–21.
- Tammiku J, Burk P, Tuulmets A. *J. Phys. Chem. A* 2001; **105**: 8554–8561.
- Smith MB, Becker WE. *Tetrahedron* 1966; **22**: 3027–3036.
- Smith MB, Becker WE. *Tetrahedron* 1967; **23**: 4215–4219.
- Holm T, Crossland I. In *Grignard Reagents: New Developments*, Richey HG (ed). Wiley: New York, 2000; chapt. 1.
- Frisch MJ, Trucks GW, Schlegel HB, Scuseria GE, Robb MA, Cheeseman JR, Zakrzewski VG, Montgomery Jr. JA, Stratmann RE, Burant JC, Dapprich S, Millam JM, Daniels AD, Kudin KN, Strain MC, Farkas O, Tomasi J, Barone V, Cossi M, Cammi R, Mennucci B, Pomelli C, Adamo C, Clifford S, Ochterski J, Petersson GA, Ayala PY, Cui Q, Morokuma K, Malick DK, Rabuck AD, Raghavachari K, Foresman JB, Cioslowski J, Ortiz JV, Stefanov BB, Liu G, Liashenko A, Piskorz P, Komaromi I, Gomperts R, Martin RL, Fox DJ, Keith T, Al-Laham MA, Peng CY, Nanayakkara A, Gonzalez C, Challacombe M, Gill PMW, Johnson B, Chen W, Wong MW, Andres JL, Gonzalez C, Head-Gordon M, Replogle ES, Pople JA. *Gaussian 98, Revision A7*. Gaussian: Pittsburgh PA, 1998.
- Boys SF, Bernardi F. *Mol. Phys.* 1976; **19**: 325–330.





*Journal of Molecular Structure (Theochem)*, **2003**, submitted.  
A. Tuulmets, J. Tammiku-Taul, P. Burk,  
Computational Study of the Grignard Reaction with Alkynes.

# Computational study of the Grignard reaction with alkynes

Ants Tuulmets,<sup>1</sup> Jaana Tammiku-Taul<sup>1</sup> and Peeter Burk<sup>2\*</sup>

Department of Chemistry, <sup>1</sup>Institute of Organic and Bioorganic Chemistry,  
<sup>2</sup>Institute of Chemical Physics, University of Tartu, Jakobi 2, 51014 Tartu,  
Estonia

## Abstract

The complexation of  $MgX_2$ ,  $MeMgX$ , and  $Me_2Mg$  ( $X = Cl, Br$ ) with propyne have been studied both in the gas phase and in the presence of dimethyl ether ( $Me_2O$ ) by means of the density functional theory (DFT) B3LYP/6-31+G\* method. Solvation was modeled using the supermolecule approach. The complex formation between disolvated magnesium compound and alkyne is connected with replacement of a coordinated solvent molecule by the alkyne, being necessary for the reaction to proceed to the end. The reaction towards end products, an acetylenic Grignard reagent and an alkane, is exothermic. The transition state has a cyclic structure, which is almost triangular with practically linear proton transfer. The transition state resembles more the reagents than the products.

Keywords: Grignard compounds; alkynes; transition states; DFT calculations.

## 1. Introduction

Acetylenic Grignard compounds and the corresponding organometallic derivatives are important intermediates in many syntheses of acetylenic compounds [1].

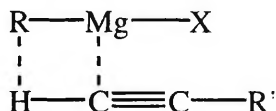
The first acetylenic Grignard reagents of the type  $RC\equiv CMgX$  ( $R = C_6H_5, n-C_5H_{11}$ ) were obtained by J. Iotsitch [2]. Subsequently the reactions of acetylenic compounds with Grignard reagents have been investigated occasionally over many years [3] and in some extent also in our laboratory. During recent years our efforts have been focused on elucidation of the mechanism of the Grignard reaction with acetylene and on the solvent effects in reactions of acetylenic compounds with Grignard reagents [4-8].

We observed large solvation effects, which depended strongly on the steric requirements of both the Grignard reagent and the donors. Using density functional theory (DFT) calculations we have shown that the replacement of a

---

\* Corresponding author. Tel.: +372-7-375-258; fax: +372-7-375-264.  
E-mail address: burk@ut.ee

coordinated solvent molecule by the alkyne in a complex of disolvated magnesium compound is necessary for the reaction to proceed [7]. An analysis of kinetic data in terms of the Koppel-Palm equation [9] revealed a rate decrease with increase in solvent polarity and polarizability [7,8] taken for evidence of smaller polarity of the transition state in comparison with the reagents. These results are well in favour of a cyclic structure of the transition state (Scheme 1) suggested by Dessy et al. [10] and supported inter alia by the significance of the nucleophilic assistance by the acetylenic group as stressed in our work [5].



Scheme 1. A cyclic structure of the transition state for a complex between magnesium compound and alkyne molecule.

Thus, the reaction with alkynes consists of replacement of a donor ligand at the magnesium centre by the alkyne followed by subsequent rearrangement of the complex to products. Our previous calculations estimated very small equilibrium constants for the complex formation [7], thus, the concentration of the complex in the reaction solution remains extremely low. This seems to be the reason for the rather feeble reactivity of alkynes, although the rate of product formation from an alkyne-Grignard complex appears to be large.

The generally accepted transition state structure in Scheme 1 is merely a symbolic sketch, representing no real bond lengths and angles or any atomic charges. No necessary experimental data are available to give more fundamental information about the transition state. For that reason, and with an aim to obtain a more detailed insight into the mechanism of the reaction, we carried out an extensive computational investigation of the reaction by means of DFT calculations. In order to save the computing time, all calculations were carried out for model compounds, i.e., we used organomagnesium compounds with methyl group and propyne as alkyne. Their reactions were investigated in the gas phase and in the solvated state, using dimethyl ether as the donor.

Solutions of alkyl- and arylmagnesium halides, particularly those of chlorides contain also dimers and higher oligomers. The degree of association increases with an increase in the concentration of the reagents [11]. Relative reactivity of monomers and oligomers is not yet clear. In this work only monomeric Grignard reagents have been considered.

## 2. Calculation methods

The calculations were carried out using the GAUSSIAN 98 [12] program package.

All geometry optimizations and vibrational analysis were done using the density functional theory (DFT) with hybrid B3LYP functional and the 6-31+G\* basis set (B3LYP/6-31+G\*). Stationary points were found to be true minima (number of imaginary frequencies,  $N_{\text{Imag}} = 0$ ) for reagents and products. The first order saddle point was found on the surface of potential energy ( $N_{\text{Imag}} = 1$ ) for the transition state. The calculated frequencies were also used for calculations of enthalpies and Gibbs energies. The reaction path from the obtained transition state was followed both in reverse (towards the reagents) and forward (towards the products) direction to verify that the correct transition state, which connects the reactants and products, was obtained [13].

Solvation was modeled using the supermolecule approach, which is the best method to describe the specific solvent effects. Up to two molecules of dimethyl ether were added to the studied species.

The basis set superposition error (BSSE) estimated according to the counterpoise (CP) correction [14] was taken into account. The BSSE arises from the mathematical fact that the basis sets are not complete and it should be considered in the case of complexation energies. The dimer (complex) energy minus the monomer energies is the directly calculated complexation energy,  $\Delta E_{\text{complexation}}$ .

$$\Delta E_{\text{complexation}} = E(AB)_{ab}^* - E(A)_a - E(B)_b \quad (1)$$

To estimate how much of this complexation energy is due to BSSE, the complex was divided into fragments, thus, four (for the unsolvated systems) up to eight (for the disolvated systems) additional energy calculations were needed. The CP correction is defined as

$$\Delta E_{\text{CP}} = E(A)_{ab}^* + E(B)_{ab}^* - E(A)_a^* - E(B)_b^* \quad (2)$$

where  $E(A)_{ab}^*$  and  $E(B)_{ab}^*$  are the monomer energies with the basis set of complex,  $E(A)_a^*$  and  $E(B)_b^*$  are the monomer energies with their normal basis sets. In all cases the monomers were calculated with the geometry they have in complex. The counterpoise corrected complexation energy,  $\Delta E_{\text{BSSE}}$ , is given as

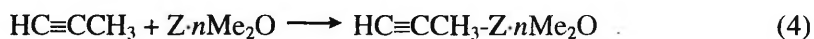
$$\Delta E_{\text{BSSE}} = \Delta E_{\text{complexation}} - \Delta E_{\text{CP}} \quad (3)$$

The BSSE had a particularly strong influence on the complexation energies of the bromine-containing compounds compared to the corresponding chlorine compounds, indicating somewhat less satisfactory description of bromine basis set. The activation energies were calculated without BSSE corrections. There is no general rule how to separate the transition state into interacting fragments.

### 3. Results and discussion

#### 3.1. Complexation energies of magnesium compounds with alkyne

The complexation energies of unsolvated, mono- and disolvated magnesium compounds with propyne were calculated from Eq. 4, where Z is  $\text{MgX}_2$ ,  $\text{MeMgX}$  or  $\text{Me}_2\text{Mg}$  ( $\text{X} = \text{Cl}, \text{Br}$ ) and the number of solvent molecules, dimethyl ether ( $\text{Me}_2\text{O}$ ),  $n$  is 0, 1 or 2.



The results are given in Table 1. The optimized structures of some unsolvated and solvated complexes are shown in Fig. 1a-d. The complexation enthalpies are exothermic for all the studied systems. The stability of the complex,  $\Delta H_0$  for unsolvated and  $\Delta H_1$  for monosolvated species, is largest for the magnesium halides,  $\text{MgX}_2$ , ( $\Delta H_0 = -8.3\dots-12.1$  kcal/mol,  $\Delta H_1 = -5.5\dots-6.6$  kcal/mol) and least for the dimethyl magnesium compound,  $\text{Me}_2\text{Mg}$ , ( $\Delta H_0 = -3.7$  kcal/mol,  $\Delta H_1 = -1.1$  kcal/mol) with intermediate values for the methylmagnesium halides,  $\text{MeMgX}$ , ( $\Delta H_0 = -5.1\dots-7.2$  kcal/mol,  $\Delta H_1 = -3.1\dots-3.7$  kcal/mol). The chlorine-containing complexes are somewhat more stable than the corresponding bromine-containing complexes because of more electronegative and smaller chlorine atom. The lowest stability of  $\text{Me}_2\text{Mg}$  complex is due to the fact that  $\text{Me}_2\text{Mg}$  is sterically the most unfavourable, as two relatively bulky methyl groups are directly bound to the magnesium atom. However, the solvation of the magnesium compounds causes a substantial change in the complexation energies. The addition of the first solvent molecule to the magnesium compound destabilizes the formed complex by 2.0...5.5 kcal/mol and the second solvent molecule has an additional 0.7...5.9 kcal/mol destabilizing effect. The complexation via hydrogen bonding between the Br-atom of the disolvated magnesium compound and the H-atom of acetylenic methyl group of propyne (Fig. 1c) appeared to be energetically unfavourable ( $\Delta H_2 = -0.2\dots-0.8$  kcal/mol). Another structure of hydrogen-bonded complex, where a hydrogen bond is formed between the Br-atom of magnesium compound and the acetylenic H-atom of propyne (Fig. 1d), is even less stable than the above-mentioned disolvated complexes, by 0.6 and 1.5 kcal/mol, respectively. It should be noted that the values of  $\Delta G$  for all complexes differ considerably from the  $\Delta E$  and  $\Delta H$ , thus, indicating a significant contribution of

entropy. The complexes are weak and  $\Delta G$  of their formation is positive in most cases.

As a consequence, the reaction only proceeds through replacement of a solvent molecule by the alkyne (Eq. 5a) and subsequent rate limiting conversion of the complex to products (Eq. 5b):



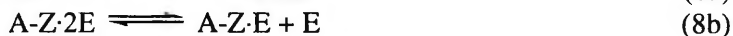
$$v = k[A \cdot Z \cdot E] = kK \frac{[Z \cdot 2E][A]}{[E]} \quad (6)$$

where Z denotes a magnesium compound, A an alkyne, and E an ether molecule.

The complex between the alkyne and monosolvated magnesium compound can form in two ways and, thus, the equilibrium constant K can be estimated either (i) from the equilibria (i.e.,  $S_N1$  mechanism of the ligand exchange)



or (ii) from the equilibria (i.e., a  $S_N2$  like mechanism)



combining the data from Table 1 and the Gibbs energies of solvation of magnesium compounds with one or two dimethyl ether molecules calculated in our previous work [15]. The thermodynamic effect is identical for the both cases and the results are presented in Table 2. According to our calculations the equilibrium is shifted far to the left, thus, the observed reaction rate is related to the fast conversion of the complex to products. Recently we found [7,8] that addition of non-donating solvents to ethereal solutions of Grignard reagent accelerated the reaction regardless of the polarity/polarizability of added cosolvents. Obviously reduced content of the ether in the reaction mixture shifted the equilibrium to the right, thus, enhancing the rate of the reaction.

### 3.2. The end products and the transition state of Grignard reaction with alkyne

The formation energies of the end products were only calculated starting from unsolvated ( $n = 0$ ) and monosolvated ( $n = 1$ ) complexes of organomagnesium compounds with propyne according to Eqs. (9) and (10):



The results are given in Table 3. The reaction towards the end products, acetylenic Grignard reagent and methane, is exothermic. As expected, the reaction in solution is by 4.2...6.0 kcal/mol more exothermic than in the gas phase,  $\Delta H = -12.5\text{...}-17.6$  kcal/mol for the unsolvated species and  $\Delta H = -18.5\text{...}-23.3$  kcal/mol for the monosolvated species, respectively. This is in agreement with the experimental enthalpy of metallation of Brønsted acid  $\text{C}_6\text{H}_5\text{-C}\equiv\text{CH}$  with pentylmagnesium bromide in diethyl ether ( $\Delta H = -30.1$  kcal/mol) determined by Holm [16].

The activation energies for the forward reaction (relative to the propyne-Grignard complex) and for the reverse reaction (relative to the end products) are given in Table 4. The activation barrier for the monosolvated reagents is lower by 4.7...5.2 kcal/mol than in the gas phase,  $\Delta H^\ddagger_{\text{forward}} = 27.6\text{...}27.9$  kcal/mol for the unsolvated reagents, and  $\Delta H^\ddagger_{\text{forward}} = 22.6\text{...}22.9$  kcal/mol for the monosolvated reagents, respectively. The heights of the enthalpy barrier for the unsolvated and monosolvated products are comparable with each other and there is no remarkable difference between chlorine and bromine-containing species ( $\Delta H^\ddagger_{\text{reverse}} = 39.1\text{...}41.0$  kcal/mol). The activation enthalpies for the reverse reaction are by 12.1...18.1 kcal/mol higher compared to the reactants, being consistent with the exothermic formation of the end products. Available rate constants for the reaction of Grignard reagent  $\text{PhCH}_2\text{MgCl}$  with proton donor  $\text{PhC}\equiv\text{CH}$  in diethyl ether [17] afforded a calculation of the activation energy equal to 16.7 kcal/mol, being in correlation with our computational activation energies for the monosolvated reagents.

The optimized structures for unsolvated and monosolvated reagents, transition states (TS), and end products are shown in Fig. 2. The structure of the transition state is consistent with the cyclic four-centre transition state postulated by Dessy et al. [10], however, the actual geometry of the transition state is almost triangular with practically linear proton transfer. From the data in Table 4 negligible entropy change during activation is obvious. From the values of the complexation enthalpies,  $\Delta H$ , and Gibbs energies,  $\Delta G$ , (see Table 1) becomes evident that the entropy change,  $\Delta S$ , lies in the range between  $-21.7\text{...}-31.2$  cal/K·mol (at 298 K). Consequently, the overall entropy loss between the initial reagents and the transition state (about  $-25\text{...}-30$  cal/K·mol)

is mainly due to complexation of the reagents. Indeed, the cycle closing actually takes place at atoms C1-H-C2 (see Fig. 2) and does not involve freezing out of many degrees of freedom.

Selected bond lengths for reagents, transition states, and products were calculated and the results are listed in Table 5. In the transition state the donor bond between the Mg-atom and the acetylenic C-atom (Mg-C2) is shortened close to a covalent bond length, while Mg-C1 bond in the Grignard moiety is stretched up by 0.12...0.15 Å. The proton transfer between C1 and C2 centres is accomplished up to an 40% extent, as regards the bond lengths C1-H and C2-H. It can be concluded that the transition state, which lies on the reaction path between reagents and products, slightly resembles the reagents. This is in accordance with the exothermicity of the reaction and with the enthalpy values for the activation, as well as with available values for kinetic isotope effects. Pocker and Exner [17] have found the kinetic deuterium isotope effect for the reactions of several organomagnesiums with phenylacetylene in diethyl ether to be  $4.6 \pm 0.2 \dots 6.2 \pm 0.2$ . The same effect in tetrahydrofuran (THF) solution was equal to  $3.0 \pm 0.2 \dots 3.6 \pm 0.2$ , accompanied with higher reactivity in THF medium [17]. The effect of stronger solvation, resulting in a shift of the transition state towards the reagents, can be observed also in our computational data, if to compare the lengthening of Mg-C1 bond in the unsolvated and monosolvated transition states.

Polarity of the transition state can be estimated regarding its dipole moment. The most straightforward comparison can be done for the propyne-Grignard complex and the corresponding transition state. The calculated dipole moments for the propyne-Grignard complexes and the transition states are presented in Table 6. It appears that the solvated initial systems are slightly more polar in comparison with the transition states. Although the change in the polarity during activation is almost negligible, it does not contradict to a slight suppressing effect of solvent polarity and polarizability found for the reaction of hex-1-yne with phenylmagnesium bromide solvated with diethyl ether and quantitatively described with Koppel-Palm equation in our previous work [7].

#### 4. Conclusions

The reaction between an alkyne and a disolvated Grignard reagent involves two consecutive steps, the first consisting in the replacement of a coordinated solvent molecule by the alkyne, followed by an unimolecular reaction of the complex. The complex formation equilibrium is shifted far towards the initial reagents, therefore, despite of a fast rearrangement of the complex to products the overall reaction is slow.



The activation barrier of the reverse reaction is considerably higher than that for the forward reaction. Thus, the formation reaction of the end products, acetylenic Grignard reagent and alkane, is exothermic. The transition state has a cyclic four-centre structure, although the optimized structure for the transition state is almost triangular with practically linear proton transfer. The cycle formation is largely connected with the complexation of reagents. From the calculated values of complexation enthalpies and Gibbs energies becomes evident that the entropy change is in the range -22...-31 cal/K-mol, which is common for cycle formation. According to our DFT calculations the transition state lies on the reaction path closer to the reagents than to the end products. All calculated values are consistent with available experimental data.

### Acknowledgements

The authors gratefully acknowledge the financial support of this research by Estonian Science Foundation (grant 4630).

### References

- [1] L. Brandsma, H.D. Verkruisje, *Synthesis of Acetylenes, Allenes and Cumulenes*, Elsevier, Amsterdam, 1981.
- [2] J. Jotsitch, *Bull. Soc. Chim. Fr.* 28 (1902) 922.
- [3] W.E. Lindsell, in G. Wilkinson (Ed.), *Comprehensive Organometallic Chemistry*, Vol. 1, Pergamon Press, 1982, Chapter 4, *Comprehensive Organometallic Chemistry II*, Vol. 1, Pergamon Press, 1995, Chapter 3.
- [4] V. Pällin, A. Tuulmets, *J. Organomet. Chem.* 584 (1999) 185.
- [5] V. Pällin, E. Otsa, A. Tuulmets, *J. Organomet. Chem.* 590 (1999) 149.
- [6] V. Pällin, A. Tuulmets, *Main Group Met. Chem.* 23 (2000) 179.
- [7] A. Tuulmets, V. Pällin, J. Tammiku-Taul, P. Burk, K. Raie, *J. Phys. Org. Chem.* 15 (2002) 701.
- [8] V. Pällin, A. Tuulmets, K. Raie, *Main Group Met. Chem.* 25 (2002) 297.
- [9] I.A. Koppel, V.A. Palm, in N.B. Chapman, J. Shorter (Eds.), *Advances in Linear Free Energy Relationships*, Plenum Press, New York, 1972, Chapter 5.
- [10] R.E. Dessy, J.H. Wotiz, C.A. Hollingsworth, *J. Am. Chem. Soc.* 79 (1957) 358.
- [11] F.W. Walker, E.C. Ashby, *J. Am. Chem. Soc.* 91 (1969) 3845.
- [12] M.J. Frisch, G.W. Trucks, H.B. Schlegel, G.E. Scuseria, M.A. Robb, J.R. Cheeseman, V.G. Zakrzewski, J.A. Montgomery, Jr., R.E. Stratmann, J.C. Burant, S. Dapprich, J.M. Millam, A.D. Daniels, K.N. Kudin, M.C. Strain, O. Farkas, J. Tomasi, V. Barone, M. Cossi, R. Cammi, B. Mennucci, C. Pomelli, C. Adamo, S. Clifford, J. Ochterski, G.A.

Petersson, P.Y. Ayala, Q. Cui, K. Morokuma, D.K. Malick, A.D. Rabuck, K. Raghavachari, J.B. Foresman, J. Cioslowski, J.V. Ortiz, A.G. Baboul, B.B. Stefanov, G. Liu, A. Liashenko, P. Piskorz, I. Komaromi, R. Gomperts, R.L. Martin, D.J. Fox, T. Keith, M.A. Al-Laham, C.Y. Peng, A. Nanayakkara, C. Gonzalez, M. Challacombe, P.M.W. Gill, B. Johnson, W. Chen, M.W. Wong, J.L. Andres, C. Gonzalez, M. Head-Gordon, E.S. Replogle, J.A. Pople, GAUSSIAN 98, Revision A.7, Gaussian, Inc., Pittsburgh PA, 1998.

- [13] J.B. Foresman, Æ. Frisch, Exploring Chemistry with Electronic Structure methods, 2<sup>nd</sup> Ed., Gaussian, Inc., Pittsburgh PA, 1996.
- [14] F.B. Van Duijneveldt, J.G.C.M. Van Duijneveldt-Van de Rijdt, J.H. Van Lenthe, Chem. Rev. 94 (1994) 1873.
- [15] J. Tammiku, P. Burk, A. Tuulmets, J. Phys. Chem. A 105 (2001) 8554.
- [16] T. Holm, Acta Chem. Scand. B 37 (1983) 797.
- [17] Y. Pocker, J.H. Exner, J. Am. Chem. Soc. 90 (1968) 6764.

Table 1

Complexation energies ( $\Delta E$ ), enthalpies ( $\Delta H$ ), and Gibbs energies ( $\Delta G$ ) of unsolvated, mono- and disolvated magnesium compounds with propyne calculated at the B3LYP/6-31+G\* level of theory. All values are in kcal/mol and include BSSE corrections.

Z	$\Delta E$	$\Delta H$	$\Delta G$
$\text{HC}\equiv\text{CCH}_3 + \text{Z} \longrightarrow \text{HC}\equiv\text{CCH}_3\text{-Z}$			
MgCl <sub>2</sub>	-12.22	-12.08	-5.06
MgBr <sub>2</sub>	-8.35	-8.31	-0.25
MeMgCl	-7.59	-7.15	-0.47
MeMgBr	-5.37	-5.06	2.81
Me <sub>2</sub> Mg	-3.92	-3.66	4.45
MgCl <sub>2</sub> ·Me <sub>2</sub> O	-7.08	-6.59	1.93
MgBr <sub>2</sub> ·Me <sub>2</sub> O	-6.02	-5.52	3.36
MeMgCl·Me <sub>2</sub> O	-4.25	-3.73	4.70
MeMgBr·Me <sub>2</sub> O	-3.48	-3.11	6.18
Me <sub>2</sub> Mg·Me <sub>2</sub> O	-1.64	-1.14	7.02
MgCl <sub>2</sub> ·2Me <sub>2</sub> O	-1.41	-0.71	6.68
MgBr <sub>2</sub> ·2Me <sub>2</sub> O	-0.78	-0.18	7.79
MeMgCl·2Me <sub>2</sub> O <sup>a</sup>	-1.54	-0.79	5.69
MeMgBr·2Me <sub>2</sub> O <sup>a</sup>	-1.24	-0.61	6.78
MeMgCl·2Me <sub>2</sub> O <sup>b</sup>	-0.96	-0.20	5.06
MeMgBr·2Me <sub>2</sub> O <sup>b</sup>	1.24	0.92	10.47
Me <sub>2</sub> Mg·2Me <sub>2</sub> O	-0.79	-0.42	6.86

<sup>a</sup> Calculated for the structure c in Fig. 1.

<sup>b</sup> Calculated for the structure d in Fig. 1.

Table 2

Estimated Gibbs energies and equilibrium constants at 298 K for the complex formation of magnesium compounds with propyne in dimethyl ether solution according to Eqs. (7a-b) or (8a-b).

Complex	$\Delta G$ (kcal/mol)	$K$
$\text{HC}\equiv\text{CCH}_3\cdot\text{MgCl}_2\cdot\text{Me}_2\text{O}$	8.32	$7.9 \times 10^{-7}$
$\text{HC}\equiv\text{CCH}_3\cdot\text{MgBr}_2\cdot\text{Me}_2\text{O}$	7.55	$2.9 \times 10^{-6}$
$\text{HC}\equiv\text{CCH}_3\cdot\text{MeMgCl}\cdot\text{Me}_2\text{O}$	6.00	$4.0 \times 10^{-5}$
$\text{HC}\equiv\text{CCH}_3\cdot\text{MeMgBr}\cdot\text{Me}_2\text{O}$	6.50	$1.7 \times 10^{-5}$
$\text{HC}\equiv\text{CCH}_3\cdot\text{Me}_2\text{Mg}\cdot\text{Me}_2\text{O}$	4.17	$8.7 \times 10^{-4}$

Table 3

Energies ( $\Delta E$ ), enthalpies ( $\Delta H$ ), and Gibbs energies ( $\Delta G$ ) for the formation reaction of the end products according to Eqs. (9) and (10) calculated at the B3LYP/6-31+G\* level of theory. All values are in kcal/mol and include BSSE corrections.

Complex	$\Delta E$	$\Delta H$	$\Delta G$
HC≡CCH <sub>3</sub> -MeMgCl	-13.08	-12.50	-14.98
HC≡CCH <sub>3</sub> -MeMgBr	-16.28	-15.59	-20.17
HC≡CCH <sub>3</sub> -Me <sub>2</sub> Mg	-18.49	-17.61	-22.88
HC≡CCH <sub>3</sub> -MeMgCl·Me <sub>2</sub> O	-19.41	-18.55	-26.20
HC≡CCH <sub>3</sub> -MeMgBr·Me <sub>2</sub> O	-20.63	-19.79	-29.49
HC≡CCH <sub>3</sub> -Me <sub>2</sub> Mg·Me <sub>2</sub> O	-23.47	-23.28	-26.52

Table 4

Activation energies ( $\Delta E^\ddagger$ ), enthalpies ( $\Delta H^\ddagger$ ), and Gibbs energies ( $\Delta G^\ddagger$ ) for the forward reaction (relative to the propyne-Grignard complex) and for the reverse reaction (relative to the end products, acetylenic Grignard reagent and methane). All values are in kcal/mol.

Z	$\Delta E^\ddagger_{\text{forwar}}$	$\Delta H^\ddagger_{\text{forward}}$	$\Delta G^\ddagger_{\text{forwar}}$	$\Delta E^\ddagger_{\text{reverse}}$	$\Delta H^\ddagger_{\text{reverse}}$	$\Delta G^\ddagger_{\text{revers}}$
	d		d			e
MeMgCl	28.05	27.60	28.59	40.71	39.68	43.16
MeMgBr	28.48	27.90	28.31	42.38	41.12	46.10
MeMgCl·Me <sub>2</sub> O	23.20	22.87	22.68	42.18	40.98	48.44
MeMgBr·Me <sub>2</sub> O	22.96	22.64	22.59	40.30	39.14	45.36

Table 5

Selected bond lengths for reagents (propyne-Grignard complex), transition states, and products (acetylenic Grignard reagent and methane) at B3LYP/6-31+G\* level. All distances are in angstroms, Å.

Bond	Reagents	TS state	Products	Comments
$\text{HC}\equiv\text{CCH}_3\text{-MeMgCl} \longrightarrow \text{Mg}(\text{Cl})\text{-C}\equiv\text{CCH}_3 + \text{CH}_4$				
Mg-C1	2.097	2.206	3.213	lengthens
Mg-C2	2.545	2.198	2.006	shortens
C1-H	3.087	1.599	1.097	shortens
C2-H	1.070	1.313	2.964	lengthens
C1-C2	3.454	2.892	3.916	both
$\text{HC}\equiv\text{CCH}_3\text{-MeMgBr} \longrightarrow \text{Mg}(\text{Br})\text{-C}\equiv\text{CCH}_3 + \text{CH}_4$				
Mg-C1	2.096	2.212	3.622	lengthens
Mg-C2	2.551	2.202	1.999	shortens
C1-H	3.000	1.608	1.096	shortens
C2-H	1.069	1.302	4.192	lengthens
C1-C2	3.395	2.890	4.108	both
$\text{HC}\equiv\text{CCH}_3\text{-MeMgCl}\cdot\text{Me}_2\text{O} \longrightarrow \text{Me}_2\text{O}\cdot\text{Mg}(\text{Cl})\text{-C}\equiv\text{CCH}_3 + \text{CH}_4$				
Mg-C1	2.117	2.239	4.818	lengthens
Mg-C2	2.675	2.272	2.039	shortens
C1-H	2.994	1.581	1.095	shortens
C2-H	1.069	1.314	4.919	lengthens
C1-C2	3.425	2.884	4.428	both
$\text{HC}\equiv\text{CCH}_3\text{-MeMgBr}\cdot\text{Me}_2\text{O} \longrightarrow \text{Me}_2\text{O}\cdot\text{Mg}(\text{Br})\text{-C}\equiv\text{CCH}_3 + \text{CH}_4$				
Mg-C1	2.113	2.263	4.664	lengthens
Mg-C2	2.671	2.266	2.038	shortens
C1-H	2.975	1.486	1.095	shortens
C2-H	1.069	1.372	4.712	lengthens
C1-C2	3.412	2.838	4.297	both

Table 6

Dipole moments (in Debye units, D) for reagents (propyne-Grignard complex) and transition states.

Complex	Reagents	TS state
$\text{HC}\equiv\text{CCH}_3\text{-MeMgCl}$	4.4760	4.9739
$\text{HC}\equiv\text{CCH}_3\text{-MeMgBr}$	4.2515	4.9715
$\text{HC}\equiv\text{CCH}_3\text{-MeMgCl}\cdot\text{Me}_2\text{O}$	6.5050	6.7737
$\text{HC}\equiv\text{CCH}_3\text{-MeMgBr}\cdot\text{Me}_2\text{O}$	6.5521	5.8134



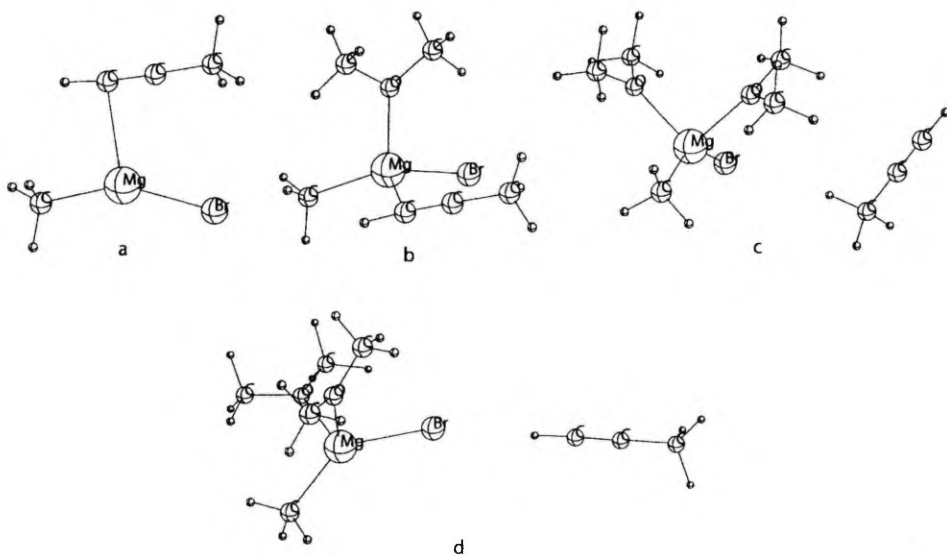


Fig. 1. The optimized (at B3LYP/6-31+G\* level of theory) structures of the propyne complexes with unsolvated methylmagnesium bromide (a), monosolvated methylmagnesium bromide (b), and disolvated methylmagnesium bromide (c) and (d).

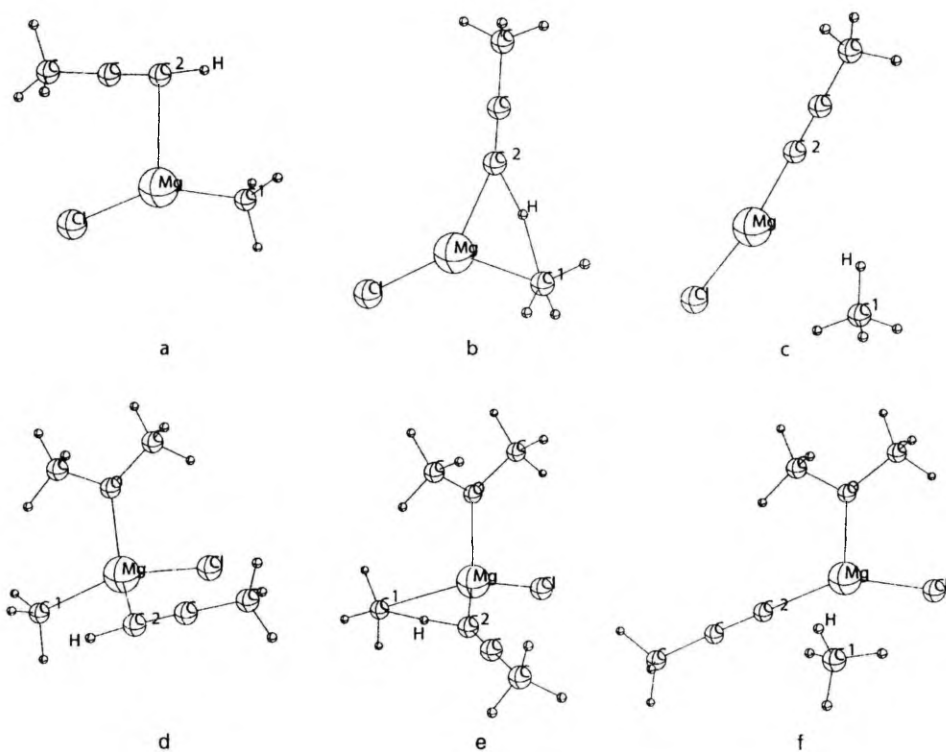


Fig. 2. The optimized (at B3LYP/6-31+G\* level of theory) structures for unsolvated and monosolvated reagents (a) and (d), transition states (b) and (e), and end products (c) and (f).

# CURRICULUM VITAE

## Jaana Tammiku-Taul

Born: August 27, 1976, Tartu, Estonia  
Citizenship: Estonian  
Marital status: married  
Address: Institute of Organic and Bioorganic Chemistry,  
University of Tartu,  
2 Jakobi St., Tartu 51014, Estonia  
Phone: +372 7 375 258  
Fax: +372 7 375 264  
E-mail: jaana@tera.chem.ut.ee

### Education

1994–1998 University of Tartu, Department of Chemistry, *B.Sc.*  
(chemistry, *cum laude*) 1998  
1998–2000 University of Tartu, Department of Chemistry, *M.Sc.*  
(chemistry, *cum laude*) 2000  
2000–present University of Tartu, Department of Chemistry, *Ph.D.* student,  
doctoral advisors prof. Ants Tuulmets and prof. Peeter Burk  
2003–present Teacher education program in University of Tartu

### Professional employment and retraining

1999–2000 University of Tartu, Centre of Strategical Competence, chemist  
2003–present University of Tartu, Institute of Chemical Physics, researcher

## Main scientific publications

1. J. Tammiku, P. Burk, A. Tuulmets, UV-VIS Spectrum of 1,10-Phenanthroline — Ethylmagnesium Bromide Complex. An Experimental and Computational Study. *Main Group Metal Chemistry*, **2000**, *23*, 301–305.
2. J. Tammiku, P. Burk, A. Tuulmets, 1,10-Phenanthroline and Its Complexes with Magnesium Compounds. Disproportionation Equilibria. *J. Phys. Chem. A*, **2001**, *105*, 8554–8561.
3. A. Tuulmets, V. Pällin, J. Tammiku-Taul, P. Burk, K. Raie, Solvent Effects in the Grignard Reaction with Alkynes. *J. Phys. Org. Chem.*, **2002**, *15*, 701–705.
4. J. Tammiku-Taul, P. Burk, A. Tuulmets, Theoretical Study of Magnesium Compounds. The Schlenk Equilibrium in the Gas Phase and in the Presence of Et<sub>2</sub>O and THF molecules. *J. Phys. Chem. A*, **2003**, *submitted*.
5. A. Tuulmets, J. Tammiku-Taul, P. Burk, Computational Study of the Grignard Reaction with Alkynes. *J. Mol. Struct. (Theochem)*, **2003**, *submitted*.
6. P. Burk, K. Taul, J. Tammiku-Taul, Proton and Lithium Cation Binding to Some  $\beta$ -Diketones. A Theoretical Study. *J. Phys. Chem. A*, **2003**, *submitted*.

## Conferences and meetings

1. J. Tammiku, P. Burk, A. Tuulmets, The Experimental and Computational Study of 1,10-Phenanthroline and Its Complex with Grignard reagent. XXV<sup>th</sup> Estonian Chemistry Days, Tallinn, 25–26.11.1999, 167–168.
2. J. Tammiku, P. Burk, A. Tuulmets, 1,10-Phenanthroline and Its Complexes with Magnesium Compounds. Disproportionation Equilibria. XXVI<sup>th</sup> Estonian Chemistry Days, Tallinn, 16–17.11.2000, 140–141.
3. J. Tammiku, P. Burk, A. Tuulmets, 1,10-Phenanthroline and Its Complexes with Magnesium Compounds. Disproportionation Equilibria. XIV<sup>th</sup> FEChem Conference on Organometallic Chemistry, Gdansk, Poland, 02–07.09.2001, 129.
4. J. Tammiku-Taul, P. Burk, A. Tuulmets, 1,10-Phenanthroline and Its Complexes with Magnesium Compounds. An Influence of Solvation on the Disproportionation Equilibria. XXVII<sup>th</sup> Estonian Chemistry Days, Tallinn, 15–16.11.2001, 136–137.
5. J. Tammiku-Taul, A. Tuulmets, P. Burk, The Experimental and Computational Study of Complexes Between 1,10-Phenanthroline and Magnesium Compounds. XX<sup>th</sup> International Conference on Organometallic Chemistry, Corfu, Greece, 07–12.07.2002, 146.
6. A. Tuulmets, V. Pällin, J. Tammiku-Taul, P. Burk, K. Raie, Solvent Effects in the Grignard Reaction with Alkynes. XX<sup>th</sup> International Conference on Organometallic Chemistry, Corfu, Greece, 07–12.07.2002, 147.

7. J. Tammiku-Taul, A. Tuulmets, P. Burk, The Experimental and Computational Study of Complexes Between 1,10-Phenanthroline and Magnesium Compounds. XXVIII<sup>th</sup> Estonian Chemistry Days, Tallinn, 21–22.11.2002, 137–138.
8. A. Tuulmets, V. Pällin, J. Tammiku-Taul, P. Burk, K. Raie, Solvent Effects in the Grignard Reaction with Alkynes. XXVIII<sup>th</sup> Estonian Chemistry Days, Tallinn, 21–22.11.2002, 152–153.
9. P. Burk, K. Taul, J. Tammiku-Taul, K. Sillar, Proton and Lithium Cation Affinities of Some Dicarbonyl Compounds: Influence of Keto-Enol Tautomerism. KISPOC-X, Fukuoka, Japan, 30.09–03.10.2003, 222–226.

# ELULOOKIRJELDUS

## Jaana Tammiku-Taul

Sündinud: 27. august 1976, Tartu, Eesti  
Kodakondsus: Eesti  
Perekonnaseis: abielus  
Aadress: Orgaanilise ja bioorgaanilise keemia instituut,  
Tartu Ülikool,  
Jakobi 2, 51014 Tartu, Eesti  
Tel: +372 7 375 258  
Faks: +372 7 375 264  
E-mail: jaana@tera.chem.ut.ee

### Haridus

1994–1998 Tartu Ülikooli keemiaosakonna üliõpilane, *B.Sc.* (keemia, *cum laude*) 1998  
1998–2000 Tartu Ülikooli keemiaosakonna magistrant, *M.Sc.* (keemia, *cum laude*) 2000  
2000–praegu Tartu Ülikooli keemiaosakonna doktorant, juhendajad emeritprof. Ants Tuulmets ja prof. Peeter Burk  
2003–praegu õpetajakoolitus Tartu Ülikoolis

### Teenistuskäik

1999–2000 Tartu Ülikooli Tehnoloogiakeskuse materjaliteaduse osakond, keemik  
2003–praegu Tartu Ülikooli keemilise füüsika instituut, teadur

## Tähtsamad teaduspublikatsioonid

1. J. Tammiku, P. Burk, A. Tuulmets, UV-VIS Spectrum of 1,10-Phenanthroline — Ethylmagnesium Bromide Complex. An Experimental and Computational Study. *Main Group Metal Chemistry*, **2000**, *23*, 301–305.
2. J. Tammiku, P. Burk, A. Tuulmets, 1,10-Phenanthroline and Its Complexes with Magnesium Compounds. Disproportionation Equilibria. *J. Phys. Chem. A*, **2001**, *105*, 8554–8561.
3. A. Tuulmets, V. Pällin, J. Tammiku-Taul, P. Burk, K. Raie, Solvent Effects in the Grignard Reaction with Alkynes. *J. Phys. Org. Chem.*, **2002**, *15*, 701–705.
4. J. Tammiku-Taul, P. Burk, A. Tuulmets, Theoretical Study of Magnesium Compounds. The Schlenk Equilibrium in the Gas Phase and in the Presence of Et<sub>2</sub>O and THF molecules. *J. Phys. Chem. A*, **2003**, *submitted*.
5. A. Tuulmets, J. Tammiku-Taul, P. Burk, Computational Study of the Grignard Reaction with Alkynes. *J. Mol. Struct. (Theochem)*, **2003**, *submitted*.
6. P. Burk, K. Taul, J. Tammiku-Taul, Proton and Lithium Cation Binding to Some  $\beta$ -Diketones. A Theoretical Study. *J. Phys. Chem. A*, **2003**, *submitted*.

## Konverentsid

1. J. Tammiku, P. Burk, A. Tuulmets, The Experimental and Computational Study of 1,10-Phenanthroline and Its Complex with Grignard reagent. XXV<sup>th</sup> Estonian Chemistry Days, Tallinn, 25.–26.11.1999, 167–168.
2. J. Tammiku, P. Burk, A. Tuulmets, 1,10-Phenanthroline and Its Complexes with Magnesium Compounds. Disproportionation Equilibria. XXVI<sup>th</sup> Estonian Chemistry Days, Tallinn, 16.–17.11.2000, 140.–141.
3. J. Tammiku, P. Burk, A. Tuulmets, 1,10-Phenanthroline and Its Complexes with Magnesium Compounds. Disproportionation Equilibria. XIV<sup>th</sup> FEICHEM Conference on Organometallic Chemistry, Gdansk, Poland, 02.–07.09.2001, 129.
4. J. Tammiku-Taul, P. Burk, A. Tuulmets, 1,10-Phenanthroline and Its Complexes with Magnesium Compounds. An Influence of Solvation on the Disproportionation Equilibria. XXVII<sup>th</sup> Estonian Chemistry Days, Tallinn, 15.–16.11.2001, 136–137.
5. J. Tammiku-Taul, A. Tuulmets, P. Burk, The Experimental and Computational Study of Complexes Between 1,10-Phenanthroline and Magnesium Compounds. XX<sup>th</sup> International Conference on Organometallic Chemistry, Corfu, Greece, 07.–12.07.2002, 146.
6. Tuulmets, V. Pällin, J. Tammiku-Taul, P. Burk, K. Raie, Solvent Effects in the Grignard Reaction with Alkynes. XX<sup>th</sup> International Conference on Organometallic Chemistry, Corfu, Greece, 07.–12.07.2002, 147.

7. J. Tammiku-Taul, A. Tuulmets, P. Burk, The Experimental and Computational Study of Complexes Between 1,10-Phenanthroline and Magnesium Compounds. XXVIII<sup>th</sup> Estonian Chemistry Days, Tallinn, 21.–22.11.2002, 137–138.
- A. Tuulmets, V. Pällin, J. Tammiku-Taul, P. Burk, K. Raie, Solvent Effects in the Grignard Reaction with Alkynes. XXVIII<sup>th</sup> Estonian Chemistry Days, Tallinn, 21.–22.11.2002, 152–153.
8. P. Burk, K. Taul, J. Tammiku-Taul, K. Sillar, Proton and Lithium Cation Affinities of Some Dicarbonyl Compounds: Influence of Keto-Enol Tautomerism. KISPOC-X, Fukuoka, Japan, 30.09.–03.10.2003, 222–226.



## DISSERTATIONES CHIMICAE UNIVERSITATIS TARTUENSIS

1. **Toomas Tamm.** Quantum-chemical simulation of solvent effects. Tartu, 1993, 110 p.
2. **Peeter Burk.** Theoretical study of gas-phase acid-base equilibria. Tartu, 1994, 96 p.
3. **Victor Lobanov.** Quantitative structure-property relationships in large descriptor spaces. Tartu, 1995, 135 p.
4. **Vahur Mäemets.** The  $^{17}\text{O}$  and  $^1\text{H}$  nuclear magnetic resonance study of  $\text{H}_2\text{O}$  in individual solvents and its charged clusters in aqueous solutions of electrolytes. Tartu, 1997, 140 p.
5. **Andrus Metsala.** Microcanonical rate constant in nonequilibrium distribution of vibrational energy and in restricted intramolecular vibrational energy redistribution on the basis of slater's theory of unimolecular reactions. Tartu, 1997, 150 p.
6. **Uko Maran.** Quantum-mechanical study of potential energy surfaces in different environments. Tartu, 1997, 137 p.
7. **Alar Jänes.** Adsorption of organic compounds on antimony, bismuth and cadmium electrodes. Tartu, 1998, 219 p.
8. **Kaido Tammeveski.** Oxygen electroreduction on thin platinum films and the electrochemical detection of superoxide anion. Tartu, 1998, 139 p.
9. **Ivo Leito.** Studies of Brønsted acid-base equilibria in water and non-aqueous media. Tartu, 1998, 101 p.
10. **Jaan Leis.** Conformational dynamics and equilibria in amides. Tartu, 1998, 131 p.
11. **Toonika Rinken.** The modelling of amperometric biosensors based on oxidoreductases. Tartu, 2000, 108 p.
12. **Dmitri Panov.** Partially solvated Grignard reagents. Tartu, 2000, 64 p.
13. **Kaja Orupõld.** Treatment and analysis of phenolic wastewater with microorganisms. Tartu, 2000, 123 p.
14. **Jüri Ivask.** Ion Chromatographic determination of major anions and cations in polar ice core. Tartu, 2000, 85 p.
15. **Lauri Vares.** Stereoselective Synthesis of Tetrahydrofuran and Tetrahydropyran Derivatives by Use of Asymmetric Horner-Wadsworth-Emmons and Ring Closure Reactions. Tartu, 2000, 184 p.
16. **Martin Lepiku.** Kinetic aspects of dopamine  $\text{D}_2$  receptor interactions with specific ligands. Tartu, 2000, 81 p.
17. **Katrin Sak.** Some aspects of ligand specificity of P2Y receptors. Tartu, 2000, 106 p.
18. **Vello Pällin.** The role of solvation in the formation of iotsitch complexes. Tartu, 2001, 95 p.

19. **Katrin Kollist.** Interactions between polycyclic aromatic compounds and humic substances. Tartu, 2001, 93 p.
20. **Ivar Koppel.** Quantum chemical study of acidity of strong and super-strong Brønsted acids. Tartu, 2001, 104 p.
21. **Viljar Pihl.** The study of the substituent and solvent effects on the acidity of OH and CH acids. Tartu, 2001, 132 p.
22. **Natalia Palm.** Specification of the minimum, sufficient and significant set of descriptors for general description of solvent effects. Tartu, 2001, 134 p.
23. **Sulev Sild.** QSPR/QSAR approaches for complex molecular systems. Tartu, 2001, 134 p.
24. **Ruslan Petrukhin.** Industrial applications of the quantitative structure-property relationships. Tartu, 2001, 162 p.
25. **Boris V. Rogovoy.** Synthesis of (benzotriazolyl)carboximidamides and their application in relations with *N*- and *S*-nucleophyles. Tartu, 2002, 84 p.
26. **Koit Herodes.** Solvent effects on UV-vis absorption spectra of some solvatochromic substances in binary solvent mixtures: the preferential solvation model. Tartu, 2002, 102 p.
27. **Anti Perkson.** Synthesis and characterisation of nanostructured carbon. Tartu, 2002, 152 p.
28. **Ivari Kaljurand.** Self-consistent acidity scales of neutral and cationic Brønsted acids in acetonitrile and tetrahydrofuran. Tartu, 2003, 108 p.
29. **Karmen Lust.** Adsorption of anions on bismuth single crystal electrodes. Tartu, 2003, 128 p.
30. **Mare Piirsalu.** Substituent, temperature and solvent effects on the alkaline hydrolysis of substituted phenyl and alkyl esters of benzoic acid. Tartu, 2003, 156 p.
31. **Meeri Sassian.** Reactions of partially solvated Grignard reagents. Tartu, 2003, 78 p.
32. **Tarmo Tamm.** Quantum chemical modelling of polypyrrole. Tartu, 2003. 100 p.
33. **Erik Teinmaa.** The environmental fate of the particulate matter and organic pollutants from an oil shale power plant. Tartu, 2003. 102 p.



ISSN 1406-0299  
ISBN 9985-56-881-7